PULMONARY DELIVERY OF ANTIMICROBIAL PEPTIDES (AMP) USING POROUS NANOPARTICLES AGGREGATES (PNAPs) FOR TARGETING ALVEOLAR MACROPHAGES AGAINST PULMONARY TUBERCULOSIS

A thesis submitted

By

Ankur Sharma

In partial fulfilment of the requirements for the degree

Of

Doctor of Philosophy

Institute of Nano Science and Technology, Mohali, India

And

Indian Institute of Science Education and Research, Mohali, India

December 2019

Declaration

The work presented in this thesis has been carried out by me under the guidance of Dr. Rahul K.Verma at Institute of Nano Science and Technology and registered at Indian Institute of Science Education and Research Mohali. This work has not been submitted in part or in full for a degree, a diploma, or a fellowship to any other university or institute. Whenever contributions of others are involved, every effort is made to indicate this clearly, with due acknowledgement of collaborative research and discussions. This thesis is a bona fide record of original work done by me and all sources listed within have been detailed in the bibliography.

Place
Date:

Ankur Sharma

In my capacity as the supervisor of the candidate's thesis work, I certify that the above statements by the candidate are true to the best of my knowledge.

Place
Date:

Dr. Rahul K.Verma
Scientist D
Institute of Nano Science and Technology, Mohali

This Work is dedicated to

My Parents

and

Thee Almighty

Acknowledgements

It gives me a great pleasure to acknowledge my heartfelt respect and depth of gratitude to my guide and mentor Dr. Rahul K. Verma Scientist INST, Mohali for his incredible mentorship, indispensable knowledge, guidance, fruitful discussions, and constant encouragement and for being there at each and every step for me throughout my research. I am totally blessed to be a part of his lab. He has been an ideal mentor for his excellent guidance, caring, patience; for providing me with an excellent research atmosphere and for allowing me to work independently. I am thankful to him for his continuous input throughout the project. Innumerable ideas, questions, answers, and fruitful discussions have been helpful in arriving to the conclusions. Most importantly, I am thankful to him for, his extraordinary kindness, openness, support and friendliness. His incredible creativity and interpretation skills have often inspired me. His encouragement for growth and perseverance is a dependable force amidst the trials of life and learning. Simply, I cannot imagine a better supervisor.

I wish to express my sincere thanks to Dr. Arvind, Director IISER Mohali for providing me opportunity to register for PhD and Dr. H.N. Ghosh, Director, INST Mohali for providing me the opportunity to avail the research facilities of the institute.

I wish to thank Dr Deepa Ghosh Dean Research INST, Mohali for providing good working facilities, a stimulating environment and a friendly working atmosphere for pleasant and stimulating discussions. Many thanks are also extended to Dr. Abir De Sarkar Dean academics INST Mohali, for providing me the necessary help and support encountered during my Ph.D. Thank you all for the invaluable scientific input and for all your personal advice.

I would specially like to thank to Doctoral committee members for guiding and advising time to time, which improved the quality and impact of my research work.

I would specially like to thank my lab mates Kalpesh and Eupa, for providing me enough co-operation and support during experimental work. They were always there to offer me great support with amazing suggestions in both professional and personal matters. I have been lucky enough to have the support of many good friends Soumen, Neha, Ruchi, Ashmeet, Rajinder, Ashmeet, Rashmi, Swati, Anirban, Sandeep, Naimat , Dimple, for noisy parties, enjoyable friendship, for the discussions, encouragement as well as providing me emotional support. They need real appreciation for their critical analysis, valuable advice and willingness to share bright thoughts and for constantly reminding me to take care of myself, for providing the light moments.

I also acknowledge the financial assistance from Department of Science and technology and INST Mohali during the tenure of this dissertation.

This work could have never been completed without the blessings and love of my parents. They provided me the path to go ahead in each and every aspect of my life. Without their support I was not able to make such a delightful carrier. It would be immoral if forgot to acknowledge the silent sacrifice of innocent mice without whom this work will never have been completed. Finally, I can't forget the blessing of almighty God for his grace and kindness.

Ankur Sharma

Abstract

The prospective to progress pulmonary tuberculosis (TB) therapy outcomes with adjunctive therapies requires investigation. The objective of the present work was aimed to investigate the role of exogenous delivery of antimicrobial peptides (AMPs) using inhalable formulations against pulmonary tuberculosis as an adjunct therapy along with contemporary anti-TB treatment with increased activity and patient compliance. Several AMPs have antimycobacterial potential which provides them as appropriate therapeutics but due to poor pharmacokinetic profile, salt sensitivity, presence of proteases in the biological system makes them highly unstable with very diminutive half-life hence, is exigent to deliver as such in biological system in a sustained and controlled way for therapeutic rationale. The study was performed to target lungs locally using various Inhalable biodegradable formulations encapsulating substantial amount of AMPs shows raised area to release AMPs locally (alveolar macrophages) at beneficial level over extended period of time at site of infection for the treatment of pulmonary tuberculosis (TB). Double emulsion method was used to prepare porous microspheres and spray freeze drying was used to develop inhalable Porous nanoparticles aggregate particles (PNAPs) containing individual AMPs alone) for pulmonary delivery. All the developed formulations had optimized aerodynamic properties to deposit into lungs with cascade impaction. MIAP, UB2, Aurin, K4, HHC-10, Indolicidin and IDR-1018 were synthesized using solid phase peptide synthesis and individually incorporated in various delivery systems with encapsulation efficiencies of ~50% to obtain particles (MP) yields of >60%. The Mass Median Aerodynamic Diameter (MMAD) of the MP was 2.2-2.4 μm within geometric standard deviations (GSD) of ≤ 0.1 μm. MP were phagocytosed by RAW 264.7 macrophages in culture and significantly ($P<0.05$) dose-dependent killing of intracellular Mtb by formulation compared to equivalent amounts of drugs in solution was observed on estimation of colony forming units (CFU). Cytotoxicity of MP towards macrophages was lower than that of dissolved drugs. The in-vivo efficacy of individual AMPs and with anti-TB combinations Isoniazid was evaluated in Swiss mice infected with virulent (H37Rv) mycobacterium after 6 weeks (5days/week) multiple dose pulmonary delivery which was further compared with standard oral Anti-TB therapy. The results reveals the formulations containing indolicidin and IDR-1018 exerts significant antimycobaterial activity against virulent Mycobacterium tuberculosis (H37Rv) in vivo. AMPs releasing inhalable microparticles demonstrated enhanced bactericidal efficacy and normalized lung and spleen morphology. Attempt was made to elucidate the cellular and molecular

mechanism by which AMP kills the bacteria. Our results suggest that different exogenous AMPs exerts multiple mechanisms to enhance bacterial killing inside inected macrophages like phagolysosomal fusion, membrane permeabilization also enhance apoptosis in infected macrophages. It is concluded that developed inhalable formulations containing AMPs can were formulated best depending upon their aerodynamic capacity, encapsulation efficiency *in vitro* and *in vivo* efficacy. These results display the advantage of pulmonary delivering of AMPs via formulation for antituberculosis application an adjunct therapy along with standard DOTS therapy.

LIST OF PUBLICATIONS

1. Sharma A, Vaghasiya K, Ray E, Gupta P, Singh AK, Gupta UD, Verma RK. Mycobactericidal activity of some micro-encapsulated synthetic Host Defense Peptides (HDP) by expediting the permeation of antibiotic: A new paradigm of drug delivery for tuberculosis. International journal of pharmaceutics. 2019 Mar 10;558:231-41.
2. Sharma A, Vaghasiya K, Gupta P, Gupta UD, Verma RK. Reclaiming hijacked phagosomes: hybrid nano-in-micro encapsulated MIAP peptide ensures host directed therapy by specifically augmenting phagosome-maturation and apoptosis in TB infected macrophage cells. International journal of pharmaceutics. 2018 Jan 30;536(1):50-62.
3. Sharma A, Verma RK. Hybrid nano-in-micro systems for lung delivery of host defence peptides (HDP) as adjunct therapeutics for pulmonary tb. In journal of aerosol medicine and pulmonary drug delivery 2018 Apr 1 (Vol. 31, No. 2, pp. A17-A17).
4. Sharma A, Vaghasiya K, Verma RK. Inhalable microspheres with hierarchical pore size for tuning the release of biotherapeutics in lungs. Microporous and Mesoporous Materials. 2016 Nov 15;235:195-203.
5. Sharma A, Vaghasiya K, Ray E, Verma RK. Lysosomal targeting strategies for design and delivery of bioactive for therapeutic interventions. Journal of drug targeting. 2018 Mar 16;26(3):208-21
6. Vaghasiya K, Sharma A, Kumar K, Ray E, Adlakha S, Katare OP, Hota S, Verma RK. Heparin encapsulated metered-dose topical “Nano-spray gel” liposomal formulation ensures rapid on-site management of frostbite injury by inflammatory cytokines scavenging. ACS Biomaterials Science & Engineering. 2019 Nov 6.
7. Vaghasiya K, Eram A, Sharma A, Ray E, Adlakha S, Verma RK. Alginate Microspheres Elicit Innate M1-Inflammatory Response in Macrophages Leading to Bacillary Killing. AAPS PharmSciTech. 2019 Aug 1;20(6):241.
8. Vaghasiya K, Sharma A, Verma R. Misdiagnosis Murder: Disguised TB or Lung Cancer. Pul Res Respir Med. 2016;3:e5-6.

Book sections

- Sharma A, Vaghasiya K, Verma RK, Yadav AB. DNA nanostructures: chemistry, self-assembly, and applications. InEmerging Applications of Nanoparticles and Architecture Nanostructures 2018 Jan 1 (pp. 71-94). Elsevier.
- Ray, E,; Sharma, A,; Vaghasiya, K, Verma, R.K* Molecular Medicines for Cancer: Concepts and Applications of Nanotechnology, CRC Press; 2018 Oct 5.
- Vaghasiya K, Sharma A, Ray E, Verma RK. (2019) Different methods to characterize nanoparticles Mucosal Delivery of Drugs and Biologics in Nanoparticles' 'AAPS Advances in the Pharmaceutical Sciences (in press)

PREFACE

The present work entitled “Pulmonary delivery of antimicrobial peptides using porous nanoparticles aggregate particles (PNAPs) for targeting alveolar macrophages against pulmonary tuberculosis” comprises of the work done by the author in Institute of Nano Science And Technology, Mohali and Department of Biological Sciences, Indian Institute of Science Education and Research (IISER), Mohali for the award of Doctor of Philosophy.

Tuberculosis (TB) caused by Mycobacterium tuberculosis is add up to one major bacterial killer around the globe. Tuberculosis transmission occurs via droplet infection. Alveolar macrophages phagocytize the mycobacterium and able to multiply within phagosomes and arrest the phagolysosomal fusion. Later the bacteria may disseminate from the lungs to other organs such as liver and kidneys. Recent reports established that, the host cells containing infection develops immunoregulatory and bactericidal mechanisms, but malfunction in these mechanisms permits the disease to develop. Currently drug sensitive TB bacteria are treated with a combination of anti-TB drugs administered by the oral or parenteral route. The most suitable route is oral route and generally the safest and least pricey. However, limitations of oral route may include a slower onset of action, high daily dose of the drugs, poor patient compliance and potentially significant first-pass effect by the liver. The development of antituberculosis drugs formulations delivered directly to the lungs is a promising avenue to explore. To work against the budding treatment of resistant M.tb bacteria immune system of the body may be explored and exploited as new way to cure.. Newer therapeutics is limited and are frequently more costly and additionally may not be safe. One of the most limitation of using current regimen is they are mostly active on replicating cells but not active on non dividing cells, Also due to emergence of MDR and XDR TB so urgent need of new drugs or delivery systems are required. In these conditions, exploitation of innate immune mechanism may work against tuberculosis. There are certain evidences of using these antimicrobial peptides against tuberculosis in *in vitro* systems bcause they are having antimicrobial activity.

In this thesis work, we have explored therapeutic prospective of exogenously supplied antimicrobial peptides to treat TB. Here, we synthesized antimicrobial peptides and developed formulations like porous micropsheres, PNAPs, nano in micro systems containing AMPs alone or/and in combination with half dose of anti-tuberculosis drugs to

treat *Mycobacterium tuberculosis*-infected macrophages, and to inspect whether these targeted delivery system possesses the capability in bacterial killing and analysed their therapeutic efficiency in *in vitro* cell lines & laboratory animal models of TB. Further, we made an attempt to elucidate cellular mechanism of anti-microbial action.

The present work carried out is incorporated into eight different chapters, which includes: Introduction, Research envisaged, Synthesis, characterization and minimum inhibitory concentration of selected antimicrobial peptides, Preparation Characterisation inhalable various AMPs loaded formulations like porous microspheres, porous nanoparticle aggregate particles (PNAPS), mucus penetrating particles (MPPs) and Efficacy studies on cells lines, Mechanistic Study, In vivo efficacy study, and Summary & Conclusions.

Introduction of this thesis introduces about the pulmonary tuberculosis, its pathogenesis, contemporary drug delivery systems, the importance of AMPs in the disease and a brief idea about inhalation delivery systems.

Research envisaged justifies the problem to be investigated along with outline of plan of action.

Experimental chapters were further divided into four sections i.e. Introduction, Experimental, Results & Discussion and Conclusions. Chapter-2 deals with synthesis and characterisation of antimicrobial peptides and determination of their MIC values against mycobacterium tuberculosis bacteria. Chapter-3 deals with the analytical method development and validation of the AMPs to be used in formulation development. Chapter-4 includes with preparation and characterization of inhalable AMPs releasing microparticles which includes spray drying methodology, particle size distribution, drug content and encapsulation efficiency determination, aerodynamic characterization of microparticles using cascade impactor, thermal studies, *and in vitro* drug release studies. Chapter-5 includes *in vitro* efficacy studies against infected cell lines, cell uptake studies on cell lines and cytotoxicity studies. Chapter-6 deals with elucidation of various mechanisms on TB infected macrophages by AMPs formulation which comprises phagosome-lysosome fusion studies, apoptosis studies, membrane degeneration.Chapter-7 includes with therapeutic efficacy studies of AMPs releasing inhalable microparticles which includes respiratory infection of animals with virulent tuberculosis bacteria, multi dosing of microparticles, Necropsy, tissue processing, histopathology and enumeration of viable bacilli in animal organs.

Chapter-8 includes Summary and conclusion which gives a short overview of the endeavours of this thesis work and future prospects of study. References appearing throughout the text are documented at end of the thesis.

TABLE OF CONTENTS

List of Tables

List of Figures

List of abbreviations

Abs	Absorbance
ACN	Acetonitrile
IDR	Innate defence regulator
AMPs	Antimicrobial peptides
AMφ	Alveolar Macrophages(s)
ANOVA	Analysis of variance
BAL	Bronchio alveolar lavage
BLK	Blank Microparticles
BSL-2	Bio Safety Level-2
BSL-3	Bio Safety Level-3
cDNA	Complimentary Deoxyribonucleic acid
Conc.	Concentration

CFUs	Colony forming units
oC	Degree Celsius
60Co	Radioactive Cobalt-60
DAPI	4, 6-Diamidino-2-phenylindole, Dihydrochloride
DCF	Dichlorofluorescein
DCFH-DA	Dichlorodihydrofluorescein diacetate
DCM	Dichloromethane
DMSO	Dimethyl Sulfoxide
DNA	Deoxyribonucleic acid
DOTS	Directly Observed Shortcourse Treatment
DPI	Dry powder inhalation
FACS	Fluorescence-activated cell sorter
FCS	Fetal calf serum
FITC	Fluorescein Isothiocyanate
x g	Relative centrifugal force
gm	Gram
H37Ra	Attenuated Mycobacterium tuberculosis strain
H37Rv	Virulant Mycobacterium tuberculosis strain
HIV	Human immunodeficiency virus
h	Hour
IAEC	Institute's Animal Ethical Committee
Inh	Inhalation
INH	Isoniazid
iNOS	Inducible nitric oxide synthase
JALMA	Japanese Leprosy mission for Asia
kGy	Kilogray (radiation unit)
kg	Kilogram

L	Liter
m	Milli
M	Molar
μ	Micro
μm	Micrometer
MDR-TB	Multi drug resistance TB
MeOH	Methanol
MIC	Minimum inhibitory concentration
mg	Milligram
min	Minute
mM	Millimolar
MOI	Multiplicity of infection
MPs	Microparticles
PNAPs	Porous Nanoparticle Aggregate Particles
Mφ	Macrophage(s)
M.tb.	Mycobacterium tuberculosis
MW	Molecular weight
nm	Nanometer
NaOH	Sodium hydroxide
N	Normal solution
NO	Nitric oxide
No.	Number
MPs	Microparticles
M.tb.	Mycobacterium tuberculosis
MTT	3-(4, 5 dimethyl-thiazol-2-yl-2, 5 biphenyl) tetrazolium bromide
O2-	Superoxide anion

OADC	Oleic acid-albumin-dextrose-catalase (OADC) enrichment medium
OD	Optical density
PBS	Phosphate buffered saline
PCR	Polymerase chain reaction
pH	Negative logarithm of hydrogen ion concentration
phox	Phagocyte Oxidase
PI	Propidium iodide
PLA	Poly(lactic acid)
PLF	Phagosome lysosome fusion
PLGA	Poly(lactide-co-glycolide)
ppm	Parts per millions
RFB	Rifabutin
RPMI	Roswell Park Memorial Institute medium
RSD	Relative Standard Deviation
RT-PCR	Real Time Polymerase chain reaction
SNP	Sodium Nitroprusside
TB	Tuberculosis
TDW	Triple distilled water
TNF-α	Tumour necrosis factor alpha
UV	Ultraviolet
v/v	Volume by volume
w/w	Weight by weight
WHO	World Health Organization
XDR-TB	Extensively drug resistance tuberculosis

Tuberculosis (TB) is a life intimidating disease results from infection of *Mycobacterium tuberculosis(Mtb)*. Recently TB infections have been found to worryingly spread all over the world and second most common leading infection which is causing death to the youth and adults worldwide. Several factors, such as HIV epidemics, immigration from developing countries and failure of DOTS (directly observed treatment short course) therapies, contributed to increase the TB incidence (1). Human TB is caused by infection caused by droplet infection with members of the *Mycobacterium tuberculosis* complex, which includes *Mycobacterium tuberculosis* itself, *Mycobacterium africanum*, *Mycobacterium bovis*, *Mycobacterium caprae*, *Mycobacterium microti*, *Mycobacterium pinnipedii* and *Mycobacterium canettii* which divide in every 16- 20 hours within the alveolar macrophages. Patients with active pulmonary-TB are the main sources of infection and the majority of people infected with *M. tuberculosis* contain it as asymptomatic latent TB infection (LTBI). Bacteria present in droplets of sputum shed by infected persons are inhaled and the infection is first established in alveolar macrophage (AM)(2). There is high risk of re-activation of disease and occurrence of LTBI in estimated 2 billion people all over the world. TB continues to spread in every corner of the globe despite the introduction of the inexpensive and effective quadruple drug therapy regimen 40 years ago (3)**.** In 2012 World Health Organization (WHO) estimated 8.6 million incidence cases of TB and 1.3 million died of TB among these deaths 170,000 arose from MDR-TB, a relatively high total compared with 450,000 incident cases of MDR-TB. Asia (58%) was the highest estimated number of cases followed by Africa (27%), Eastern Mediterranean region (8%), Europe (4%) and America (3%).TB management or treatment can be improved by pulmonary delivery of antitubercular drugs(anti-TB) using the novel drug delivery system (NDDS) which can release the agents in a controlled manner. But the increasing number of multi drug-resistant (MDR) *Mtb* isolates that can be exceedingly difficult and expensive to treat is of particular concern (4) The combination of the increased frequency of infection due to *Mtb* and the increase in multidrug resistance is a great concern worldwide.

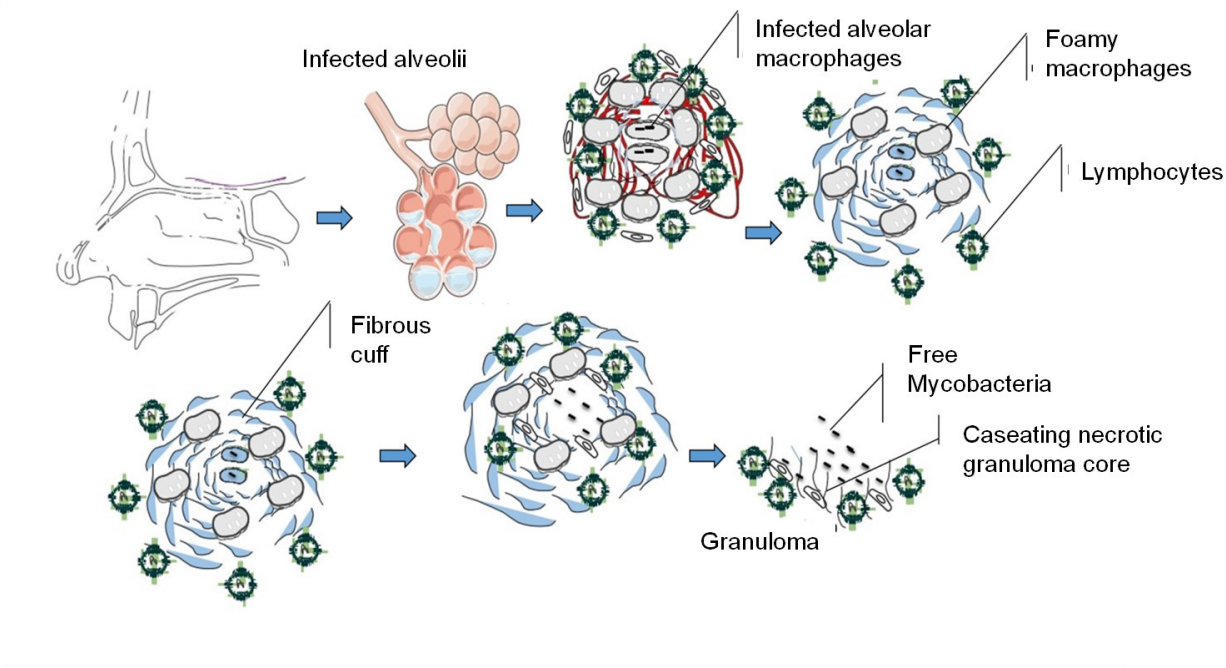

Figure 1.1. Pathogenesis of mycobacterium tuberculosis (pulmonary TB) in humans

1.1. Current treatments

The goals of chemotherapy are to cure patients without relapse, to minimize the risk of death and disability, to prevent transmission of Mtb to other persons the emergence of drug resistance (5). To achieve these goals, treatment of active TB including a single drug should never be attempted or be added to a failing regimen, the result being the development of MDR-TB (Iseman, 1993). As suggested by WHO (2011), treatment of TB and drug resistant cases requires a combination of multi-drug regimens over long periods. The initial intensive phase consists of a combination of first-line drugs (three or more) for at least 2 months to reduce the rapidly dividing bacilli load. In the continuation phase, a combination of two or three drugs is used for at least 4 months to sterilize lesions containing fewer and slow-growing bacilli. There are, at present, five 'first-line' anti-TB agents: Isoniazid (INH), Rifampicin (RIF), pyrazinamide (PZA), Ethambutol (ETB) and Streptomycin (SM)(6).

1.2. Shortcomings of current treatment

Existing TB therapy includes the grouping of anti-TB drugs administered by the oral or may be parenteral route depending on the type of patient. The oral route is normally the most suitable route of administration which is the safest and least pricey. Still the limitation of an oral route may comprise of having the slower onset of action, fail to attain high drug retention in the

pulmonary region and potentially noteworthy first-pass effect by the liver. Parentral route may have highest bioavailability but it recurrently seems as a painful route of delivery for which appropriate treatment observance can be difficult since it leads to uneasiness for the patient and it requires supervision of an expert. Parentral as well as oral route fail to achieve therapeutic level the site of infection (pulmonary alveolar region) due to poor pulmonary distribution of most of the systemically administered drugs. It is essential to note that, both of these conventional delivering routes may lead to sub-therapeutic levels of anti-TB drugs at the site of infection due to poor pulmonary allocation of most systemically administered therapeutics. As a consequence, drug-resistant strains may come into sight swiftly. The rise of multi drug-resistant (MDR), extensively drug-resistant (XDR) and completely resistant strains, are creating concerns regarding how to effectively treat TB infections by these recalcitrant strains(7). Conventional antimicrobials do not work and new pragmatic approach with novel drugs or combinations is essential to control this fatal ailment.

The development of anti-TB drugs formulations delivered directly to the pulmonary region is a promising possibility to investigate. Several research groups have investigated the direct delivery of anti-TB drugs by nebulization of drug solutions, and also via particulate pulmonary drug delivery formulations. Numerous particulate delivery systems including microparticles(8), nanoparticles(9-11), liposomes(12, 13), drug powders(14, 15) etc with or without inhalable excipients has been investigated for delivery of anti-TB drugs(16). Apart from non-invasive nature, the pulmonary delivery offers several advantages: (i) dwindling in dose and frequency of the drugs to avert side effect therefore, rising patient compliance; (ii) better targeting of the drugs directly to the lungs and reduce systemic toxicity; (iii) MDR-TB cases can be reduced by providing drugs directly to the lungs; (iv) avoid the degradation of the drugs in GI tract and reduce first-pass metabolism. (17)

1.3. Survival strategies of Mycobacterium inside macrophages

The survival and pathogenesis of Mtb inside macrophages and monocytes depend on the ability to evade the host's defence mechanisms and manipulate the host cell organelles and membrane trafficking (18).

1.3.1. Inhibition of phagosomal maturation

The survival and pathogenesis of Mtb) inside macrophages and monocytes depends on an ability to control the host cell machinery and evade host's defense mechanisms (19). TB bacteria (virulent H37Rv) successfully reside in macrophages due to its ability to "hijack" phago-lysosome biogenesis and inhibit host-cell apoptosis, as its survival strategy within the host macrophage (20, 21). Inside the macrophages, Mtb escapes the lethal effects of lysosomal enzymes and free radicals by halting phagosomal maturation(19). In this perspective, Desjardins and coworkers proposed an interesting "Kiss and Run" model for phagosome maturation in which microbe bearing phagosomes can momentarily/partially fuse (Kiss) with endosomes to permit exchange of some selective solutes, which is followed by quick fission (Run) but not result in complete and irreversible fusion of two membranes (22). Several reports suggested that the activated macrophages enhance the maturation of phagosomes containing mycobacterium and kill mycobacteria through innate antimicrobial effectors(23). As macrophages kill microbes by mechanisms which involve the participation of lysosomal contents, attention has been focused on lysosomes in macrophages. Subsequent biochemical events in infected macrophages decide the fate of microbe and macrophage(24).

1.3.2. Neutralisation of oxidative stress

Reactive oxygen species (ROS) are produced by the macrophages when there is any microbial infection in the body. Mtb being a smart bacteria, it tries to scavenge the ROS produced by biochemical pathways inside macrophages that includes enymes like super-oxide dismutase (SOD) and catalase. (25, 26).

1.3.3. Inhibition of apoptosis

The induction of apoptosis is one of the powerful mechanisms to inhibit mycobacterial growth because activated macrophages can reduce bacterial burden by inducing this mechanism(27). The interplay between M.tb and host macrophages exerts an antimicrobial effect on intracellular Mtb, as evidenced by reduced bacterial viability upon infection of macrophages and subsequent chemical induction of apoptosis (21). In TB infection, Mtb cause dysregulation of apoptosis in macrophages as its survival strategy. The induction of apoptosis specifically in Mtb infected macrophages can be an important anti-mycobacterial defense mechanism (28, 29).

1.3.4. Mycobacterial cell wall impermeability to drugs

One of the important determinants of resistance of M.tb is an atypical hydrophobic and multi-layered nature of mycobacterial cell-wall structure with mycolic-acid and wax-D, which restricts permeability of both hydrophobic and hydrophilic drugs into bacteria.

1.3.5. Excessive mucus production

A well-known characteristic of pulmonary infection with mycobacteria is a hyper-secretion of cough. Mucus production is associated with of many lung diseases. The mucus obstacle protects unknown materials and microorganisms from ingoing and/or infecting lungs. In normal lungs, the inhaled matter is naturally trapped in airway mucus and then cleared from the lungs via whipping performance of cilia or hair like strands, to the stomach to be ultimately ruined. unhappily, this necessary defensive machinery also prevents a lot of inhaled therapeutics from getting their objective(30).

1.4. Need for new drug regimen

World Health Organization (WHO) recommended treatment strategies for drug-susceptible and drug-resistant TB. Still there numerous challenges to treat normal as well as MDR TB. Hence, novel anti-TB drug-discovery is still a priority for scientific and communal healthiness. The challenges with current therapeutics for drug-susceptible strains includes high daily dose of the drugs, prolonged duration of therapy for at least six months , which leads to non-compliance of patient, which further may lead to development of drug resistant cases. Thereby, we need a new drug regimen which can reduce the treatment time as well as cost of the drugs. In case of latent TB, mycobacteria remain in dormant stage and are not susceptible to anti-TB drugs which can further enhance the duration of the treatment. Hence, treatment of MDR-TB and XDR-TB cases need less lengthened, more tolerable, more proficient drugs.

1.5. Host directed therapies

Host-directed therapy (HDT) is a latest and budding thought in treating TB, where host response is modulated by treatment with host-directed agents with or without adjunct antibiotics,. Targeting and manipulating host factors can be used for HDT to control TB infection and dissemination within/outside the lung(31). Various Host directed agents act

by various mechanisms including upregulation of antimicrobial peptides, enhancement of reactive oxygen species (ROS) and induction of autophagy in infected cells.

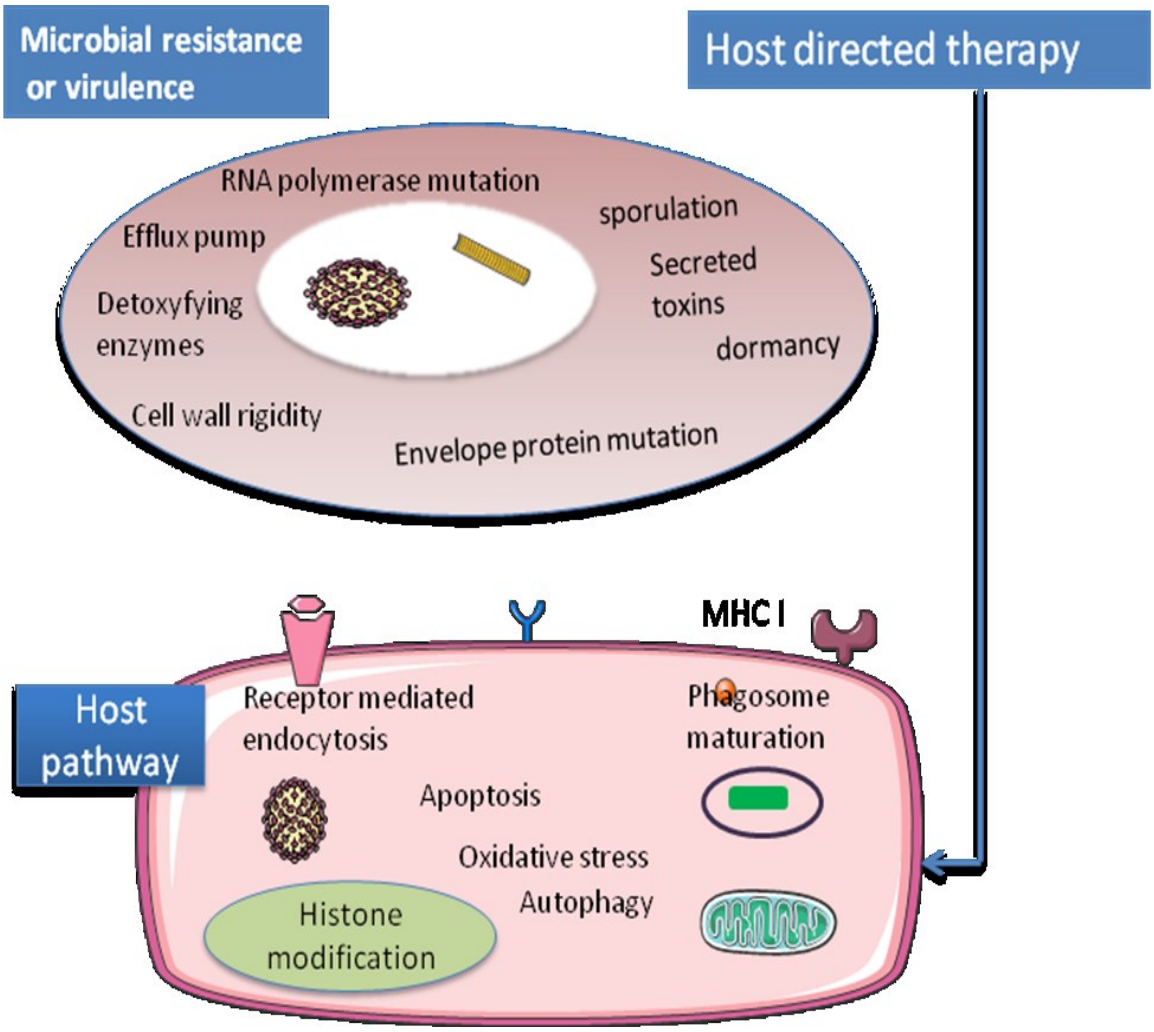

Figure 1.2. Mechanism of host directed therapy in overcoming resistance

1.6. Antimicrobial peptides against tuberculosis

Antimicrobial peptides (AMP) or Host Defense Peptides(HDP) are produced by multicellular organisms as a key component of innate defence systems and act as first line of defence against various pathogenic microbes(32, 33). Recently, AMP became a popular topic of research and over 750 eukaryotic AMP have been reported(34). Pioneering studies have led to the discovery of various types of these AMP — including defensins, cecropins, magainins and cathelicidins — with remarkably different structures and bioactivity profiles. Thousands of

AMP have evolved within bacteria, plants, and animals. Extensive research has led to the realization that these bioactive peptides do not merely act as direct antimicrobial agents but also represent important effectors and regulators of the innate immune system that are able to profoundly modulate the immune response through a range of activities (35). Indeed, many AMP are under clinical development for treating a wide variety of diseases. While a single mechanism does not underlie all effects of AMP. The bactericidal activities of AMP often depend on their abilities to permeabilize the membranes of bacteria by creating pores or disrupting the organization of the lipid bilayer(36, 37). Partial depolarization of the cytoplasmic membrane by AMP interferes with electron transport and oxidative metabolism, leading to cell death(38, 39). Directly or indirect, exposure of AMP interferes in the activities of essential cellular processes including synthesis of protein, DNA, RNA, and the bacterial cell envelope(40). The activities of AMP and their species specificity are also determined by resistance systems that directly recognize structural motifs in specific AMP and then bind, degrade, or extrude them from the membrane. Membrane transporters also serve to extrude AMP from the cytoplasmic or inner membrane. The proliferation of intracellular pathogens within host cells is often dependent on their abilities to sense and activate these resistance systems. (41)The resistance to the AMP occurs to a much lesser degree because they attack various targets by multiple mechanisms. The resistance to the AMP can be developed via external trapping of peptides to the cell surface, presence of proteases which can degrade the peptides before reaching to the site of action. Earlier studies demonstrated therapeutic roles of AMP in various diseases like dermatitis(42, 43), Crohn's disease(44-46), Cystic fibrosis(47-49), Pneumonia(50, 51), wound healing(52, 53), TB(39, 54, 55), leishmaniasis(56-58) etc. Moreover these AMP can also signaling mediators in host defence and inflammation. The major group of AMP in humans is defencins and cathelicidins. Recent studies have emphasized the role of AMP like LL-37, PR-39, thymopentin, IDR-1018(59), α helical peptides, hepcidin, HNP-1, HNP-2, HNP-3 as antimycobacterial agents. Portell-Buj et al. investigated the antimycobacterial activity of 12 different AMP on Mycobacterium tuberculosis and M. avium clinical isolates using microtitre and risazurin assay(60). Linde et al. investigated the *in vitro* activity of the proline arginine rich peptide PR-39 against TB. They used the BACTEC radiometric method for mycobacterial activity(61). HNP-1, HNP-2, HNP-3 showed antimycobacterial effects at the concentration of 50μg/ml with killing

efficiency of up to 87.2%. B. Rivas-Santiago et al. investigated the role of LL-37, CRAMP and other peptide derived compounds E2, E6 and CP26 against mycobacterium using microdilution assay *in vitro(62)*. Gareth Griffith and his coworkers also cocluded that LL-37 have some in vitro activity against mycobacterium(63). It has been reported that alteration in the production of these molecules increase susceptibility to infections like TB(27).

1.7. Contemporary Drug Delivery Systems for Tuberculosis

It is difficult to introduce AMP into lungs and alveolar macrophages in which bacteria resides, for therapeutic purpose due to their susceptibility to proteases inside the body. The applicability of the AMP is stuck due to the unavailability of the appropriate delivery system which can deliver them to the target site. In recent years various drug delivery systems like liposomes, niosomes, polymeric microparticles, nanoparticles, and solid lipid nanoparticles have been investigated for the successful administration of the drugs to the site of infection. The promising benefits of the inhalable particles includes lung targeting, sustained release effects, drug protection etc. The optimum size to target lung alveolar macrophages is 1-5 μm which is amenable to inhalation and phagocytosis.

1.8. Pulmonary drug delivery system

Pulmonary drug delivery has been an area of attention for numerous disciplines. Pulmonary drug delivery improves the deposition of the drug directly to the lungs. Extensive efforts are being carried out to persuade the factors implicated in deposition of inhaled particulate delivery systems. It is the non-invasive, and widely accepted approach for treating lung diseases to reduce side effects of systemically administered drugs and enhance therapeutic efficacy (64). Confined deliverance may escort to high drug concentration specifically in the lung might reduce the period of therapy and preventing drug resistant cases.

Inhalation therapy is increasingly gaining popularity over conventional treatment strategies for delivery of various types of drugs to target alveolar macrophages. Pulmonary delivery for TB may help in targeting drug to AMϕ where bacteria reside. The particulate delivery systems get deposited inside the lungs by three key mechanisms named inertial impaction and gravitational sedimentation and diffusion (65). Bigger particle size leads to deposition by gravitation force or inertial impaction and smaller particle size leads to deposition via diffusion.TB bacteria residing alveolar macrophages can be targeted via various delivery systems with appropriate aerodynamic

properties which can deposit into the deep lung and be phagocytosed by alveolar macrophages. The appropriate particulate delivery system with correct size anywhere between 1 and 5 μm help to deposit them deposit into the terminal bronchioles and alveolar regions of the pulmonary bed (66). Formulations having aerodynamic diameters in the 1–3 μm range are proper for deep lung delivery. To deal with this challenge, continuous efforts are made to develop advanced particle-engineering technologies to obtain optimal therapeutic outcomes (67, 68). Within pulmonary drug delivery system development liposomes, microparticles, porous microspheres, porous nanoparticle aggregate particles (PNAPs), hybrid Nano in Micro (NIM) and solid lipid nanoparticles are being developed

Microparticles are delivery systems for inhalation or pulmonary route include the use of 1-5μm size inhalable particles to target drugs direcly to the lungs. Polymers like poly (lactic-coglycolic acid) is widely used polymer which FDA approved to form polymeric microspheres (69, 70). Other polymers like PLA(71), fucoidan (72) guar gum (73) can also be used to develop inhalable microsphere formulation for TB.

Porous nanoparticles aggregate particles(PNAP) are inhalable powder dosage forms comprised mainly of nanoparticles held together by physical forces such as van-der waal forces or may be aggregated using binders such as polymers, phospholipids or sugars like trehalose, lactose, mannitol. PNAP can be of two types based on their shape and internal structure: hollow nanoaggregates, and nanocomposites. Both types of particles can be prepared using spray drying process with slight modification.

Liposomes are sub-microscopic spherical vesicles composed of a phospholipid bilayer surrounding the aqueous core. Liposomes are most versatile and studied carriers for drug delivery which can be avidly taken up by the macrophages and control the release rate of drug. Pandey et al developed the rifampicin and isoniazid loaded multi-lamellar liposomes and tested their *in-vivo* efficacy on guinea pig model of TB and found that high concentration of drugs reached to the lungs(74). Chimote et al developed Isoniazid(INH) loaded surfactant liposomes which were 750nm in diameter and having encapsulation efficiency of 36.7±1.8% , demonstrated good anti-mycobacterial activity with improved stability(75). Oral delivery of liposomes leads to degradation of the liposomes due to intestinal lipases. Solid lipid nanoparticles are suspension. SLN loaded with different anti-TB drug was developed using emulsion solvent diffusion method. Sustained release of the drug was maintained up to 5 days in plasma and 7days in the organ(76).

1.9. Methods of preparation of Inhalable delivery systems

1.9.1. Double emulsion solvent evaporation method

In this method organic or oil phase is mixed with aqueous phase to from oil/water primary emulsion. This primary emulsion is again added to continuous phase to from water/oil/water secondary emulsion. The organic phase is completely evaporated and particles formed are collected either by centrifugation or filtration and then lyophilized.

1.9.2. Spray drying

Spray drying is the process which atomizes the polymeric solution/ emulsion/suspension to form a spray that immediately comes in contact with hot gas that converts droplets into solid nanoparticles/microparticles. The ratio of time required for droplet to dry and time required for particles to diffuse from surface to centre of the droplet is known as Peclet number (Pe). In case of hollow nanoaggregates the peclet number is large enough (>>1). Various researchers have optimized and described the different types of variables like inlet temperature, feed rate, droplet atomization efficiency, type of polymer, pH, feed concentration, surfactant concentration, addition of excipients and its concentration. Nanocomposites are also formed by binding of nanoparticles agglomeration with other excipients. The variables which are optimized in forming nanocomposites are inlet temperature, type of sugar, nanoparticles to excipient ratio, size of the nanoparticles required for different inlet temperature.

1.9.3. Spray freeze drying

During spray drying drugs/bioactive are exposed to harsh condition like thermal stress, high shear stress inside the nozzle, and high adsorption at the liquid-air interface of the spray solution. These harsh conditions can affect the active ingredient, polymer matrix and re-dispersibility of the particles formed. In spray freeze drying method the atomized droplets produced by spraying are frequently frozen in liquid nitrogen to form particles, which are finally lyophilized.

1.10. Aim of the research work

The prime objective is to explore the possibility of using Antimicrobial peptide (AMP) as a novel adjunct therapy to the chemotherapeutic regimen for tuberculosis. We proposed research is to develop and characterize Porous Nanoparticles aggregates (PNAP) containing Antimicrobial

peptide alone or/and in combination with half dose of anti-TB drugs to *Mycobacterium tuberculosis*-infected macrophages, and to investigate whether this targeted delivery system possesses the ability to reprogram the activation status of the infected macrophage, contributing to bacterial killing.

The sub objectives of this proposal are:

- To prepare and characterize inhalable PNAPs containing HDP alone/ and in combination with anti-tuberculosis drugs by industrially-scalable process and define their specifications.
- To compare PNAP delivery system with other inhalable drug delivery system to ensure its suitability.
- To evaluate the formulation to target *Mycobacterium tuberculosis* infected macrophages.
- To evaluate whether PNAPs would activate infected macrophages to mount a bactericidal innate response.
- To compare the efficacy of the PNAPs containing HDP and free drugs in *Mycobacterium tuberculosis* clearance from macrophages in infected cell lines and animal models.

Infection and replication of M.tb occurs preferentially inside alveolar macrophages merely ~10% of infected population develop active TB. For that reason, the relations among bacterial pathogenesis and the extent of the host immune response corroborate the outcome of the disease. The appearance of *M.tb* strains resistant to the few principal drugs that are at present existing makes it extremely not easy, to cure lethal infections. AMP produced by the immune system can help to oppose disease. Since AMP have broad range of antimicrobial activity a lot of AMP have good antibacterial activity beside a wide range of microbes and there is a less chance of pathogens acquiring resistance, they correspond to hopeful latest avenues for antibacterial drug development, especially for multidrug-resistant strains. To understand the important role AMP in the host defense against mycobacteria, it is important to delineate their capability to kill the mycobacterium inside lungs. It has been well accepted that AMP contributes significantly to host defence against intracellular pathogens. Endogenous AMP are well recognized components of the innate immunity and have been suggested to have an important role in TB infections. It has been reported that alterations in the production of these molecules increases susceptibility to infectious diseases, including TB. There are several reports of the immuno-modulatory effects of these peptides in TB and other models. Such peptides possibly inhibit microbial growth either directly through membrane/nucleic acid disruption or indirectly through immune-modulation to efficiently clear the infection.

It was of some interest, whether exogenously supplied AMP could kill the pathogen like mycobacterium. Endogenous AMP are well recognized components of the innate immunity and have been suggested to have an important role in TB infections. It has been reported that alterations in the production of these molecules increases susceptibility to infectious diseases, including TB.

However, due to lack of specificity toward target cells, short half-life, salt sensitivity, presence of proteases, poor pharmacokinetics and first pass metabolism, it is challenging to introduce AMP as such in biological system in a controlled manner by using conventional delivery systems. To kill the bacilli residing in alveolar macrophages, it is essential to deliver a sufficient amount of AMP into the lungs and alveolar macrophages where bug actually resides. The applicability of AMP as antimicrobial therapeutic agents for TB is hampered due to unavailability of appropriate delivery system which can carry and deliver required payload to AMP to the targeted site.

The purpose of present work is to elucidate and exploration of the novel role of AMP as

chemotherapeutic regimen for pulmonary TB. The aim of this thesis was to develop a novel particulate delivery system for peptide to improve the treatment of pulmonary disease, particularly TB. The inhalable DPI formulations possessed properties suitable for efficient deposition into the lungs, the ability to target macrophages and provide extended drug release. As it evade first-pass metabolism, smaller dose are required as compared to the oral route. Hence, it is hypothesized that intracellular delivery of AMP using inhalable Porous Nanoparticle-Aggregate Particles (PNAPs) that would provide benefits in the chemotherapy of TB. These microparticles may prove to be useful as adjunct therapy with co-administration with conventional DOTS therapy or with inhalable microparticles containing anti-TB drug.

In the current work we proposed and focus on the pharmaceutical product development of inhalable polymeric (*poly* Lactic acid-co-glycolic acid (PLGA), PLA and PCL) dry powder inhaler (DPI) formulations containing enough amount of selected individual synthesized AMP with or without incorporation of anti TB drug isoniazid (INH). Consequently, to characterize the AMP releasing formulations in terms of size, shape, peptide release pattern, aerodynamic properties, macrophage uptake and stability and *in vitro* efficacy of the formulations in Mtb infected macrophages in culture. With the understanding that exogenous AMP can also activate other innate bactericidal mechanisms of the host like apoptosis, reactive oxygen species, nitric oxide release, autophagy. We also proposed to study biochemical and cellular responses of AMP-releasing PNAPs on Mtb infected macrophages. Finally, we proposed to evaluate the efficacy of the selected formulations in therapeutic efficiency in Mtb infected laboratory animals.

In this present work, the proposed plan of work includes:

1. Peptide synthesis

2. Preformulation and Analytical methodology

3. Preparation and characterization of formulation

- Spray freeze drying
- Particle size
- Drug content analysis
- *In vitro* drug release studies
- Aerodynamic characterization
- Storage stability studies (as per ICH guidelines)

4. Efficacy studies on cells lines

- Cell uptake studies
- *In vitro* efficacy studies on macrophage cell lines
- Cytotoxicity studies

5. Therapeutic efficacy studies in TB infected animal model

- Respiratory infection of animals with virulent TB bacteria
- Multi dosing of porous nanoparticle aggregate particles
- Necropsy, tissue processing and histopathology
- Enumeration of viable bacilli in animal organs

6. Biochemical and cellular responses on TB infected macrophages

- Membranolysis study
- Phagosome-lysosome fusion studies
- Apoptosis studies
- ROS estimation

The solid- phase peptide synthesis method is one of the essential tools for the synthesis of various types of peptides. It has been the method of choice to generate the biologically active peptides. The chemically synthesized peptides help to study various mechanisms including hormone action, enzyme-substrate interaction, antigen-antibody reaction, protein-DNA interaction and other various effects. Another method of peptide synthesis is the classical solution phase peptide synthesis method developed by Emil Fisher and Curtius in the early phase of the last century. The difference between solution phase and solid phase peptide synthesis is lies in the coupling reaction that is carried out in solution and progress of the reaction is monitored by simple techniques like thin layer chromatography (TLC). After every step of synthesis, purity of the product is determined, so principally this is the unsurpassed means of obtaining marked peptide in homogenous state (77). The main shortcoming of classical solution phase peptide synthesis is that, it is a tedious and lengthy process; and other restriction was the insolubility of the peptide chain in solvents engaged in development.

The notion of solid based polypeptide synthesis was given by R. B. Merrifield in 1963, which helped to conquer numerous of preparative problems encountered in the previous conventional method. The Merrifield method with a number of methodological changes still enjoys the method of selection for the synthesizing of peptides or proteins(78). The basic idea of solid phase approach involves the covalent anchoring of the C-terminal wing peptide chain to an insoluble resin support. This technique helps the removal of excess reagent by simple filtration and repetitive washings with suitable solvents. The target peptide-sequence is formed in a stepwise manner from the C-terminal to the N-terminal using activated Nu-protected amino acids. Usually large molar excess of the soluble reagents is often used to ascertain the completion of the reaction at every stage of the multistep synthesis. Once the chain assembly is completed, the crude peptide is cleaved from the support by various techniques depending upon the type of anchoring between the polymer support and the peptide sequence. In Merrifield's technique, the C-terminal amino acid with a temporary N"-protecting group t-butyloxycarbonyl (Boc) is attached to the chloromethyl resin by an ester linkage. The temporary amino protecting group is removed under acidic condition using 1M HCI in glacial acetic acid, 4N HCI in trioxane or with 30% TFA in Dichoromethane (DCM). Although, above methodology is an excellent way to prepare polypeptides, the synthesis using Fmoc-amino acids developed by Sheppard et al. is widely accepted, as it avoids the repeated Nu-deprotection with trifluoroacetic acid(TFA) during

peptide chain elongation. However, Fmoc-method is also based on the same principle as Merrifield's method but the temporary Nu-deprotection is carried out.

The solid phase peptide synthesis offers the following advantages over the classical solution phase peptide synthesis(79). The peptide is synthesized with its C-terminus is covalently attached to an insoluble polymeric support. This permits easy separation of the byproducts or constituent amino acids from the growing peptide. All reactions can be driven to completion by using excess of the soluble reagents, which results in the high yield, and purity of the target peptides. No loss occurs because growing peptide is released by the polymer in a single reaction vessel throughout the synthesis. Increases solvation and decreases aggregation of the intermediate products. The physical operations of the heterogeneous system are simple, rapid and amenable to automation. Furthermore, the spent resin can be recycled.

2.1. Experimental

This study involved the synthesis of short AMP peptides using solid phase peptide synthesis method, purification of peptides by RP-HPLC and their characterization using MALDI-TOF.

2.1.1. Materials

Chemicals

Fmoc-Rink amide resin, and all the Fmoc amino acids were procured from Novabiochem, India. Di-methyl formamide (DMF), Acetone, Methanol, trifluoro acetic acid (TFA), anisole, thioanisole, Ether and other reagents used in the study were of analytical grade purchased from Merck India. Purified water from a Milli Q (Millipore corp.) water purification system was used.

Bacteria

M. tuberculosis H37Rv [*M.tb* H37Rv Code: PN7 was procured from All India Institute of Medical Science (AIIMS)] were grown in Sauton's medium supplemented with 0.2% glycerol, 0.05% Tween 80, and 10% Oleic acid-Albumin-dextrose-Catalase (OADC) enrichment (BD, USA). Colony forming units (CFU) in dilutions were estimated by plating dilutions on Middlebrook 7H11 agar supplemented with 0.5% glycerol and 10% OADC. Plates were incubated at 37°C, 75% RH for up to 4 weeks. The absorbance at 600 nm correlated with CFU obtained on agar plates after serial dilutions and was used to generate a standard plot for routine estimation of CFU

2.2. Solid Phase Peptide synthesis

Synthesis of all the AMP were carried-out by Fmoc Solid Phase Peptide Synthesis (SPPS) method using Liberty-blue^{TM} automated microwave peptide synthesizer (CEM Corporation, NC, USA)(80). Fmoc-Rink amide resin was utilized as the solid support (100-200 in mesh size). De-protection of Fmoc-amino acids was done using 20% piperazine solution in DMF (initially dissolved in ethanol and than DMF was added to with continuous vortexing) and cleavage of the crude peptide from resins was performed by cleaving it from the support resin using a cocktail solution of tri-fluoro-acetic acid (90%), thio-anisole (5%), ethane-diol (3%), and anisole (2%) for 3h. the optimum cleavage method depends on individual amino acid and sequence. TFA acts as cleaver and reagents like ethane diol act as acid scavengers which helps in preventing acid catalysed oxidation of amino acids like tryptophan and methionine etc. This procedure was followed by precipitation with cold diethyl ether. Crude peptide was purified by semi-preparative reversed-phase high-performance liquid chromatography (Waters Corporation, USA) on a C_{18} column with an acetonitrile-water gradient. The mobile phase consisted of acetonitrile (ACN) and de-ionised water containing 0.1% TFA which was used as a gradient program as follows: Flow rate of 5 ml/min was linearly increased from 10 to 45% of Solvent-A (Acetonitrile); while 90–55% Of Solvent B (water containing 0.1% TFA) was used. Purity of lyophilized peptides was confirmed by analytical RP-HPLC [Waters Spherisorb ODS1, C18, (250×4.6 mm, 5µm)] and MALDI-TOF (Applied bio-systems 4700 proteomics analyser, MA USA)(81)

Table 2.1. Selected and synthesized antimicrobial peptide

Sno.	Selected Anti-Microbial Peptides	Sequence
1	LLKK-18	KEFKRIVKRIKKFLRKLV
2	IDR-1018	VRLIVAVRIWRR-NH2
3	HHC-8	KIWWWWRKR
4	HHC-10	KRWWKWWRR
5	Temporin-B	LLPIVGNLLKSLL
6	Indolicidin	ILPWKWPWWPWRR
7	L5k5W	KKLLLKWLKKLL
8	Aurin 1.1	GLFDIIKKIAESI
9	K4 peptide	KKKKPLFGLFFGLF
10	α-helical peptide	$M(LLKK)_2M$
11	UB_2	STLHLVLRLRGG
12	MIAP	GIGKFLKSKGKFGKA
13	D-LFIN 17-30	FKCRRWQWRMKKLG

2.3. Characterization

2.3.1. Circular Dichroism (CD)

Secondary structure of the synthesized peptides was evaluated by using a spectropolarimeter (JASCO J-1500, JASCO international, Tokyo Japan). The CD spectra of each sample were recorded spectro-polarimeter equipped with a temperature-controlling unit, over a range of 180–260 nm using a quartz cuvette of 0.2 cm path length. CD data represent average value of three separate recording with three scans per sample at a scan rate of 1 nm/sec. The individual scans were corrected by subtracting with the blank. All CD measurements are reported as ellipticities.

2.4. Minimum inhibitory concentration (MIC) estimation

Broth micro dilution method (82) was utilized for estimation of MIC of peptides against mycobacterium. This assays was performed using stock solutions of all the synthesized peptides diluted serially from 100 to 0.78µg/ml to a final volume of 100 µl. Bacterial suspension (2×10^5 CFU/mL, 100µL) in Middlebrook media was added to 96 well cell-culture plate and then different concentrations of AMP was added to the designated wells. The bacterial growth was estimated by measuring absorbance at different time intervals (3, 6, 12, 24, 48 and 96h) at 37°C.

The optical density (OD) of each well was measured at 600 nm in an ELISA reader (BioRad, model 450, Hercules, CA, USA). We used pure broth-medium as negative control and INH treated bacteria as positive-control in designated wells. MIC values were calculated from the dose-response curve. The minimum AMP concentration that showed 50% inhibition of visible growth of *M.tb* considered as MIC_{50}. This experiment was repeated thrice to obtain mean MIC values.

2.5. Results and Discussion

2.5.1. Peptide synthesis and purity

The crude peptide showed the yield of ≥40% which was slightly sticky in nature. The peptide purity (>91%) was confirmed by analytical RP-HPLC and the masses were confirmed by MALDI-TOF. Obtained peptide was purified by preparative reversed-phase high-performance liquid chromatography (Waters Corporation, USA) on a C_{18} column with an acetonitrile-water gradient. The collected liquid extract was lyophilized for 48 hours. Purity of lyophilized peptides was confirmed by analytical RP-HPLC [Waters Spherisorb ODS1, C18, (250×4.6 mm, 5µm)]. Single peak in analytical HPLC chromatogram indicated high purity of synthesized all the peptides (>95%) (Figure-2.1).

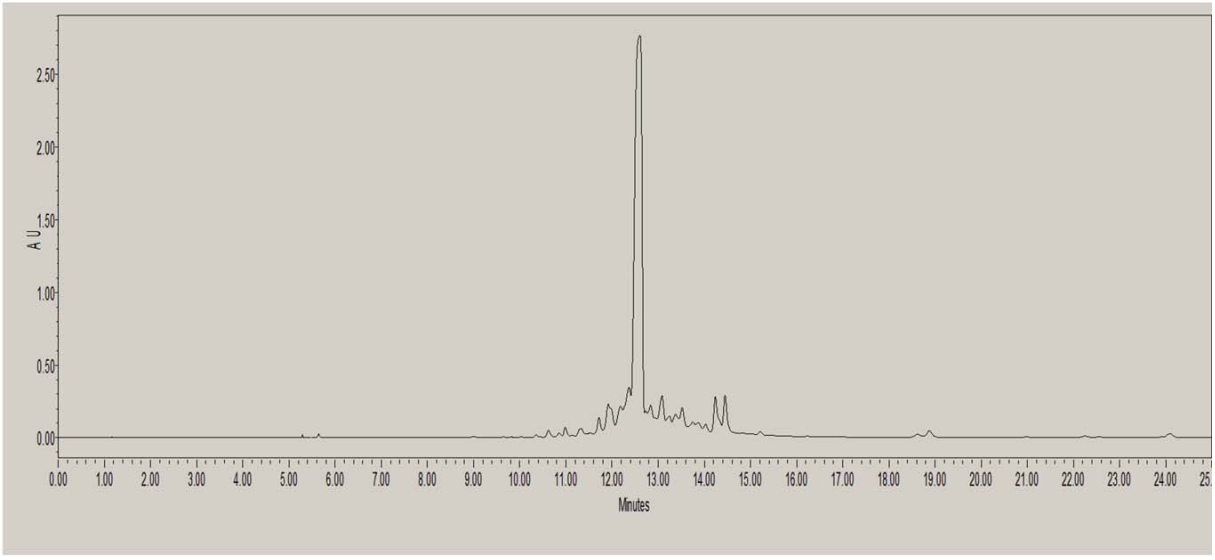

Figure 2.1: Chromatogram of the synthesized antimicrobial Peptide (Model peptide-MIAP) showing the purity of the peptides

Mass spectrum display the purity and expected molecular weight of the synthetically designed peptides UB2, K4 and Aurien1.2, indolicidin, IDR-1018 and MIAP are shown in Figure 2.2. The mass of the purified peptides determined by MALDI-TOF analysis corresponded to the anticipated theoretical-mass of peptides (Ub2:1320.68; K4:1668.91; Aurien1.2:1479.72, indolicidin: 1906.9, IDR-1018: 1535.9, MIAP: 1564.81).

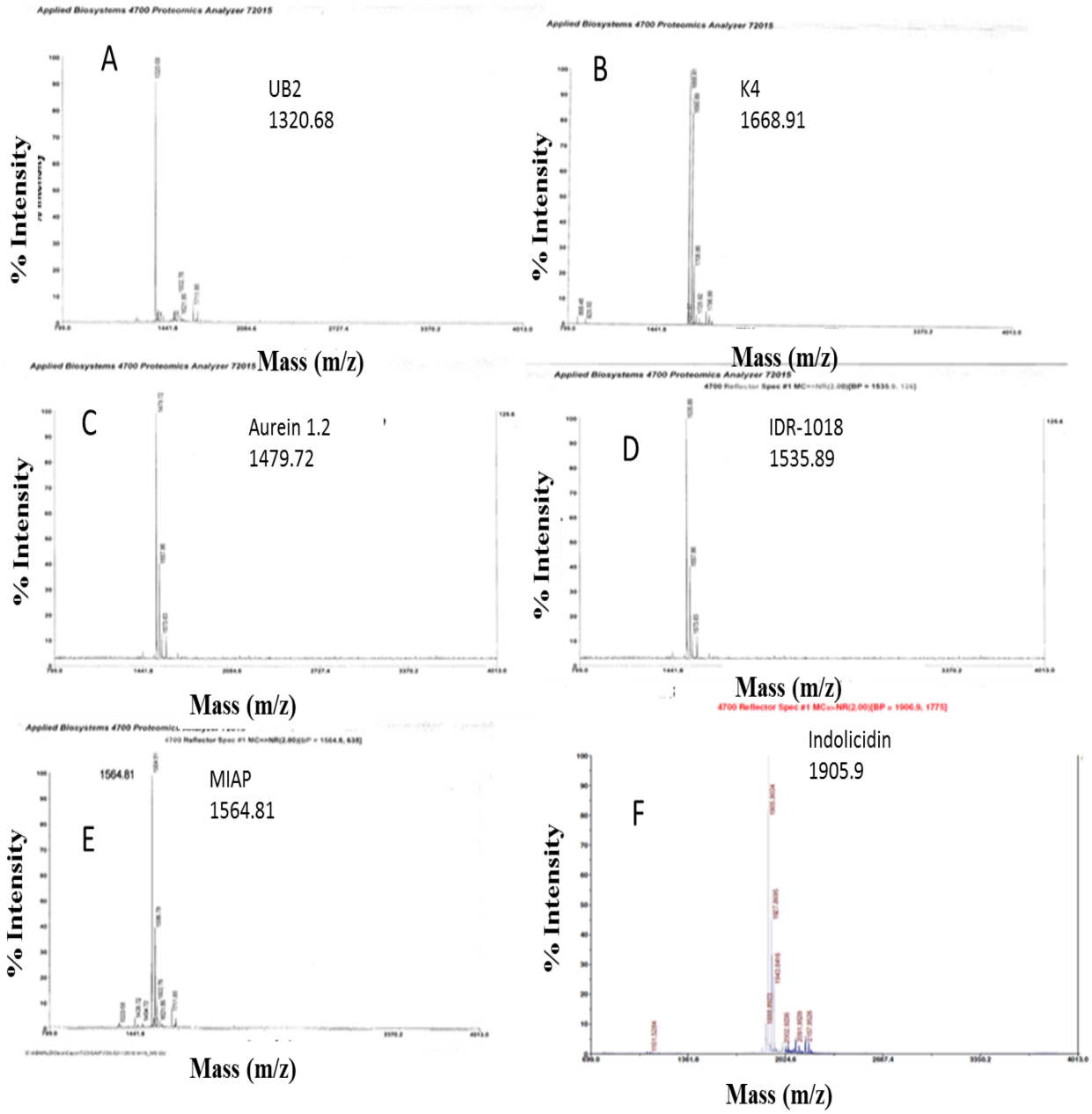

Figure 2.2: Identification of selected synthesized peptides MALDI-TOF mass spectrum presenting the predictable molecular weight

2.5.2. Minimum inhibition concentration (MIC)

Direct anti-*M.tb* activity of AMP was evaluated using liquid micro-dilution method and compared with their potential to kill mycobacteria. The MIC_{50} values of the selected AMP against M.tb are shown in Table-1. This study confirmed the mycobactericidal property of given peptides and their potency of activity was in the order:

LLKK-18< HHC-8< Temporin-B <D-LFIN 17-30< L5k5W< $M(LLKK)_2M$< Aurin 1.1< MIAP< K4 peptide< Indolicidin< HHC-10< UB_2< IDR-1018.

Comparing the activity of these selected antimicrobial peptides, MIAP, Aurin1.2, K4, Indolicidin, Ub2, and IDR-1018 demonstrated significant bactericidal activity with lower MIC-values. Further, formulation development, *in-vitro* and *in-vivo* efficacy studies were carried out by using these screened peptides.

Table 1.2. Synthesized antimicrobial peptide with their MIC values

Sno.	Selected Anti-Microbial Peptides	Sequence	MIC
1	LLKK-18	KEFKRIVKRIKKFLRKLV	121.76±6.8
2	IDR-1018	VRLIVAVRIWRR-NH2	15.4 ±1.2
3	HHC-8	KIWWWWRKR	118.43±7.2
4	HHC-10	KRWWKWWRR	21.42±2.5
5	Temporin-B	LLPIVGNLLKSLL	98.71±4.3
6	Indolicidin	ILPWKWPWWPWRR	28.25±5.1
7	L5k5W	KKLLLKWLKKLL	79.87±8.9
8	Aurin 1.2	GLFDIIKKIAESI	43.9±4.7
9	K4 peptide	KKKKPLFGLFFGLF	29.6±3.1
10	α-helical peptide	$M(LLKK)_2M$	62.5±6.2
11	Ub_2	STLHLVLRLRGG	17.4±1.5
12	MIAP	GIGKFLKSKGKFGKA	30±2.5
13	D-LFIN 17-30	FKCRRWQWRMKKLG	88.62±5.1

2.6 Conclusion

AMP are promising field for the development of antimicrobial agents for TB, mainly due to the fact that these peptides are fast acting and have no cross reactivity with current anti TB and anti HIV drugs. Thirteen AMP were synthesized for evaluating the anti-Mtb efficacy. *In vitro* direct bactericidal activity of all the synthesized peptides were evaluated which revealed that some of the peptides (MIAP, Aurin1.2, K4, Indolicidin, Ub2, and IDR-1018) were showing good bactericidal response. The developed peptides may have potential to use as anti-TB agents against the drug sensitive as well as resistant strains because due to their non-specific mechanism of action. Further, studies were carried out with the selected six peptides having lower MIC values.

This chapter explains the development and validation of sensitive chromatographic and spectrophotometric methods to quantify content, release and stability of the anti-TB drugs and AMP present in various formulations. Precise HPLC methods for Rifampicin and Isoniazid (INH) determination were developed. Spectrophotometric methods (UV-Vis) were developed for AMP used in the study, i.e. IDR-1018, indolicidin, UB2, K4, Aurin1.1, and MIAP. HPLC methods were not deemed suitable for AMP, since the time essential for sample preparation was too extensive to avoid deprivation in an aqueous and mildly acidic situation. Analytical methods were validated as per ICH guidelines in terms of system sensitivity, reproducibility, recovery from matrix, intra- and inter-batch variations in accuracy and precision.

3.1. Experimental

This study encompasses the individual isocratic RP-HPLC method for the analysis of RIF & INH and UV-Vis spectrophotometer method for AMP incorporated in particle matrix.

The experimental work is discussed under the following heads:

3.1.1 Material

3.1.2 Analytical method development and validation

(A) HPLC Method for Rifampicin (RIF)

(B) HPLC Method for Isoniazid(INH)

(C) Spectrophotometric method for different AMP

3.1.1. Materials

3.1.1.1 Chemicals

Potassium dihydrogen orthophosphate, ortho-Phosphoric acid and Triethylamine were procured from Merck, India. Acetonitrile (ACN), Dichloromethane (DCM), was purchased from Merck, (Bangalore, India). Triple filtered water was used for all buffer preparations. A 0.22 µm PVDF membrane filter of Pall Corporation was used for the filtration of buffers. Parafilm was purchased from American Can Company (Neenah, USA) was used for sealing tubes. All reagents and solvents used were of analytical grade.

3.1.1.2. HPLC instrumentation

The HPLC system consist of waters 1525 binary HPLC pump with autosampler 2707, injector with a 20 µL fixed loop and a 2998 PDA detector, 2424 ELS detector, waters 2475 fluorescence detector . HPLC separation was performed on Agilent c-18 column (particle size 5 µm; 4.6 x 250mm spherisorb).The HPLC system was equilibrated for approximately 30 min before commencement of analysis and chromatography was carried out at ambient temperature. Data was acquired and processed using Empower 3.

3.1.1.3. HPLC method for Rifampicin (RIF)

Rifampicin is a semi-synthetic anti-TB agent. A validated reverse phase HPLC (RP-HPLC) method was used for its determination in polymeric formulations (83). In this isocratic chromatographic method, mixture of phosphate buffer and ACN is used as mobile phase and drug was analyzed at 275 nm using UV detector. Phosphate buffer (50 *mM*) was prepared by dissolving KH_2PO_4 in filtered water. The buffer was filtered through a 0.22 µm membrane filter under vacuum using a Millipore pump. The mobile phase was a mixture of acetonitrile and phosphate buffer in ratio of 55:45. Method was isocratic and chromatography was performed at 25°C at a flow rate of 1 mL/min.

3.1.1.4. HPLC method for Isoniazid (INH)

INH is also a common drug used alone or in combination for treatment of TB. RP-HPLC is performed using mixture of Triethylamine (TEA) with ACN as the mobile phase and measuring absorbance at 262 nm. The mobile phase was a mixture of Triethylamine (TEA)-buffer and ACN in ratio of 97:3. This solves the problem of peak tailing commonly observed for INH. All the components were filtered through 0.22 µm filter using Millipore filter assembly and degassed by sonication before use. Method was isocratic and chromatography was performed at 25°C at a flow rate of 1 mL/min. A reversed phase C_{18} column was used. Injection volume was 20 µL.

3.1.1.5. Spectrophotometer Instrumentation

A UV-Vis spectrophotometer (Perkin Elmer AX-1, USA) with 1cm matched quartz cuvette was used for the estimation (84).

3.1.1.6. Spectrophotometric method for AMP

The objective of the present study was to develop simple, precise, accurate and validated, analytical methods for the estimation of AMP in pure form and in pharmaceutical formulations. The developed analytical method was validated as per the ICH guidelines. Stock solution (100 µg/mL) was prepared by dissolving 10 mg of AMP in 100 mL of PBS. Stock solution was used to prepare working solution, which was further utilized for constructing calibration standard curve. A 10 µg/mL solution was prepared by dilution from stock solution for determination of wavelength maxima. This solution was scanned in the wavelength range of 190-500 nm. From the spectra of drug, λ_{max} was selected for the formation of simultaneous equation.

3.2. Results

3.2.1. Method development: Rifampicin

The method of Rif was specific and there was no interference in the region of rifampicin. The extraction procedure and chromatographic conditions yielded a clean single chromatogram for RFB. The retention time in proposed method is found to be 6.5 minutes (Figure 3.1).

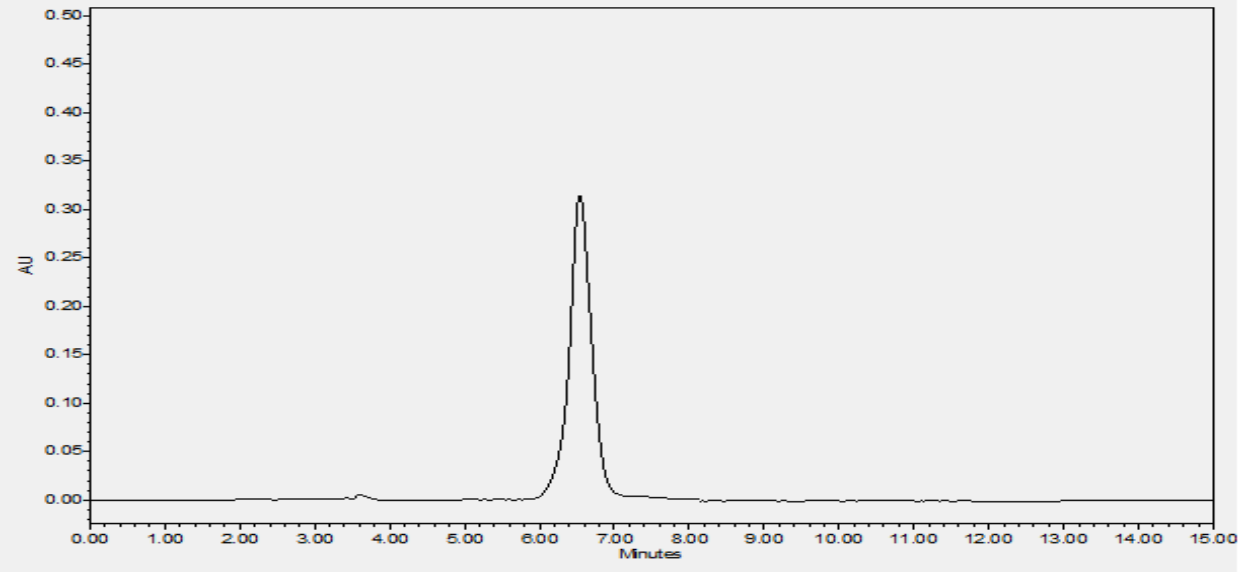

Figure 3.1 Typical chromatograms of Rifampicin

3.2.2. Method development: INH

No interference was observed in the region of INH after injecting processed blank sample obtained from mixture of blank MP and INH. This indicated that the method is specific for INH. The extraction procedure and chromatographic conditions yielded a clean chromatogram. The retention time in the proposed method is 6.8 min .

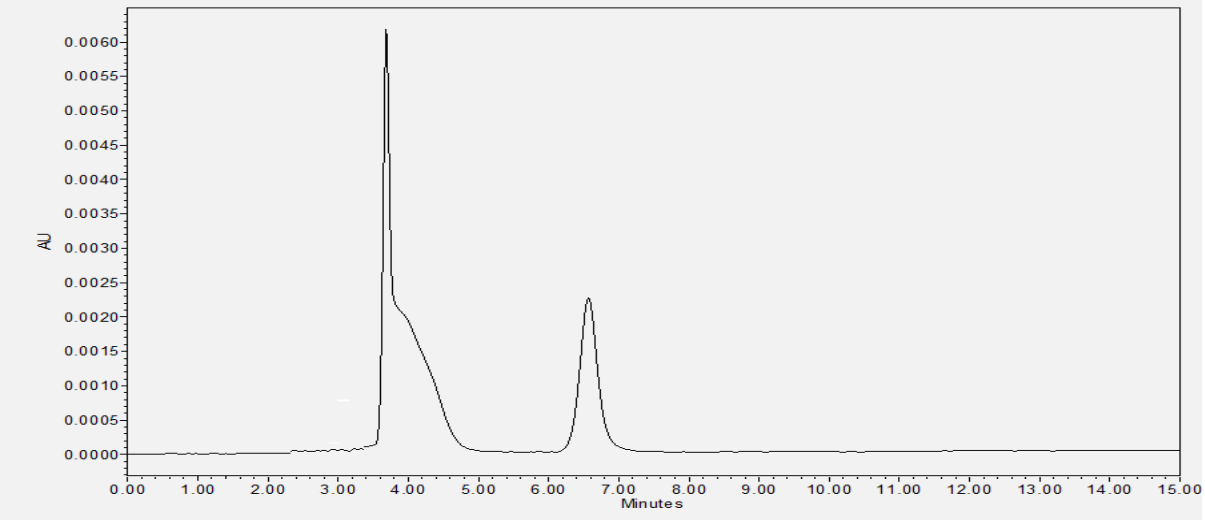

Figure 3.2 Typical chromatograms of Isoniazid

3.3. Spectroscopic method for AMP

3.3.1. Specificity

To ensure the interference of blank at the working wavelength, the blank solution was scanned from 200-600 nm. No interference was observed at the working wavelength of 217 nm, indicating that the UV-Vis spectroscopic method presented in this study is specific for IDR-1018.

3.3.2. Linearity

An eight point standard curve was obtained in the concentration range of 2-16 µg/mL (Figure 3.3). The linearity of this method was evaluated by linear regression analysis. Slope, intercept and correlation coefficient (r^2) of the standard curve are given in Table 3.1. Beer's law is obeyed over the concentration range 2-16 µg/mL for all AMP concentrations.

Table 3.1: Linearity response of synthesized peptides

Sl. No.	Concentration(µg/mL)	Absorbance of IDR-1018 at 217nm	Absorbance of MIAP peptide	Absorbance of UB2 peptide	Absorbance of K4 peptide	Absorbance of Indolicidin peptide	Absorbance of Aurein 1.2 peptide
1	2	0.071333	0.055667	0.059333	0.070667	0.072333	0.064667
2	4	0.127	0.123333	0.121333	0.129333	0.129333	0.132
3	6	0.239333	0.237333	0.233333	0.241	0.239	0.240333
4	8	0.356667	0.355667	0.350333	0.355	0.354667	0.353333
5	10	0.570333	0.561333	0.567667	0.572	0.569333	0.568
6	12	0.745333	0.747667	0.746	0.744667	0.747	0.743333
7	14	0.864667	0.874	0.874667	0.870667	0.873	0.873
8	16	0.993	0.991667	0.993333	0.988333	0.991667	0.991
9	Slope	0.0707	0.0717	0.0718	0.0706	0.0708	0.0709
10	Intercept	0.14	0.1518	0.1528	0.1388	0.14	0.1425
11	R^2	0.9842	0.9859	0.9843	0.984	0.9833	0.9848

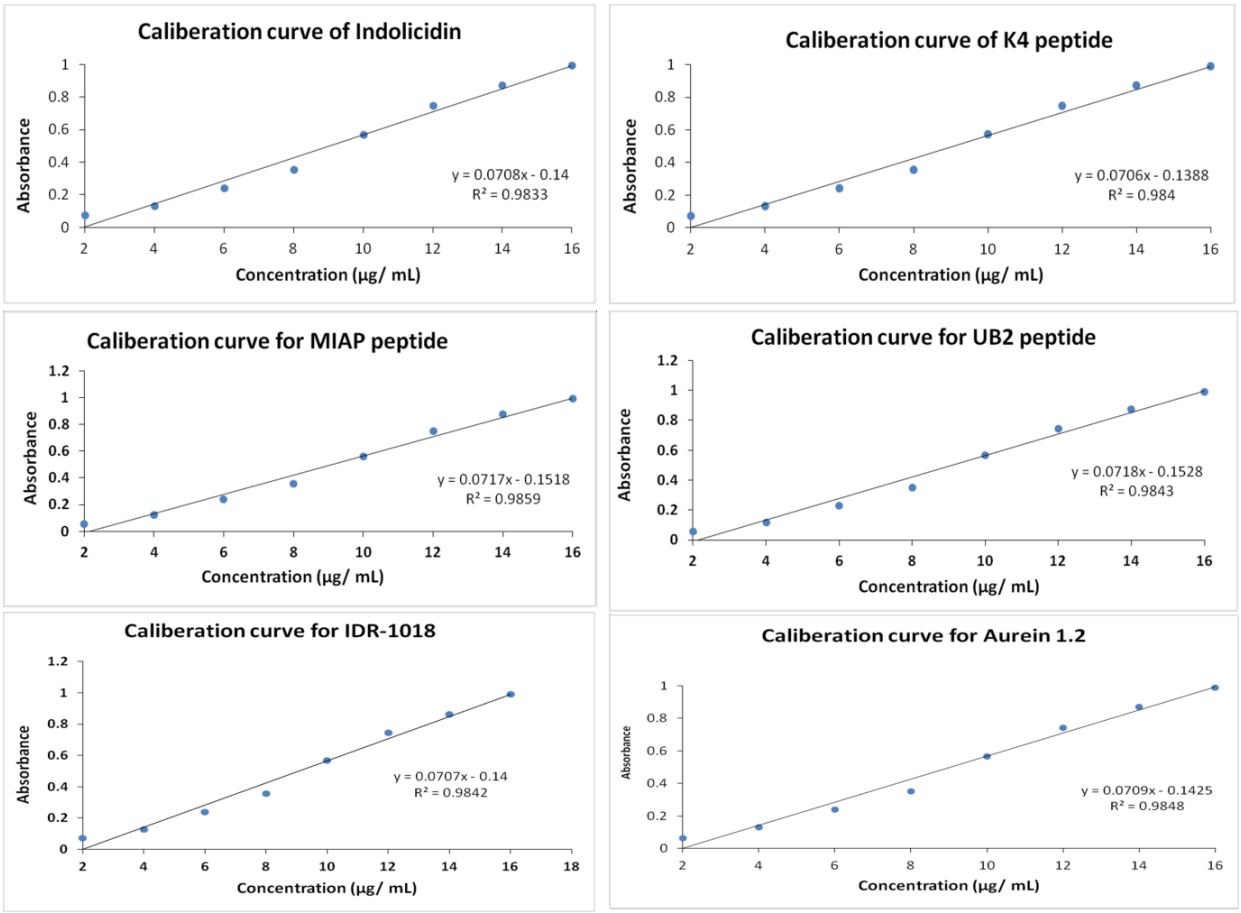

Figure 3.3 Calibration curve of synthesized peptides. Results are means (n = 3, ±standard deviation).

3.4. Conclusion

According to the results of this study, the UV-Vis spectrophotometric method can be considered as an effective and accurate way to determine the concentrations of Indolicidin, MIAP. K4, Aurein 1.2, UB2 and IDR-1018 in MP. It was found that only one peak is observed at 217 nm for IDR-1018 and at 218 nm for Indolicidin and obeyed Beer's law over the concentration range 2-16 μg/mL The mean slope and intercept values are within the 95 % confidence it can be concluded that from the data obtained that analytical methods can be accepted.

Present work was aimed to prepare and evaluate the inhalable polymeric Porous Nano Particles Aggregates Particles (PNAP) formulations for efficient delivery of antimicrobial Peptides (AMP) with or without anti-TB drugs and compare these novel formulations with other similar inhalable formulations include microspheres, hybrid nano-in-Micro system and mucus penetrating microspheres. Dry powder inhalable PNAP particles having respirable size range (1-6 μm), good encapsulation efficiency, regular spherical morphology and high product yield were developed. Micron sized inhalable particles with nano-scale physiognomies were designed to improve delivery of AMP inside lungs and enhance their stability.

To obtain optimal aerodynamic properties and maximum deposition into lungs, AMP loaded nanoparticles of size around ~300 nm were developed by double emulsion solvent evaporation method and further processed into porous micron-sized inhalable nano-assemblies i.e. Porous Nanoparticle Aggregate Particles (PNAP) (~1-6 μm) using spray freeze dying (SFD) technique. These particles were also optimized for aerodynamic properties for deposition in respiratory tract, using a cascade impactor (Anderson cascade impactor).

The developed particles were characterized for following parameters : Particle size distribution(PSD) were measured by the dynamic laser scattering(DLS) technique, morphology and shape using scanning electron microscopy(SEM), *in vitro* drug release by dialysis membrane method, and stability study of the released AMP using circular dichroism(CD). The specific surface areas of PNAP and microspheres was evaluated by the Brunauer Emmett Teller (BET) multipoint technique and the pore size distribution was calculated using Barrett-Joyner-Halenda (BJH) method (Autosorb IQ2, Quantachrome instrument, USA).

4.1. Experimental

The present study includes the preparation and characterization of AMP loaded formulations with and without anti-TB drugs under the following parameters:

4.1.1. Materials

Biodegradable 50:50 poly (D, L-lactic acid) (PLGA), Mw=7000 17,000, acid terminated with an intrinsic viscosity of 0.24 dl/g, Polyvinyl alcohol (PVA), Isoniazid (INH) and Rifampicin (RIF) were purchased from sigma Aldrich (St Louis, USA), AMP were synthesized using solid phase peptide synthesizer. Dichoromethane, Acetone, Methanol, and other chemicals and solvents used in the experiments were obtained from Sigma Aldrich, India. Purified water from a Milli Q (Millipore corp., USA) water purification system was used. All reagents and solvents used were of AnalaR grade.

4.1.2. Preparation of inhalable formulation for amp delivery with or without anti-tb drugs

4.1.2.1. Microspheres (MS)

PLA-MS was prepared using w1/o/w2 double emulsion solvent evaporation method. Briefly, 500mg of polymer was dissolved in organic solvent mixture of acetone/chloroform (3:1) and then freshly prepared aqueous solution of either Isoniazid (INH) or individual antimicrobial peptides (AMP) was added drop wise to the polymer solution with intermittent sonication using probe-sonicator in ice bath (10 pulse of 5 s each, 20% amplitude) to obtain primary emulsion. In the microspheres containing rifampicin, the drug was added in organic phase. The primary emulsion was added drop-wise to a beaker containing 40 ml of polyvinyl alcohol (PVA) solution (1%, w/v) and re-emulsified using magnetic stirrer for overnight at room temperature under fume hood for evaporation of organic solvent. The particles were harvested by centrifuging at 10,000 rpm for 15 min, washed three times with milliQ water and lyophilized for 48 h to get freely flowing MS. Blank MS were also prepared without AMP or drugs. The various parameters that influence the ultimate morphology of PLA-MS

4.1.2.2. Porous microspheres

Porous PLA-MS of different pore size and topology were prepared using w1/o/w2 double emulsion solvent evaporation method. Briefly, 500mg of polymer was dissolved in organic solvent mixture of acetone/chloroform (3:1) and then freshly prepared aqueous solution of porogen/osmogen was added drop wise to the polymer solution with intermittent sonication using probe-sonicator in ice bath (10 pulse of 5 s each, 20% amplitude) to obtain primary emulsion. A wide range of porogens/osmogens like hydrogen peroxide, sodium bicarbonate, sodium chloride, polyethylene glycol, sucrose, ammonium bicarbonate and phosphate buffer saline (PBS) were utilized for fabricating and tuning the size of the pores, surface morphology and internal structure of micro-matrix. The concentration of porogen/osmogen was specifically and precisely optimized, depending upon the prerequisite pore size in MS. The primary emulsion was added drop-wise to a beaker containing 40 ml of polyvinyl alcohol (PVA) solution (1%, w/v) and re-emulsified using magnetic stirrer for overnight at room temperature under fume hood for evaporation of organic solvent. The particles were harvested by centrifuging at 10,000 rpm for 15 min, washed three times with milliQ water and lyophilized for 48 h to get freely flowing porous MS. The various parameters that influence the ultimate morphology of PLA-MS were individually evaluated for the formation of pores and morphology(85, 86).

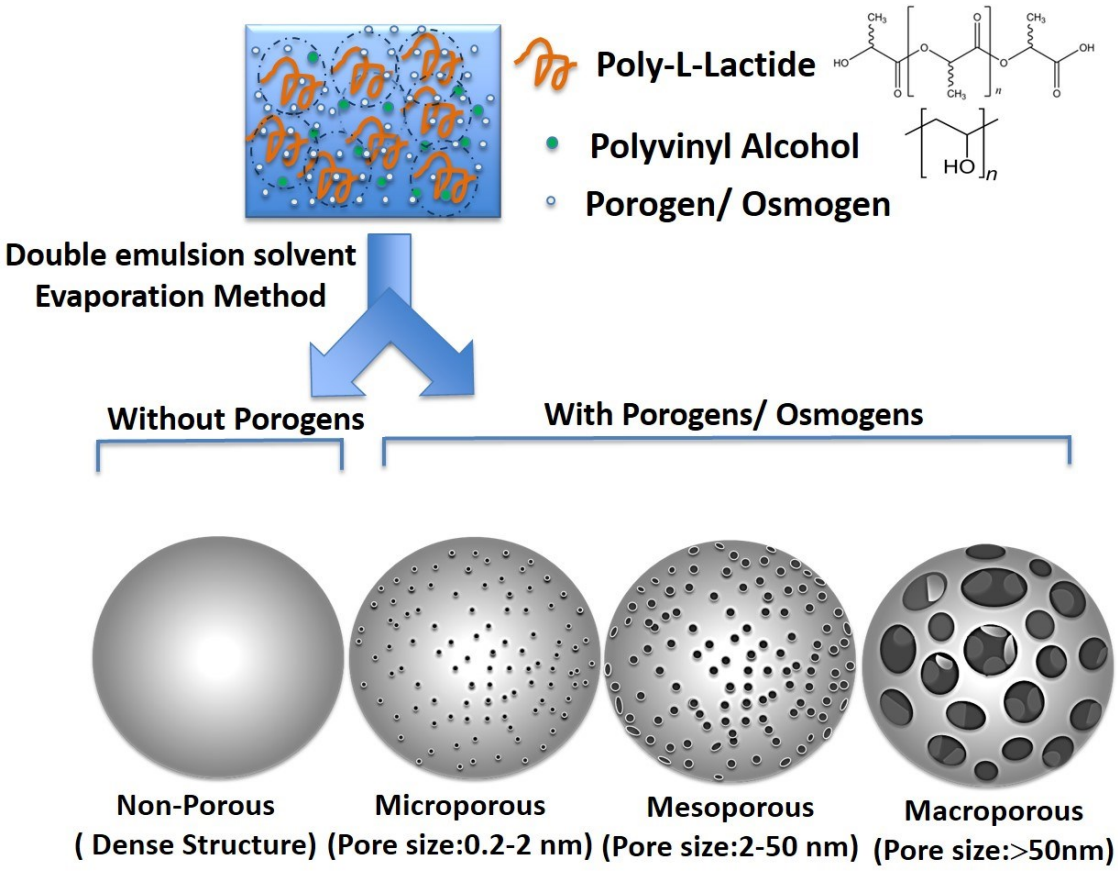

Figure 4.1. Schematic illustration of the fabrication procedure of porous PLA-MS.

4.1.2.3. Mucus penetrating Microparticles

- **Preparation of porous microparticles**

Microspheres were prepared using a double emulsion-solvent evaporation method. Briefly 50 mg peptide was dissolved in 100 µl of Phosphate Buffer Saline(PBS). PLGA was dissolved in 5 mL methylene chloride at 500 mg/ml concentration. Polymer and peptide solutions were mixed and sonicated at 10,000 rpm for 1 min in the ice bath using a sonicator to form W1/O emulsion. The freshly prepared aqueous solution of porogen (2%, sodium bicarbonate) was added drop wise to the polymer solution with intermittent sonication using probe-sonicator. The primary emulsion was added dropwise to PVA solution (2%, 30 ml) with continous stirring to form w/o/w emulsion. After evaporation of methylene chloride (6 h), the microspheres were collected by sieve and washed repeatedly with deionized water. Finally, the microspheres were lyophilized

for 24 h and stored in a desiccator at 4 °C before further investigation. Similarly, Isoniazid loaded microparticles were prepared.

- **N-acetylcysteine (NAC)-functionalized coating of PLGA MP**

Coating of porous PLGA MP with N-acetylcysteine(NAC) was optimized using different NAC concentrations, like 5, 10 and 25 mg/mL. PLGA MPs were incubated with a solution of 0.2M 1-Ethyl-3-[3-dimethylaminopropyl] carbodiimide hydrochloride) (EDC) and different NAC concentrations, in 0.1 M (N-morpholino)ethanesulfonic acid (MES; Sigma-Aldrich) buffer for 2 h, at 37 °C and 100 rpm. NAC coated PLGA MPs were centrifuged at 10000 rpm and then rinsed twice and lyophilized, were stored in a desiccator kept in the refrigerator at 4 °C until further use.

4.1.2.4. Porous nanoparticles aggregate particles (PNAPs)

- **AMP loaded nanoparticles**

Polymeric [poly(lactic-co-glycolic acid), PLGA, 50:50) microspheres loaded with individual AMP (MIAP, Aurin1.2, K4, Indolicidin, UB2, IDR-1018) were prepared by double emulsion solvent evaporation method with minor modifications(87) Briefly, 200mg PLGA was dissolved in 5ml dichloromethane (organic phase) and an aqueous solution (0.5ml) containing different types of AMP (5mg) was prepared separately (inner aqueous phase). Primary emulsion (w/o) was made by adding aqueous peptide solution into organic polymer phase with repeated episodes of sonication (5s each). The resultant solution was further added dropwise to an aqueous solution of 1% (w/v) poly vinyl Alcohol (PVA) with continuous mechanical stirring. The emulsion was stirred with a mechanical stirrer at 200rpm for 12h to ensure complete solvent evaporation of the organic solvent. MS formed were separated by centrifugation (10,000×g for 20min at 4°C) and then washed to remove excess of PVA. Blank-PLGA-NP were also prepared with the same procedure except for the addition of peptides during the preparation of formulation. All the nanoparticles were then lyophilized for 48h and stored in a desiccators at 4°C until further use.

- **Processing of Nanoparticles into Porous nanoparticles aggregate particles (PNAPs)**

To obtain optimal aerodynamic properties and maximum deposition into lungs, NP (~300 nm) were further processed into porous micron-sized inhalable nano-assemblies i.e. Porous Nanoparticle Aggregate Particles (PNAP) (~1-6 μm) using spray freeze dying (SFD) technique. Freshly prepared AMP-NP/drug-NP (20 mg/ml) were suspended in mannitol (10

mg/ml) solution and sprayed into liquid nitrogen using 0.7mm spray dryer nozzle (Techno Search instruments, Mumbai, India). Liquid nitrogen was kept in 5 L closed container which was continuously agitated using magnetic stirring (Fig. 1). In spray freeze drying method the atomized droplets produced by spraying are frequently frozen in liquid nitrogen(88). Finally the particles are lyophilized to produce the porous particles with inhalable characteristics(89, 90). Volume particle diameter of blank and AMP/drug loaded PNAP was measured by a Mastersizer 2000 (Malvern instruments, UK). Surface morphology of the PNAP along with porosity was studied using scanning electron microscopy (JEOL, JSM-IT300, Japan). The specific surface areas of PNAP were evaluated by the Brunauer Emmett Teller (BET) multipoint technique and the pore size distribution was calculated using Barrett-Joyner-Halenda (BJH) method (Autosorb IQ2, Quantachrome instrument, USA). The release kinetics and stability of AMP/drug was evaluated in simulated lung pH conditions.

4.1.3. Physical characterization of formulations

4.1.3.1. *Yield*

The production yields of particles of various formulations were calculated using the weight of final product after lyophilisation with respect to the initial total weight of the drug/AMP and polymer used for preparation MS/PNAP, the percent production yields were calculated using equation 4.1.

$$\text{Percent Yield} = \frac{\text{Wt of Drug/AMP loaded MS/PNAP}}{\text{Wt of PLGA+Drug/AMP taken in batch}} \times 100 \quad \text{..... (4.1)}$$

4.1.3.2. *Particle size distribution (PSD)*

- **Nanoparticles:** The average hydrodynamic particle diameter (z-average) and polydispersity index (PDI) of the NP were measured by dynamic light scattering (DLS) equipment (Nano ZS, Malvern Instruments, Malvern, UK) under physiological temperature (37±1°C). Dynamic light scattering (DLS) measures the correlation of the time-dependent fluctuations in the light scattered by a suspension of nanoparticles (autocorrelation function), which is determined by their Brownian motion.
- **Microspheres/PNAP:** The mean particle size of the developed Microspheres/PNAP formulation was studied by Malvern master-sizer (Malvern Instruments, UK). For

microsphere analysis, five milligrams of MS were suspended in 2ml of filtered water (0.22µ syringe filter, Millipore Merck, USA) which was added to the beaker of the system until a laser obscuration factor of 10% was achieved. For PNAP analysis, dry assembly of the equipment was used. Each sample batch was analysed in triplicates and average reading was considered for data analysis.

4.1.3.3. Morphology of particles

The surface morphology of drug/AMP loaded NP, PNAP and microspheres (MS) were observed by using a scanning electron microscope (SEM) and Atomic force microscopy (AFM).

- **Scanning Electron Microscopy (SEM)**

A thin layer of freeze dried dry powder particles (NP, MS, PNAP) was made on individual stubs (covered with double faced adhesive tape), mounted on a sample holder followed by coating with gold, using a sputter coater. The particles were examined with the beam of electrons using scanning electron microscope (Jeol 6400; Jeol MA, USA). For AFM studies, suspension of freeze dried powder in milliQ water was spread on freshly cleaved mica surface and air-dried. The observation was performed with AFM (Bruker MultiMode 8, NanoScope V controller, Santa Barbara, USA) with silicon probes with pyramidal cantilever having force constant of 0.2 N/m.

- **Atomic Force Microscopy (AFM)**

Further, atomic force microscopy (AFM) was used to further confirm the size-distribution and particle morphology of the particles (NP, MS, PNAP). Dispersion of individual particles (NP, MS, PNAP) was spread on the surface of the silicon-wafer and viewed under the AFM (Multimode 8 Nanoscope V, Bruker, USA) at a scan rate of ~0.996 Hz over a selected field. The AFM was operated in tapping-mode where images were acquired using a commercial RTESP silicon probe tip-cantilever.

4.1.3.4. Porosity and surface area estimation

The specific surface area of different particulate formulations was determined by the N_2 molecule adsorption-desorption using Brunauer-Emmett-Teller (BET) (Autosorb iQ2 Quantachrome instrument, USA) multipoint method and the pore size distribution was obtained using the Barrett-Joyner-Halenda (BJH) curve. Samples were prepared by purging overnight under N_2 at

40°C in vacuum. The Brunauer-Emmett-Teller (BET) surface area was calculated from the adsorption branches in the relative pressure range of 0.05–0.25(91).

4.1.3.5. Drug Content and encapsulation efficiency determination

A known amount of AMP/drug-loaded microspheres/PNAP (10mg) was dissolved in 2ml of dichloromethane (DCM) with intermitted vortex shaking. Phosphate buffer (2ml, 10mM, pH-7.4) was added to the obtained organic solution to precipitate the polymer. The solution was then agitated and intermittently sonicated (5s each) for 5min (in ice) to extract the peptide/drug. The dispersion was centrifuged (10000×g; 15min), the supernatant was collected and dried under vacuum at 4°C. The residue sample was reconstituted by adding 1ml PBS and filtered through a 0.45µ filter. The extracted solution of drug and peptide was analysed using HPLC and Uv-Vis spectroscopy respectively. The peptide entrapment efficiency was calculated using the following equation:

$$\text{Entrapment efficiency} = \frac{\text{Amount of AMP/drug in particles}}{\text{Amount of AMP/drug initially added}} \times 100 \qquad ...(4.2)$$

4.1.3.6. Aerodynamic characterization of particles using Cascade impaction.

The dispersion performance of individual powdered AMP/ drug loaded formulations was accessed in vitro using eight-stage cascade impactor (Graseby-Andersen, Atlanta, GA, USA) with a pre-separator. Twenty milligrams of each formulation was loaded into individual hard gelatin-capsules (size 3), which was positioned in a Rotahaler apparatus coupled with an assembled cascade impactor. The cascade impactor stages (1–8) had apertures of effective cut-off diameters of 8.6, 6.5, 4.4, 3.3, 2.0, 1.1, 0.54 and 0.25µm, respectively. The impaction was performed at a flow rate of 28.3L/min for 2min. The mass of MS deposited at each stage of the cascade impactor was determined gravimetrically. Mass median aerodynamic diameter (MMAD), Fine particle fraction (FPF) and Geometric Standard deviation (GSD) were calculated from the plot of cumulative mass-percentage undersize against the effective cut-off diameter (ECD) of the cascade impactor on a log-probability graph(92).

4.1.3.7. *In vitro* peptide release studies

In-vitro release studies of AMP and Anti-TB drugs from MS and PNAP was carried out in Phosphate buffered saline (PBS) at 37 °C for the period of 10 days. PBS containing 1% ascorbic

acid and 0.05% sodium azide at pH conditions of 7.4 was used for this purpose. AMP-MS and AMP- PNAP (equivalent to 50 mg of AMP) were transferred into individual pre-treated dialysis membrane (Sigma, molecular weight cut-off>1200 Da, 25mm 16 mm), which was suspended in a beaker. The beaker was positioned over a magnetic stirrer (50 rpm) and the temperature was maintained at 37 2 C throughout the procedure. Sample was withdrawn at predetermined time intervals and replaced with the same amount of PBS to maintain sink condition. The samples were stored at −20 C and the amount of drug and peptide released was analyzed using RP-HPLC and Uv-vis spectroscopy respectively.

4.1.3.8. Stability studies of AMP

Conformational stability and secondary structure of the AMP released from particles (MS and PNAP) during processing and release periods were determined and compared with native peptide by using a spectropolarimeter (JASCO J-1500, JASCO international, Japan). The CD spectra of each sample were recorded spectro-polarimeter equipped with a temperature controlling unit, over a range of 180-260 nm using a quartz cuvette of 0.2 cm path length. CD data represent average value of three separate recording with three scans per sample at a scan rate of 1 nm/s. The individual scans were corrected by subtracting with the blank. All CD measurements are reported as ellipticities.

4.2. Results and discussion

4.2.1. Formulation yield

Spray freeze drying and double emulsion solvent evaporation method was optimized for individual particles containing AMP (IDR-1018, MIAP, K4, UB2, aurin1.2, indolicidin, HHC-10 peptides) and anti-TB drugs (INH and RIF). The product was recovered at percentage yields above 52±2.40% and, 68.5±2.85% for Microspheres and PNAP respectively of starting material. The production yield of PNAP was significantly smaller compared with Microspheres. The smaller yield observed for PNAP may be explained by the presence of two-step in the process of preparation including double emulsion solvent evaporation method and Spray freeze drying. There was some loss of the formulation at each step.

4.2.2. Drug content, content uniformity and entrapment efficiency

All particles showed high entrapment efficiency and drug loading. Drug content and content uniformity for all formulations was in the range of 90-110% w/w. MP were prepared with encapsulation efficiencies shown in Table 4.1.

Table 4.1. Showing the developed formulations with their drug loading, encapsulation efficiency, % yield

S.No.	Formulation	Drug	Yield (%)	Drug loading (%)	Encapsulation efficiency (%)
1	Microspheres	UB2	61.45±5.89%	12.35±1.53%	46.1± 8.120
2	Microspheres	Aurin	59.78±8.68 %	13.44±1.27%	41.8±9.3 24%
3	Microspheres	K4	69.8±10.21%	13.01±1.83%	39.6±4.814
4	Mucus penetrating MP	IDR-1018	64.25±4.1%	11.25±1.27%	51.2±3.814%
5	PNAP	Indolicidin	61.25±7.58	14.25±1.27%	43.82±7.542%
6	PNAP	MIAP	68.72±13.08%	13.19± 4.85%	41.92±8.545%
7	Microspheres	UB2	61.45±5.89%	12.35±1.53%	46.1± 8.120

4.2.3. Scanning electron microscopy (SEM)

- **Porous Microspheres**

Spherical shaped hierarchically porous polymeric microspheres with uniform size distribution and regular pore morphology were obtained. Figure. 4 represents the morphological images of various porous PLA-MS displaying different type of pores induced on the surface and micro-matrix. Porogens induced well-distributed pores of diameter ranged from 2.4 nm to 872.4 nm on the surface, with well-ordered interconnected three dimensional channels inside the matrix (Fig. 4.2).

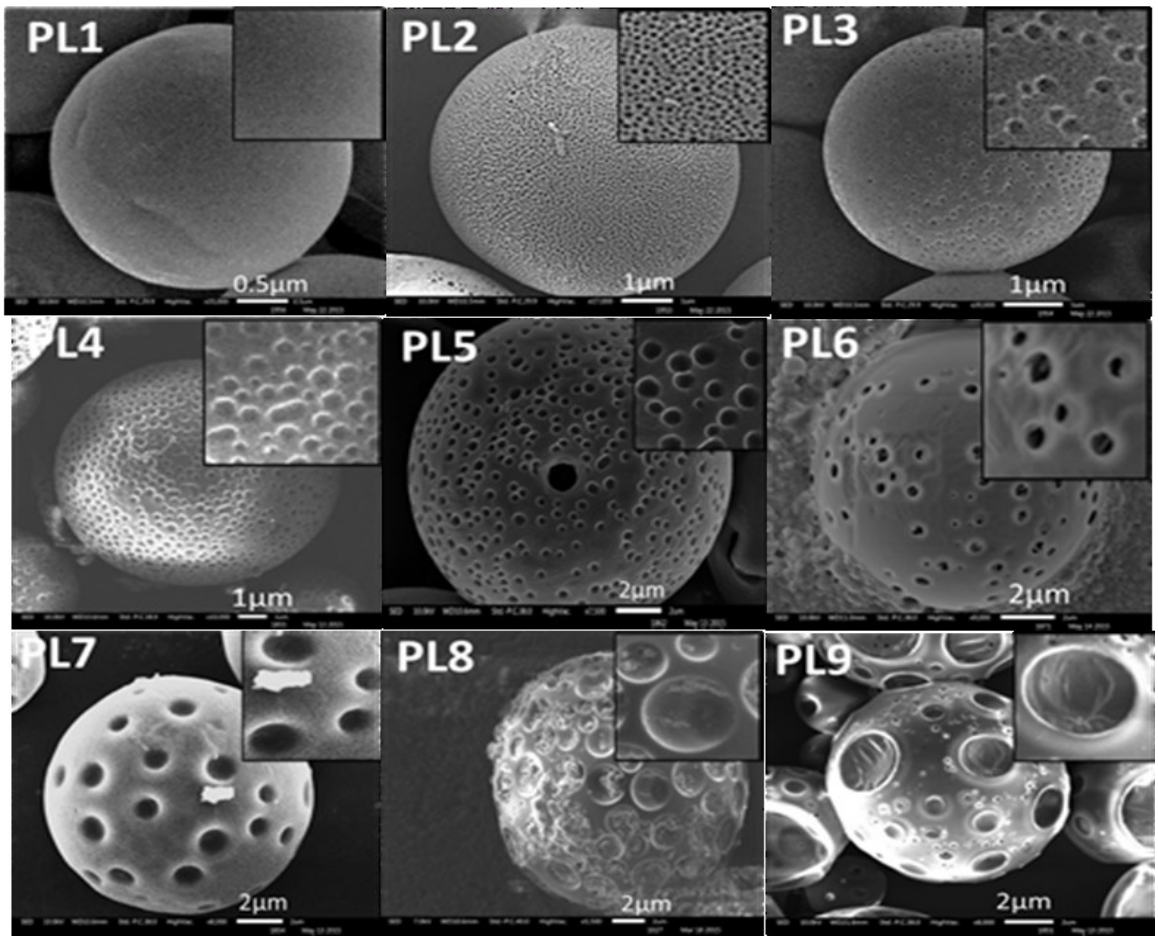

Figure 4.2. Scanning electron micrographs (SEM) showing shape and surface morphology of Porous prepared by double emulsion solvent evaporation method

The nature and concentrations of the porogens significantly influenced the pore architecture, particle size and morphology of PLA-MS (Fig. 3). Adjusting the polymer to porogens ratio could vary the porosities of the micro-scaffolds and the pore size could be controlled independently by varying the concentration of porogens. The particle size and morphology of the developed formulation was further studied by SEM analysis which reveals that all the microspheres were regular, spherical, non-aggregated, with smooth surfaces. The apparent geometric size of the MS ascertained with SEM is in agreement with the laser diffraction data.

- **Mucus penetrating microparticles(MPP):**

Scanning electron microscopy (SEM) images were used to visualize the particle diameter, structural and surface morphology of the Porous PLGA and NAC coated microparticles. The

micrographs indicate that the porous PLGA-MP was spherical in shape with well-defined porous domains all over the surface and unimodal particle size distribution (Figure 4.3). Sodium bicarbonate was decomposed and released carbon dioxide during the emulsification to generate pores in particles.

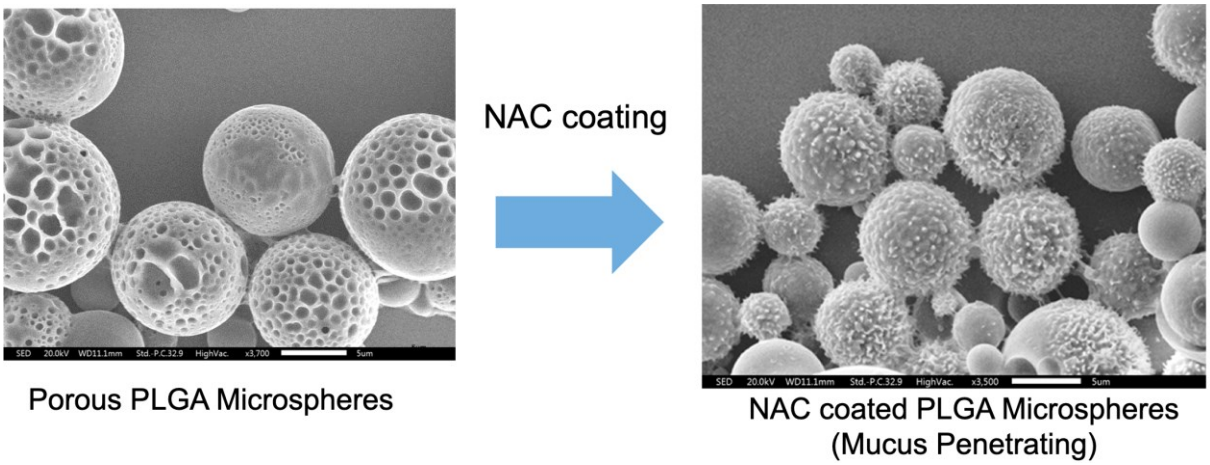

Figure 4.3. Scanning electron micrographs (SEM) mucus penetrating particles prepared by coating of porous particles

The nanoporous microparticles are beneficial for prolonged drug release. Mean size of porous PLGA-MP was 5.14±0.87µm, while NAC coated particles (MPP) have roughened surface due to the coating of the NAC on the surface of smooth particles, demonstrated slighly larger size 6.24±1.04µm. The spherical MP with narrow particle size distribution of ~5µm exhibited optimal properties for inhalation and phagocytic uptake. NAC coated particles (MPP) have roughened surface due to the coating of the NAC on the surface of smooth particles. The SEM images show that they MPP were uniformly dispersed without any aggregation (Figure 4.3).

- **Porous Nanoparticles Aggregates (PNAP)**

Scanning electron microscopy (SEM) was performed to study the particle geometry (morphology and size) of PNAPs the formulations. SEM investigation confirmed the size range, mono-dispersity, spherical shape with smooth surface topology of NP. It also demonstrates that texture and shape of the NP was not significantly influenced by encapsulation of peptide. SEM images revealed that PNAPs (mulberry shaped) are composed of visible aggregated nanoparticles having spherical structure (Figure 4.4).

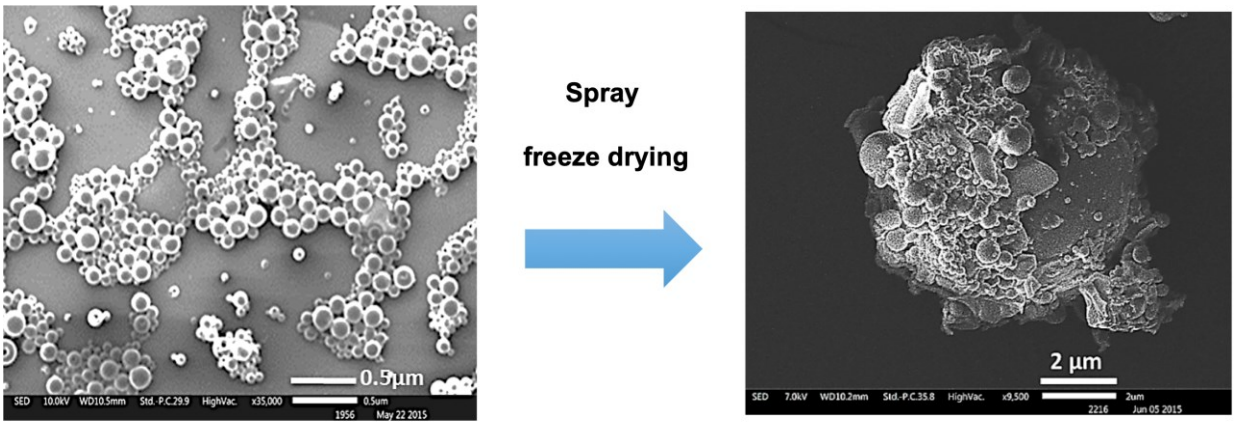

Figure 4.4: processing of AMP-NP into Porous Nanoparticles Aggregates

4.2.4. Particle size distribution

Particle size distribution and volume-based mean diameter was analyzed by using a Malvern Mastersizer. The particles (MS and PNAP) displayed a lognormal distribution of cumulative volume-average sizes between 1 and 10 µm. This size range is considered to be suitable for pulmonary administration we have found that this size of particles is adequate for targeting to lung macrophages in experiments with mice. More than 90 % of particles had a particle size below 10 µm with a median in the range ~5 µm. The Nano porous microparticles are beneficial for prolonged drug release. Mean size of porous PLGA-MP was 5.14±0.87µm, while NAC coated particles (MPP) have roughened surface due to the coating of the NAC on the surface of smooth particles, demonstrated slightly larger size 6.24±1.04µm. The spherical MP with narrow particle size distribution of ~5µm exhibited optimal properties for inhalation and phagocytic uptake. NAC coated particles (MPP) have roughened surface due to the coating of the NAC on the surface of smooth particles. The SEM images show that they MPP were uniformly dispersed without any aggregation. The median hydrodynamic diameter of the prepared primary AMP-loaded NP was found to be 312.6 ± 17.8 nm as determined by DLS. AMP showed a surface charge (zeta potential) of -3.22±0.048 mV, with a low poly-dispersity index (PDI) of 0.102 (Figure.4.5). The low value of the PDI reflects the uniformity in size of particles.

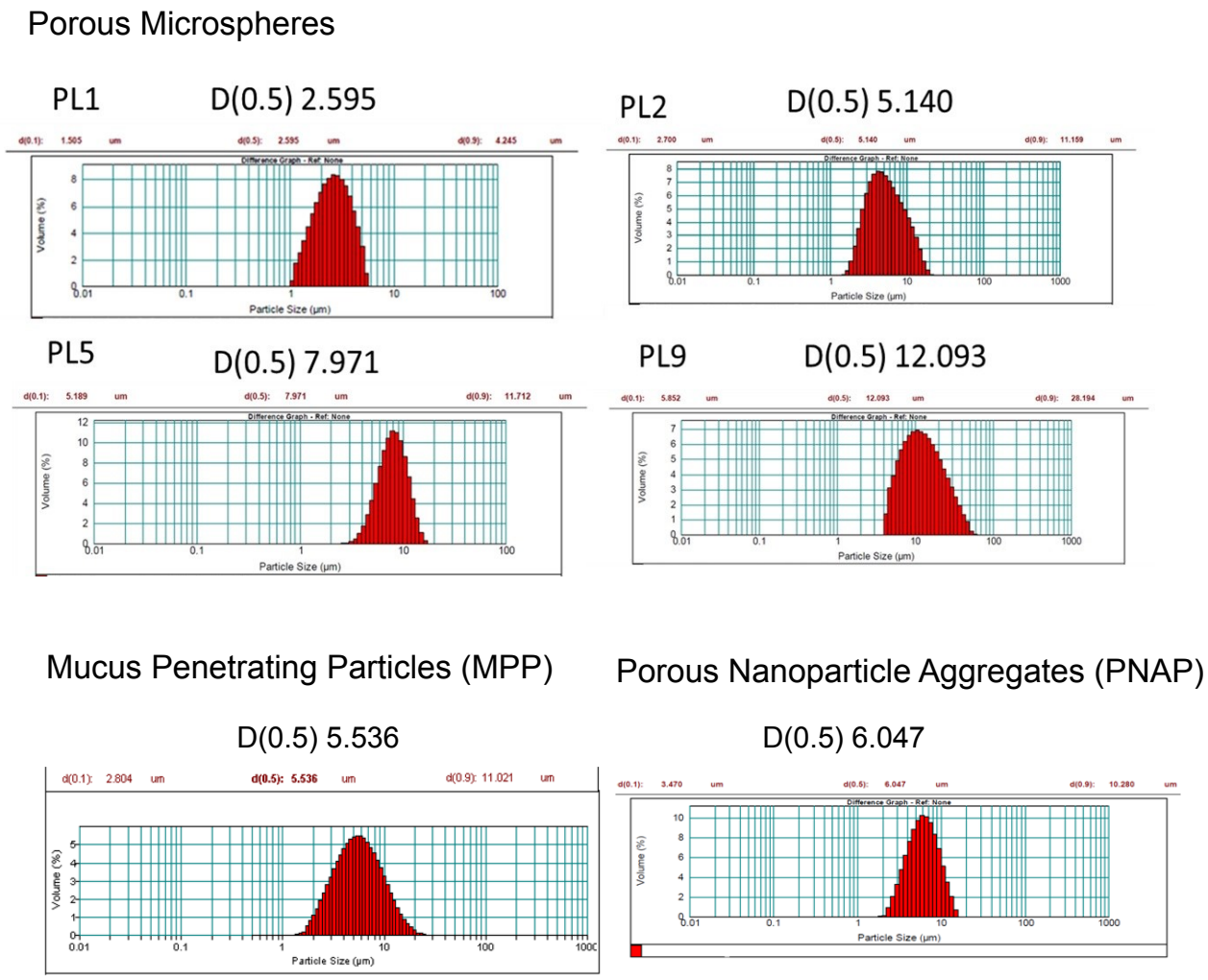

Figure 4.5. Particle size distribution of selective porous microspheres, mucus penetrating particles, porous nanoparticles aggregate particles

4.2.5. Porosity and surface area estimation

Surface area and pore diameter of MS was determined by BET and BJH method respectively. Furthermore, diameter of MS and pore structures were confirmed by SEM analysis. Spherical shaped hierarchically porous PLA-MS particles with uniform size distribution and regular pore morphology were obtained. Figure-4.6 represents the morphological images of various porous PLA-MS displaying different type of pores induced on the surface and micro-matrix. Porogens induced well-distributed pores of diameter ranged from 2.4nm to 872.4nm on the surface, with well-ordered interconnected three-dimensional channels inside the matrix. The nature and concentrations of the porogens significantly influenced the pore architecture, particle size and morphology of PLA-MS. Adjusting the polymer to porogen ratio could vary the porosities of the

micro-scaffolds and the pore size could be controlled independently by varying the concentration of porogens.

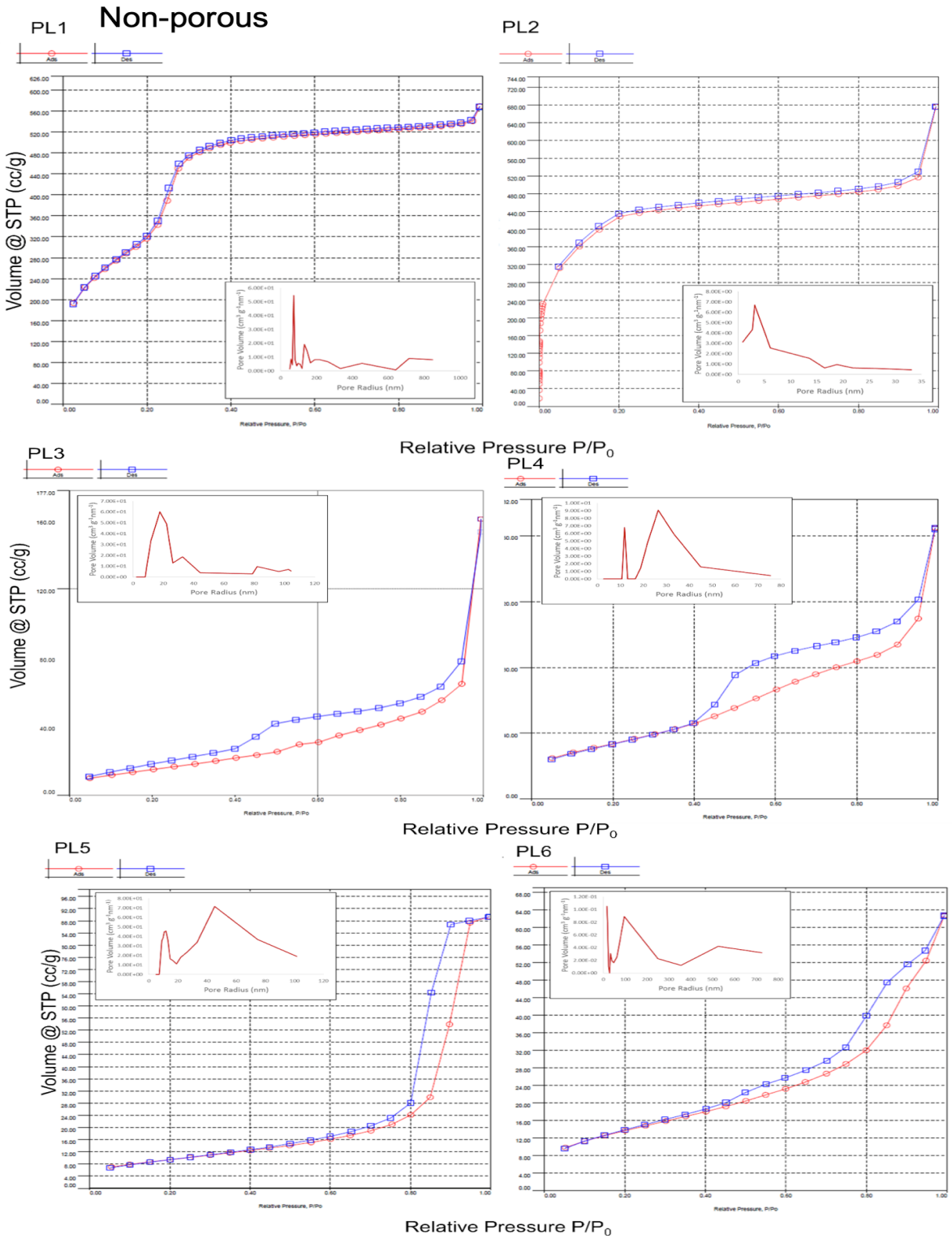

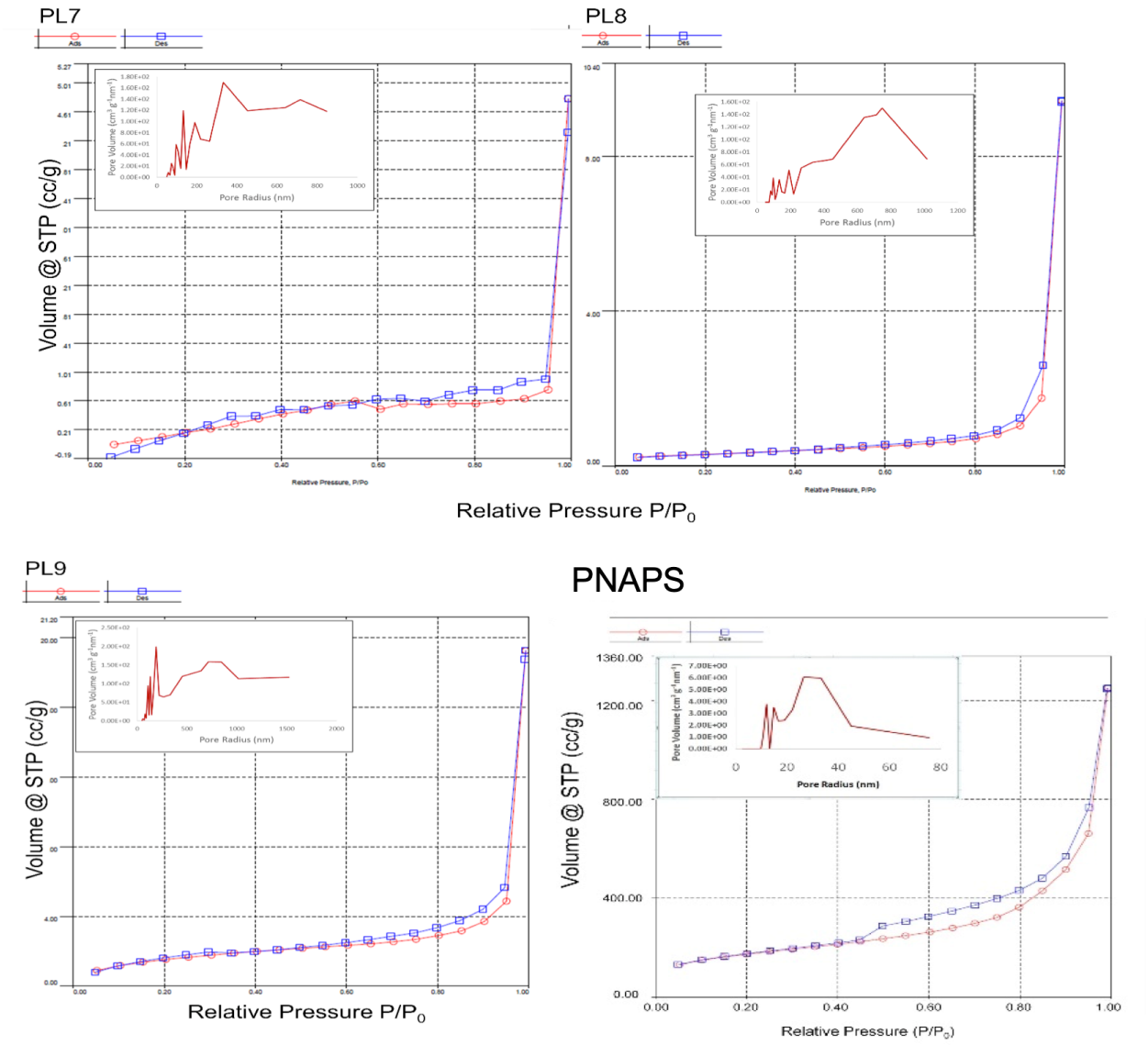

Figure: 4.6. BET and BJH curve for surface area and porosity determination of the various delivery systems developed

As noted, PL2-PL6 MS exhibits well-defined porous structures uniformly dispersed on the surface as well as inside the MS, with interconnected open-pore structures. H_2O_2(1%), Sucrose (3%) PBS (5%), NaCl (2%), NaOH (5%) and NH_4CO_3 (5%) induced porosity with fine interconnectivity in PLA-MS. PL7 to PL9 show rough surface with closed pores showing reduced interconnectivity in the micro matrix. SEM micrographs (PL7-PL9) showed that $NaHCO_3$ (5%) and higher concentration of H_2O_2 (3%) generated partially deformed MS with uniform pockmarks and dimples on the surface of the MS with closed pore structure. Regulating concentrations of porogens considerably influenced pore density on the surface and inside the

micro-matrix, but pore diameter remains unchanged. The pore diameter varied as a function of nature of porogens. Ordered porous domains can be seen all over the surface of MS that permit the inclusion of bio-therapeutics in them and convenient in making sustained release formulations. Owing the internal porous structure with numerous binding sites can solve the drawback of nonporous MS with low encapsulation efficiency and slow release of bio-therapeutics. BET and BJH of PNAP revealed the total pore surface area (m^2/g) of 521.82±71.14 m^2/g and mean pore size 34.5±9.12 nm respectively.

4.2.6. Aerodynamic parameters determination

The tendency of an aerosol particle to get deposited on various regions of respiratory tree of lungs depends on its aerodynamic properties. The aerosol performance of dry powder inhalable MIAP-PNAP for pulmonary deposition was assessed *in-vitro* using an eight-stage Anderson Cascade Impactor (ACI) (Graseby-Andersen, Atlanta, GA, USA) interfaced with Rotahaler (Cipla, Gujrat, India). Cascade impactor's functioning on inertial impaction assess the distribution of particles in a manner that represents as closely as possible, the aerosol actually inhaled by a patient and its behavior in the respiratory tract. The size distribution of particles depositing in various parts of the pathways will affect the transport rates and hence the bioavailability. Experimental studies by cascade impactor demonstrated the distribution of inhalable of MS and PNAPs in different respiratory strata according to particle size. Aerodynamic features of formulations were determined by calculation of Mass median aerodynamic diameter (MMAD), Geometric standard deviation (GSD) and Fine Particle Fraction (FPF). The MMAD and GSD, representing the measures of central tendency and spread, respectively, were calculated. A FPF value advocates deep penetration and retention of the PNAPs into central region of lung. Powder collected at different stages of cascade impactor after actuation of Rotahaler was estimated by gravimetric method and the probability plot of the cumulative mass distribution was plotted against effective cut-off diameter. All type of particles showed high emitted dose >85% from Rotahaler, with very low retention in device.

- **Porous Microspheres**

All developed porous PLA-MS were evaluated for *in-vitro* lung deposition using Andersen Cascade impactor. The emitted fractions (EFs) of all developed MS (PL1-PL9) from Rotahaler apparatus were in the range of 92.6 ± 15.9 to 96.1 ± 6.4%. Dry powder MS inhalation produced

fine particle fractions (FPF) in range of 32.3 ± 5.8 to 56.6 ± 6.8% and mass median aerodynamic diameters (MMAD) as low as 3.1 ± 1.5 to 5.2 ± 1.3 mm (Table 1). MS under investigation had a mean geometric deviation ranging from 1.3 ± 0.6 to 2.0 ± 0.7 mm and mass densities of approximately 0.08e0.76 g/cm3 (Table 1). Increase in porosities and reduction of density in MS of almost similar geometric size led to decrease in aerodynamic diameters. Large porous PLA-MS (>5 mm) hold smaller MMAD and FPF than non-porous MS of the almost similar size. In this respect, porous PLA-MS under study with geometric size > 5μm appear to be more suitable for pulmonary delivery of bioactives with good aerodynamic properties with high lungs deposition. The MMAD, GSD and FPF of emitted dose of AMP-Microspheres [Ub2-MS (3.01±1.24, 1.24±0.43 and 64.71±3.15 μm), K4-MS (3.59±1.14, 1.52±0.29 and 56.43±4.51 μm) Aurien1.2-MS (3.53 ± 2.1, 1.49±0.82 and 60.36±5.72 μm] found to be in range that is appropriate for powder dispersibility and inhalation delivery.

- **Porous Nano Particle Aggregates (PNAP)**

The MMAD, GSD and FPF of emitted dose of blank-PNAP (3.17 ±0.89μm, 1.81±0.62μm and 67.95±5.58%) and MIAP-PNAP (3.34 ±0.57μm, 1.79±0.21μm and 51.47 ± 8.08%),found to be in range that is appropriate for powder dispersibility and inhalation delivery. Particles >5 μm are expected to deposit mainly in the oropharynx, whereas those less than 0.7 μm are likely to be exhaled during normal tidal breathing. These aerodynamic values of the particles indicate that PNAP have adequate mass fraction of particles 1-5 μm, suitable for getting into interior regions of respiratory tree. Aerodynamic result suggests that the aerosol was highly respirable and likelihood of carrying large fraction of formulations gets deposited to the mid region of the lung available for alveolar uptake.

4.2.7. In-vitro Drug release profile from particles

- **Porous microspheres**

The in-vitro release profiles indicate the differences between PLA-MS caused by the variability in porosity (Fig. 4.7). The pore geometry and internal structure of micro-matrix significantly influenced the release profile of the incorporated molecules. Indeed, the release of the bioactives from different MS was temporally diverse. The delivery rate of biotherapeutics in release medium from porous. PLA-MS increases with increase in pore size from ~2.4 to 872 nm.

Microporous and mesoporous MS found to be more suitable for the delivery of biotherapeutics as compared to nonporous and macroporous MS due to their appropriate porosity, surface area and microstructure.

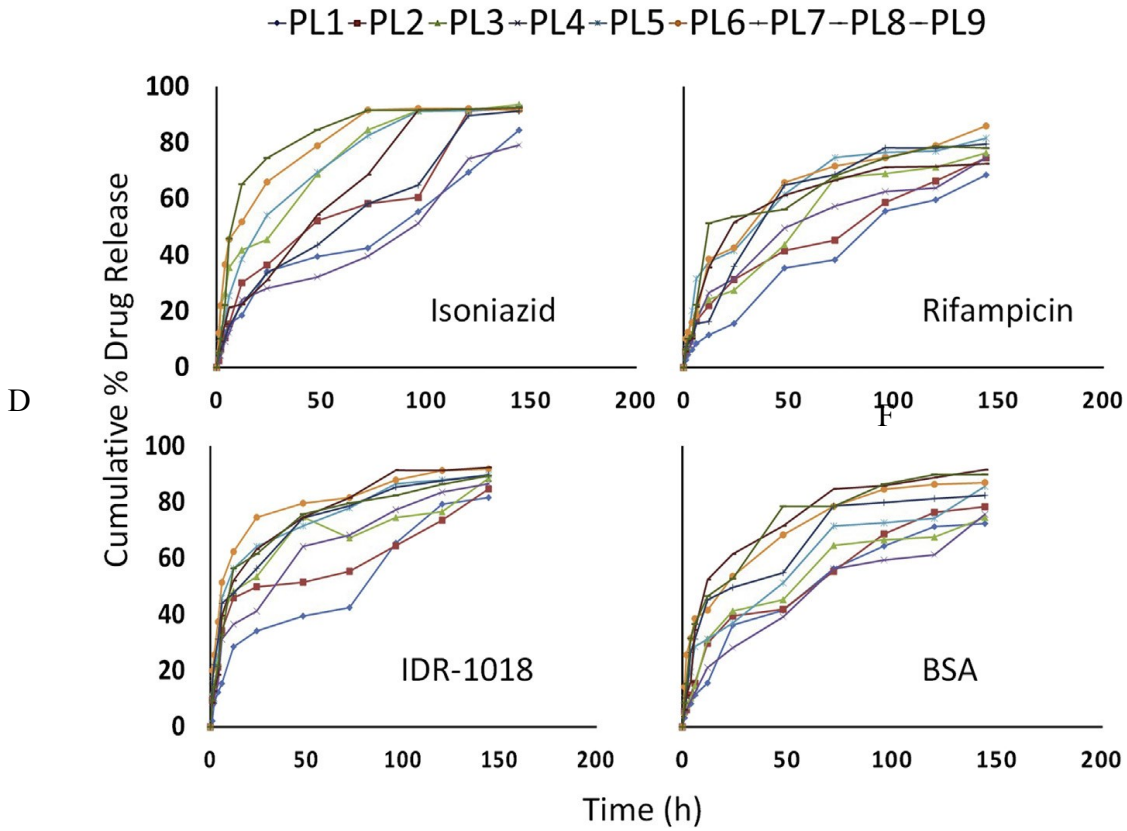

Figure 4.7. Release kinetics of bio-therapeutic molecules of significantly diverse size from PLA-MS of varied porosity in release buffer of pH 7.4.

For drugs and molecules having molecular weights less than 2000 g/mol (INH, RIF, IDR-1018 peptide), PLA-MS (PL2, PL3, and PL4) with a small pores size (~2.4-27.5 nm) were found to be suitable for controlled release. PLA-MS under investigation with variable pore sizes ranging ~20-350 nm (PL4-PL6) showed apparently sustained release of high molecular weight protein (66 kDa protein). The burst release of small molecules (INH and RIF) from non-porous (PL1) and selective porous MS (PL2, PL3, PL4) was minimal and estimated to be 8-17% in the first 2 h, which was followed by slow release pattern. MS with pore sizes >100 nm demonstrated high initial burst of all model drugs used in study and sustained behavior was absent. Hence, the proper pore size choice maximizes efficiency of MS.

- **Peptide release from porous microspheres**

The release profiles of Ub2, K4 and Aurien1.2 from respective microspheres are shown in Figure 4.6 All the AMP were gradually released from porous MS matrix in a biphasic mode. The first phase is characterized by a fast release which probably results from the solubilisation of peptides that usually present near the surface. The second phase is characterized by a slow release which could be attributed to the degradation of polymer matrix leading to the diffusion of the entrapped peptide. Due to degradation of PLGA into monomers, the pH value of the release medium slightly decreased from 7.4 to 7.1, after 3 days, but it did not affect the release and stability of AMP. The cumulative release characteristics of AMP from the PLGA matrix showed sustained release pattern leading to total release to ~91-94% in 7 days (Figure-4.8 A). The extents of Ub2, K4 and Aurien1.2, released in the first day, were about ~62%, 71% and 53% respectively. The release rate of relatively smaller K4 from PLGA-MS was higher than that of Aurein1.2 and K4 over 8 days which indicates that release kinetics of the A from MS are influenced by the physicochemical characteristic of each peptides.

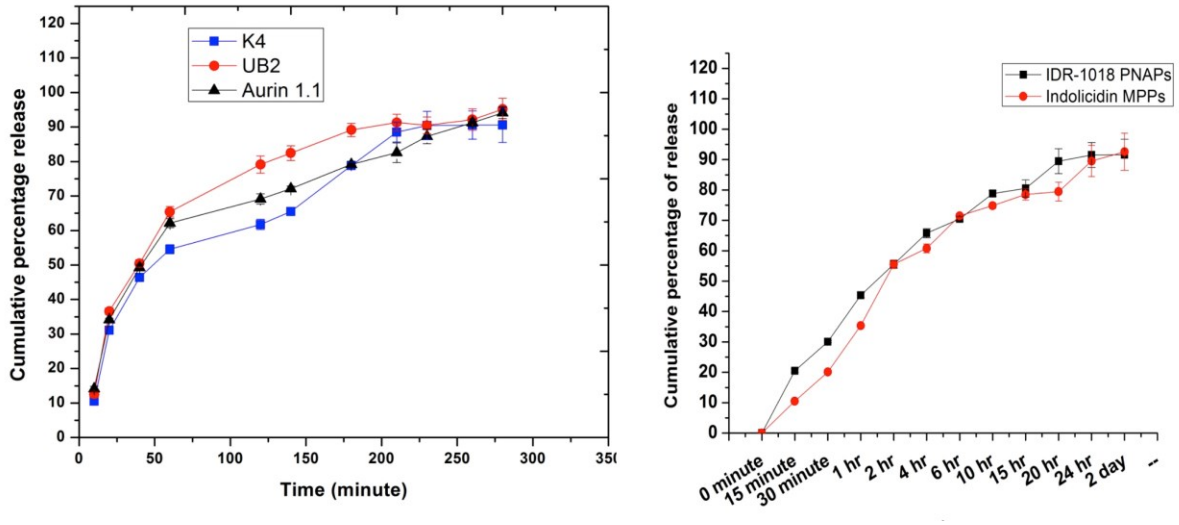

Figure 4.8. (A) Release pattern of K4, UB2 and Aurein1.2 from microspheres in release buffer of pH 7.4 (B) Release pattern of Indolicidin from indolicidin-MPPs and IDR-1018 from IDR-1018 PNAPs in release buffer of pH 7.4

- **Porous Nanoparticle Aggregates (PNAP)**

Drug carriers that offer sustained drug release in the lungs could enhance efficacy of inhaled medicament. Therapeutic outcomes are critically dependent on onset, release and duration of

retention of drug in lungs. The release kinetics of MIAP from the optimized formulations of NS and PNAP were studied for 10 days in simulated lung buffer (PBS, pH 7.4) at 37±2°C and observed continuous peptide release throughout this interval. MIAP release from both NS and PNAP demonstrated dual biphasic pattern that was categorized by initial burst, followed by slower secondary linear sustained release pattern (apparent zero order phase) of peptide. Processing of MIAP-NP into MIAP-PNAP reduced the pace of peptide release which permitted prolonged release. From the release graph it is evident that PNAP showed lower burst release (16.7%) compared to NP (21.4%). MIAP-PNAPs show sustained liberation of peptide for longer period of time (8 days) as compared with MIAP-NP (5 days) leading to total cumulative release to ~95% (Figure 4.9). Initial burst release may be due to surface desorption, diffusion, and dissolution and sustained erosion and degradation of polymer matrix.

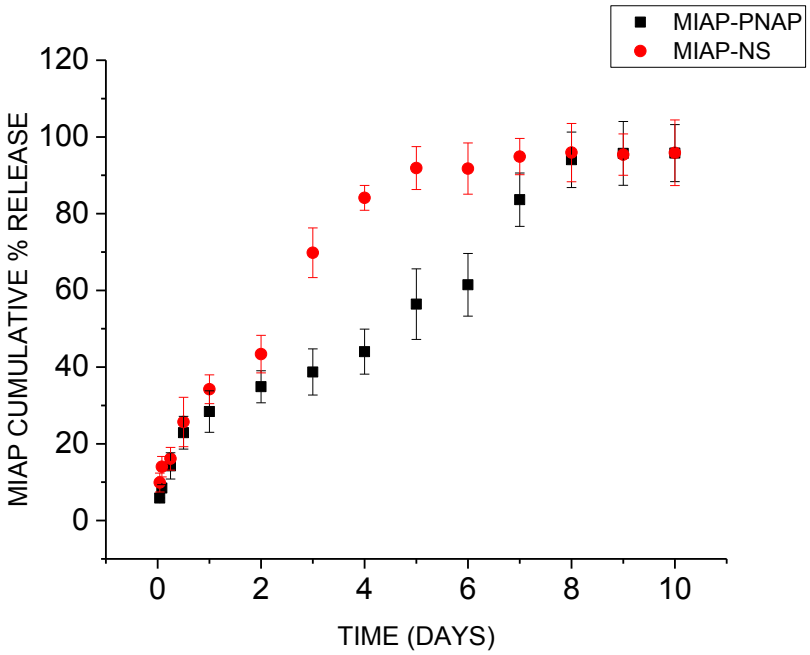

Figure 4.9. Release kinetics and Stability of MIAP (A) Release pattern of MIAP from MIAP-NP and MIAP-PNAP in release buffer of pH 7.4

4.2.8. Stability of peptides

Circular Dichorism (CD) analysis as shown in Figure-4.10 B, C & D, indicated that the Ub2, K4 and Aurein1.2 peptides released from individual MS matrix at different time intervals (0, 24, 96 and 192hr) over eight days had the similar polarity as the native original peptide. Slight reduction

of pH due to degradation of PLGA did not affect the conformation of peptide in release medium. This shows that the PLGA-MS is able to preserve α-helical secondary structure of incorporated peptides during release kinetics.

Circular Dichorism (CD) analysis as shown in Figure-10 A indicated that the MIAP peptide released on different time intervals from 1st day to the 8th day had the same polarity as the native original peptide. Due to degradation of PLGA, pH of the medium was slightly decreased but this alteration of pH did not affect the peptide as acylation of peptide was not identified in medium. This shows that the PNAP is able to preserve random coil secondary structure of MIAP during release kinetics.

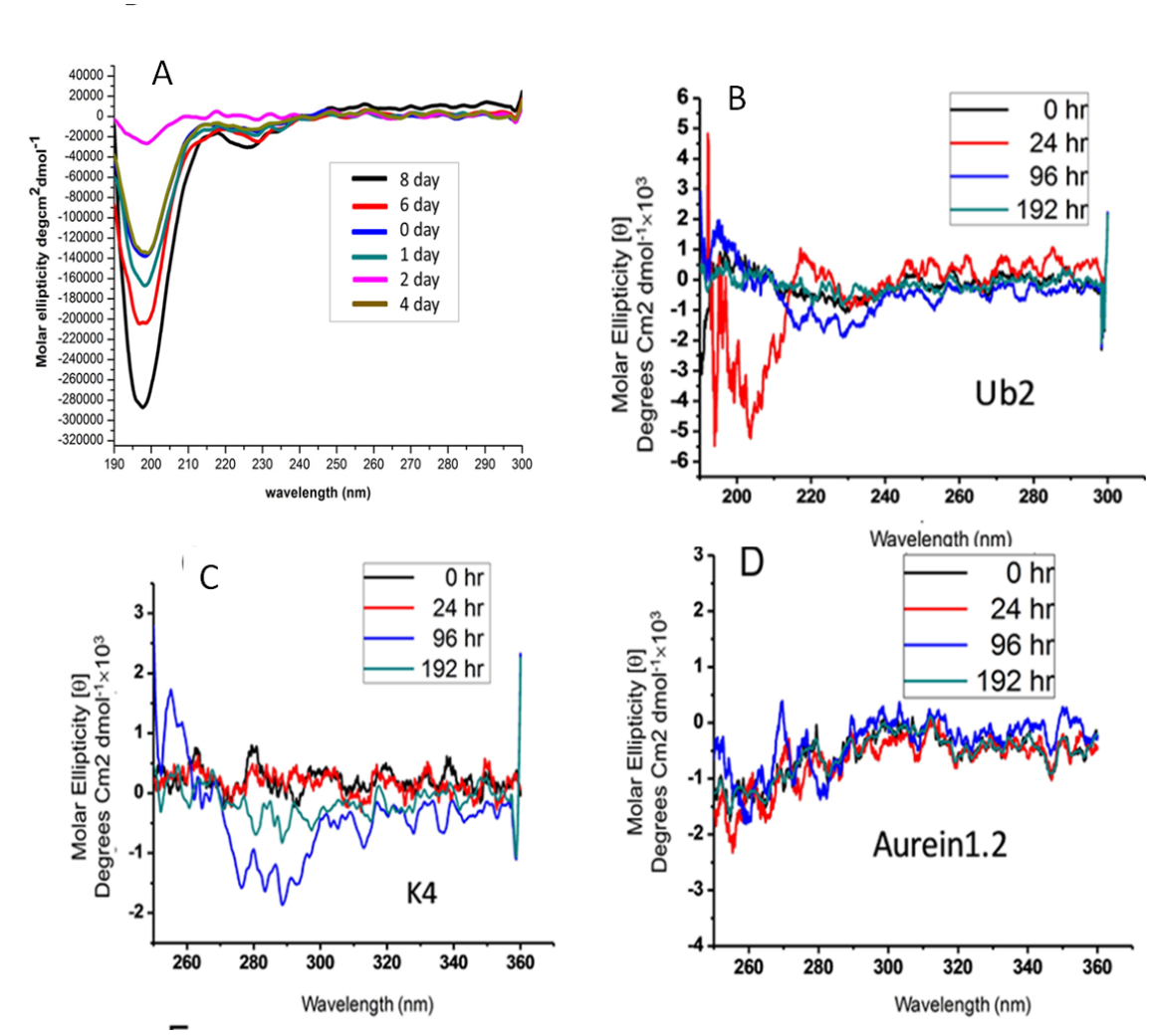

Figure 4.10. : Circular dichroism of released peptides from the different formulation (A) MIAP (B) UB2 (C) K4 (D) Aurein1.2

4.3. Conclusion

Various inhalable formulations like conventional non porous microspheres, porous microspheres, porous nanoparticles aggregates, mucus penetrating particles were developed using various methods. We demonstrated that precise control over particle sizes and porosity of PLA-MS can be attained by using varied concentrations of porogens/osmogens. A range of MS of hierarchical pore size with either open or closed porosity, with diverse topology was synthesized. MS were capable of efficiently encapsulating model molecules of variable molecular sizes. Our results confirm that prototypes with potential therapeutic utility for pulmonary delivery of drugs can be prepared by this convenient technique. Typically, the crucial size range for inhalable particles is 1 5 m microns for local lung delivery, whereas nanosize particles (<1 m) are prone to be exhaled during breathing process. Several limitations have been recognized in delivering peptides

by inhalation delivery, which encompasses lack of correct dosing, unavailability in targeted part of respiratory tree, stability and immunogenicity. Here, we designed MIAP-peptide loaded Porous Nanoparticle aggregate Particles (PNAP) the micron-size particles of dual features

Possessing aerodynamic properties comparable to low-density microspheres for optimum lung deposition whereas encapsulation and dispersion properties of nanoparticle. Mucus penetrating particles can cleave the mucus of lungs can easily penetrate the lungs which are having optimim aerodynamic properties.

It has been well accepted that antimicrobial peptides (AMPs) have demonstrated promise as a class of broad-spectrum antimicrobial agents. Antimicrobial peptides (AMP) show meticulous importance, either for delivering as monotherapy or in combination conventional drugs. These plausible molecules have remarkable potential to bacilli in the body and have important role host defense against M.tb in humans. Particles containing AMP could apparently be phagocytised by the alveolar macrophages and control the release.

In the present chapter we assessed *in-vitro* anti-mycobacterial activity of free AMP and their respective formulations against *M.tb* H37Rv in mycobacterium infected macrophages. We also assess the formulation toxicity, macrophage uptake of the developed formulations.

5.1 Experimental

Cell uptake study of developed particulate formulations was studied in macrophage (RAW264.7) cell culture.

5.1.1. Material

5.1.2. Cell uptake study
- 5.1.2.1. Preparation of florescent particles
- 5.1.2.2. Flow cytometry
- 5.1.2.3. Confocal microscopy

5.1.3. *In vitro* efficacy studies
- 5.1.3.1. *In Vitro* Infection and Treatment
- 5.1.3.2. Colony Forming Unit (CFU) Count analysis
- 5.1.3.3. Formulation cytotoxicity study (MTT assay)

5.1.1. Materials

5.1.1.1. *Chemicals and drugs*

Middlebrook 7H10 agar medium and OADC (Oleic-Albumin-Dextrose-Catalase) growth Supplement was purchased from BD. Dulbecco's Modified Eagle's medium (DMEM), Fetal bovine serum (FBS), 2, 7-Dichlorofluorescein Diacetate (DCFDA), Fluorescein Isothiocyanate (FITC), 4', 6-Diamidino-2-Phenylindole (DAPI), glycerol, cyclohexamide MTT reactant 3-(4,5-

Dimethyl-2-thiazolyl)-2,5-diphenyl-2H-tetrazolium bromide, Paraformaldehyde, Poly-L-Lysine, and TritonX-100 was purchased from Sigma, St Louis, USA. LysoTracker Red DND-99 was obtained from Molecular probes, Invitrogen.

Macrophage culture: Mouse RAW264.7 macrophages ((National Centre for Cell Science, Pune, India) were cultured in Dulbecco's modified Eagle's medium (DMEM) containing 4mM L-glutamine, 1.5 g/L sodium bicarbonate, 4.5 g/L glucose, 5 mM HEPES supplemented with 10% fetal bovine serum, 50 U/mL penicillin, and 50 mg/mL streptomycin. Cells were maintained in 75cm^3 and 25 cm^3 culture flasks at 37°C, 5% CO_2, and 95% relative humidity(93).

5.1.1.2. Mycobacterium growth conditions

M. tuberculosis H37Rv [*M.tb* H37Rv Code: PN7 was procured from All India Institute of Medical Science (AIIMS)] were grown in Sauton's medium supplemented with 0.2% glycerol, 0.05% Tween 80, and 10% Oleic acid-Albumin-dextrose-Catalase (OADC) enrichment (BD, USA). Colony forming units (CFU) in dilutions were estimated by plating dilutions on Middlebrook 7H11 agar supplemented with 0.5% glycerol and 10% OADC. Plates were incubated at 37°C, 75% RH for up to 4 weeks. The absorbance at 600 nm correlated with CFU obtained on agar plates after serial dilutions and was used to generate a standard plot for routine estimation of CFU (94).

5.1.2. Cell uptake

5.1.2.1. Preparation of florescent particles

The phagocytic uptake of porous MS, PNAPs, and MPPs was evaluated using confocal microscopy. Particles encapsulating florescent Fluorescein isothiocyanate (FITC) (0.02% w/w of the polymer mass) were prepared. The presence of FITC did not change the size, surface properties, porosity or aerodynamic characteristics of the particles(95).

5.1.2.2. Confocal microscopy

RAW264.7 macrophages (1.5×10^6 cells/well) grown on lysine coated 22× 22 mm coverslips, placed in a 6-well tissue culture plate. Florescent MS/PNAP (12µg/mL) incorporating FITC were incubated in designated wells for 2h at 37°C. After incubation, cells were washed 3 times with PBS (pH-7.4). Then cells were fixed by incubating them with 4 % paraformaldehyde for 20 min

at 4°C. Cells were then washed two times and permeabilized with Triton-X-100 solution (0.01% in PBS). Cells were then washed three times with distilled water and stained with 0.5 µg/mL 4, 6-diamidino-2-phenylindole, dihydrochloride (DAPI) for 10 min at room temperature. After five times repeated washings, coverslips were mounted with buffered glycerol solution (90% in PBS) and sealed with nail polish. Confocal microscopy was performed at 63X on a Zeiss Laser Scan Inverted 510 microscope (Carl Zeiss, Inc.). An argon/krypton laser (excitation, 488 nm; emission, 505–530 nm) was used for detection of FITC fluorescence (96, 97).

5.1.2.3. Flow cytometry

Prior to experiments, RAW464.7 macrophages seeded at a density of 1.5×10^6 cells/well in 6 well plates. The cells were washed with incomplete medium (without FBS) and fresh complete medium was added to the adherent cells, and incubation continued for another 10h. The culture medium was replaced with fresh medium containing individual MS/PNAP (12µg/mL) incorporating FITC (Fluorescein Isothiocyanate) dye as fluorescent marker (0.001 mol %) in designated wells. After 3h of incubation, the cells were washed three times with PBS (10mM, pH 7.4) in order to remove surface-bound MS/PNAP(98). The cell-associated fluorescence was measured by flow cytometry (99).

5.1.3. Infection and treatment *in vitro*

We assessed *in-vitro* anti-mycobacterial activity of free AMP and their respective formulations against *M.tb* H37Rv in mycobacterium infected macrophages (100). Macrophages ($2x10^5$) were infected with *M.tb* in 96 wells culture plate at multiplicity of infection of 10 (MOI). After incubation of 2h, wells were washed using PBS to remove extracellular bacteria. MS/PNAP were suspended in DMEM to get theoretical concentrations of 10, 50, and 100µg/ml of peptide. Corresponding amounts of pure peptides in solution were also added to designated wells for comparison. Similar treatment group was also made in combination with half dose of standard anti-TB drug (Isoniazid; 1.5µg/ml). Blank MS/PNAP equivalent to highest concentration of MS/PNAP used in experiment were added to designate well. Cells were washed after incubation of 3h to remove extracellular microspheres. Cells were incubated for different time intervals (0, 6, 12, 24, 48, 72 and 96h) which was then washed and lysed using lysis buffer (1% TritonX-100) and plated in triplicates on to 7H11 middle brook agar plates supplemented with 0.5% glycerol,

10% OADC and incubated at 37°C in incubator. The growth bacterial colonies were counted after 28 days. The results were expressed as log (CFU/ml) ± Standard Deviation and compared with control groups (94).

5.1.4. Cytotoxicity toward Macrophages

To estimate cell viability and cytotoxicity of AMP and their formulations in solution towards *M.tb* infected RAW264.7 macrophages, the 3-(4, 5 dimethyl-thiazol-2-yl-2, 5biphenyl) tetrazolium bromide (MTT) assay was used (101). Briefly, cells (2×10^5 cells/well) exposed to various concentrations of AMP (as used for bactericidal activity) in particulate or soluble form in designated wells for different time intervals (6, 12, 24, 48, 72 and 96h) and then probed with 25µl of MTT solution (1 mg/mL in complete RPMI) per well. Cells were incubated with the MTT solution for 4 h, then supernatants were discarded and formazan crystals formed in viable cells dissolved in dimethyl sulfoxide (DMSO). Absorbance at 570nm was read by a microplate reader and viability calculated as a percentage of the reading obtained with untreated, uninfected cells(2)

5.2. Results and discussion

5.2.1. Macrophage uptake studies

TB bacteria reside inside the alveolar macrophages of lungs, hence the phagocytic uptake of the prepared particles by macrophages was evaluated using flow-cytometry and confocal microscopy(5) (Figure.5.1).

- **Porous microspheres**

Fluorescence Confocal laser Scanning Microscopy (CLSM) was used to demonstrate the association and uptake of fluorescently labeled (FITC) porous PLA-MS by mouse macrophages RAW264.7 cells. Nonporous and low porosity spherical particles were efficiently phagocytized in higher numbers compared to particles with high porosity (Figure.5.1).

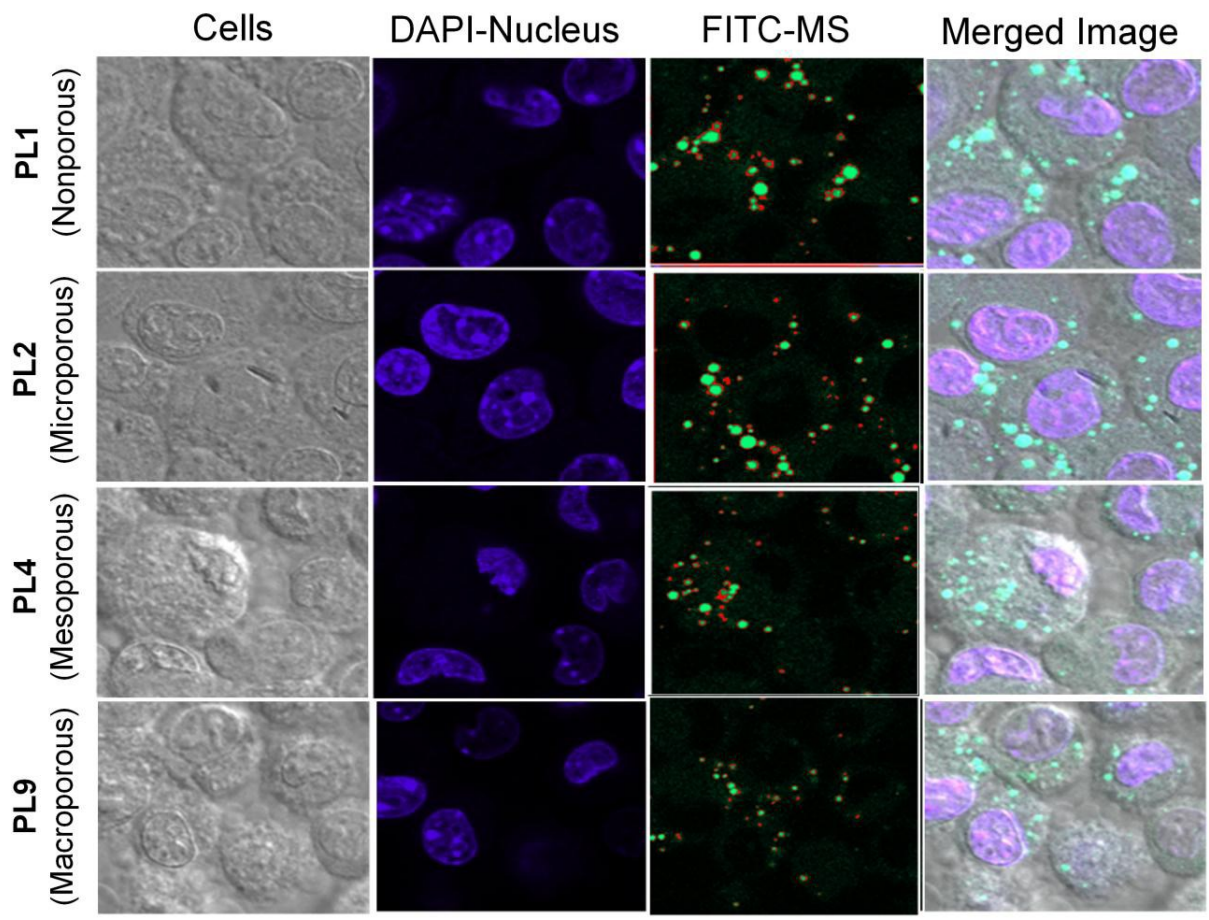

Figure 5.1. Confocal laser scanning microscopy images of RAW264.7 macrophages cells after 2 h incubation with selective FITC-conjugated PLA-MS at 37 C. Image processed by ImageJ

Evidently, in addition to particle size and surface properties, the cellular association and uptake was also found to be porosity dependent. The internalization of PLA-MS into macrophages was in the order PL1 > PL2 > PL3 > PL4 > PL5> PL7 > PL8> PL6> PL9. The maximum uptake by the cells occurred with nonporous PL-MS (PL-1). The uptake of PL1-MS was approximately ~2.1 times that of PL2, ~4.6 times that of PL4 particles, and ~5.2 times that of PL9 particles. Figure.5 shows the cellular uptake of selected PLA-MS with significant different porosity and size. It is speculated that both size and porosity influence the cellular adherence, phagocytosis and their downstream cellular outcomes.

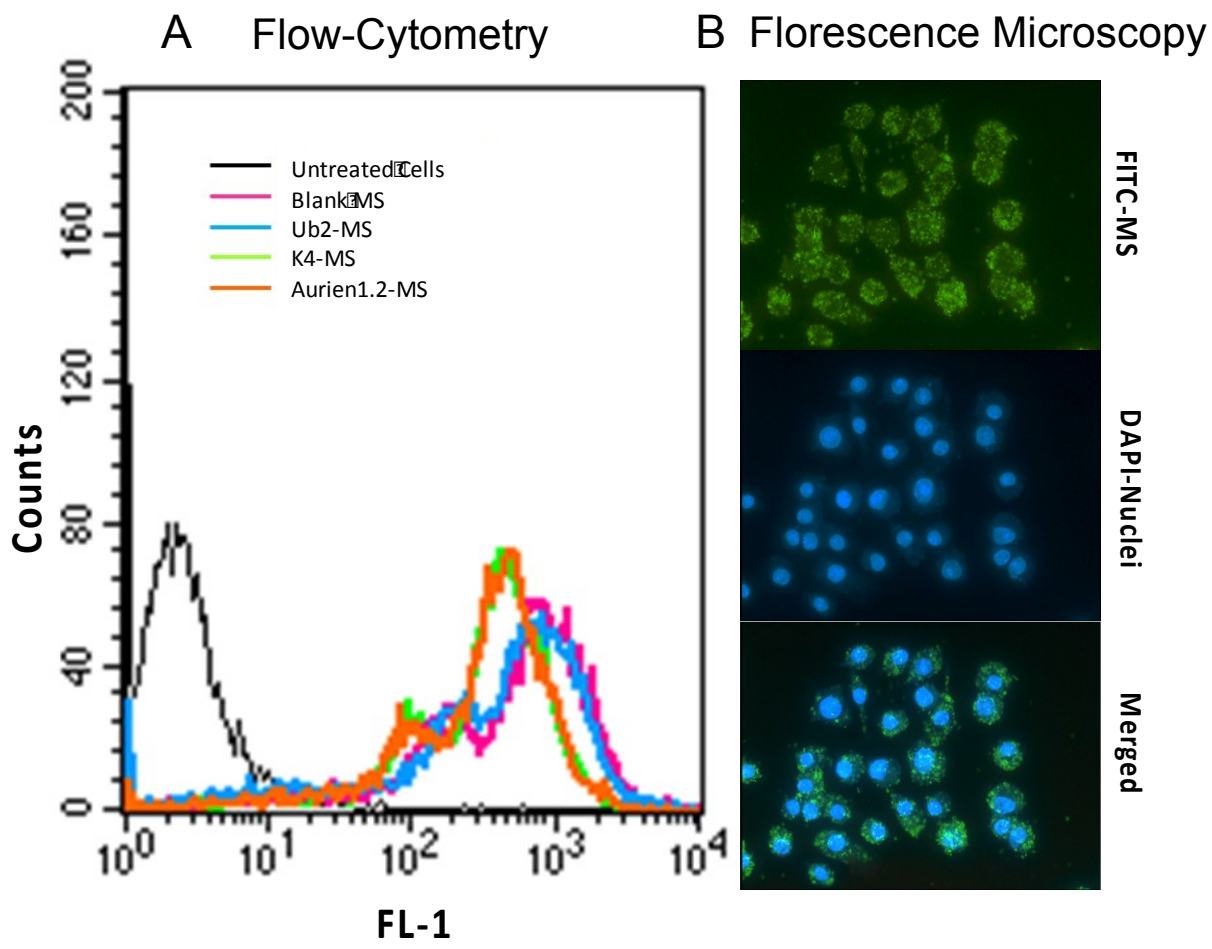

Figure 5.2. Macrophage uptake of MS loaded with UB2, K4 and Aurein 1.2 by (A) Flow Cytometry histogram profiles of macrophage cell incubated with different fluorescent PLGA-MS loaded with Ub2, K4 and Aurein1.2 (B) Fluorescence Microscopy show visualized distributions of different fluorescent AMP -PLGA MS in cultured macrophages (one representative image). Green fluorescence represents AMP -MS and blue fluorescence represents nuclei of the macrophage cells (RAW 264.7). Scale bars represent 20μm.

The uptake of FITC labelled AMP-MS/PNAP by macrophages was measured by flow cytometry where instrument was set to collect 10000 events for each sample. Labelled and unlabelled cells were used to set respective gates. Flow cytometry histograms in Figure-5.2A show significant macrophage uptake of blank and individual AMP-MS/PNAP formulations internalized by cells. Further, fluorescence microscopy confirmed the efficient internalization of most of the AMP loaded microspheres. Figure-5.3 showed one representative image of cellular uptake of AMP-MS/PNAP which suggest that these AMP-MS/PNAP are good enough to target alveolar macrophages(6).

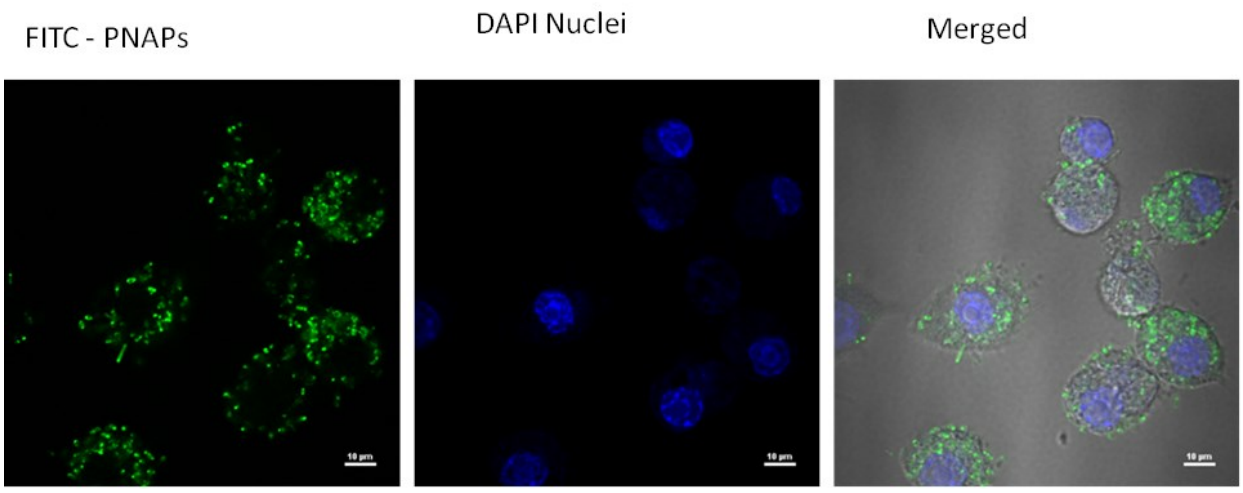

Figure 5.3.: Fluorescence Microscopy show visualized distributions of different fluorescent AMP -PLGA PNAPs in cultured macrophages (one representative image). Green fluorescence represents AMP -PNAPs and blue fluorescence represents nuclei of the macrophage cells (RAW 264.7). Scale bars represent 10μm.

5.2.2. Bactericidal activity of formulation

- **Porous Microspheres**

Of the AMP tested, K4, Ub2, Aurin-1.2 exhibited potent anti-TB activity in a dose- and time-dependent manner at micro-molar concentrations, whereas other peptides demonstrated killing at higher concentrations (> 100μg/ml) hence omitted from study. Compared with either untreated or control blank PLGA-MS (containing no drug), treatment of *M.tb*-infected macrophages with either pure or PLGA loaded peptides reduced the number of intracellular bacteria over a 4-day treatment. In contrast, lower doses (10 & 50 μg/ml), free peptide and low dose of AMP -MS (10μg/ml), revealed no significant inhibition on the growth of *M.tb*. Cellular uptake and retention studies confirmed prolonged peptide release from PLGA particles and hence substantial bacterial killing was observed till 4 days. The effectiveness of the Ub2 peptide was most promising followed by K4 and then Aurelin1.2. The number of viable bacteria in cell lysates prepared at different time intervals (0, 6, 12, 24, 48, 72 and 96h) after exposure with AMP in solution or MS was enumerated in terms of $\log_{10}$CFU/mL of cell lysate. In the absence of treatment, the colony count was 6.21±1.09 $\log_{10}$ CFU/ml. Previous studies have demonstrated that poly (lactic acid) (PLA) MS can activate macrophages and augment their ability to kill intracellular *M.tb* (102). But we did not found similar results with PLGA-MS in these study, PLGA-MS of similar size

did not did not have a statistically significant effect on growth of *M.tb*. Drug free blank MS equivalent to the highest dose used in studies did not demonstrate significant bactericidal activity (5.78±0.95 $\log_{10}$ CFU/ml). At lower doses of pure AMP (10 and 50µg/ml in solution), the differences in activity were not statistically significant at a probability level of 0.05. Bonferroni's *post hoc* test (* $p<0.05$) for comparison of means following one-way ANOVA indicated that the bactericidal activity of AMP -MS was significantly higher than that of peptides in solution at 50 and 100µg/ml. At highest experimental concentration (100 µg/ml) of AMP used in the study, Ub2-MS, K4-MS and Aurein1.2-MS demonstrated significant inhibition of mycobacterium (~3.41±0.12 $\log_{10}$CFU/ml, 2.3.2±0.73 $\log_{10}$CFU/ml, and 2.06±0.52 $\log_{10}$CFU/ml, respectively) compared to the untreated bacteria (6.21±1.09 $\log_{10}$CFU/ml). All AMP showed significant inhibition of *M.tb* for up to 4 days, suggesting prolonged drug retention and release from the MS within macrophages. The significance in bactericidal activities of the AMP -MS followed the order: Aurein1.2<K4<Ub2. The results shown that the mycobacterial inhibition by combination of AMP plus INH (1.5µg/ml) was superior to INH alone at different concentrations of AMP as shown in Figure-5.4. All three peptides had additive effects with INH against *M.tb* that could substantially decrease the concentration of the conventional anti-TB antibiotics in therapy, indicating that the peptides are potential feed additives to reduce the antibiotic dose. Bar shown as mean ± SEM of three independent experiments.

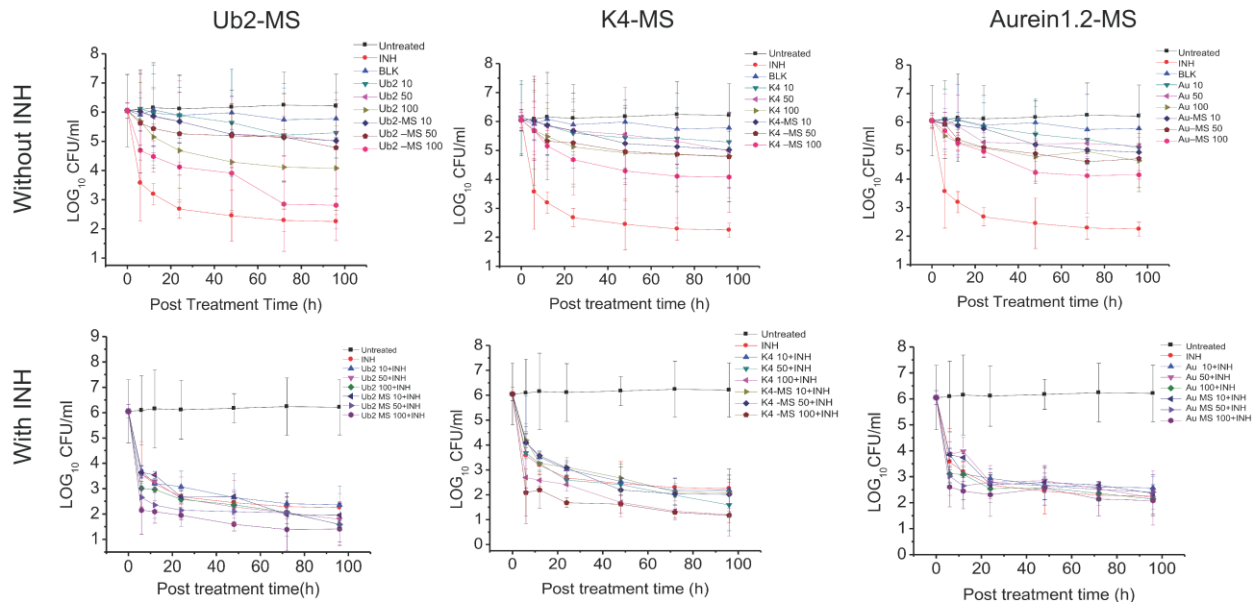

Figure 5.4. Anti-Mycobacterial activity by Colony Forming Unit (CFU) Assay. Efficacy of pure and micro-encapsulated AMP (Aurin1.2, Ub2, K4) against virulent Mtb (H37Rv) present in macrophage cells (RAW 264.7) (A) Panel:1 Activity of AMP without anti-TB drug INH (B) Panel:2 Activity of highest concentration of AMP with sub-optimal dose of anti-TB drug INH. Absolute bacterial numbers in logarithmic scale after treatment with either AMP or AMP -MS. Results are means (n=3, ± standard deviation).

- **Mucus Penetrating Particles (MPP)**

In order to determine intracellular antitubercular efficacy and drug delivery of the developed formulation, we infected the RAW 264.7 cells with virulent Mtb H37Rv bacteria and then cells were treated with free IDR-1018 and NAC/IDR1018 MPPs at 50 and 100µM concentration. There was dose dependent reduction of intracellular Mtb. In the absence of treatment, there was growth of the mycobacterium tuberculosis (H37Rv) and the colony count was 7.60± .51 Log10CFU/ml. Free IDR-1018 and NAC/IDR-1018 MPPs demonstrated significant dose dependent mycobactericidal effect. At the concentration of free 50 µM IDR-1018 there was 2.1 log CFU reduction of intracellular bacteria. At 10, 50, 100 µM concentration of the MPP formulation 0.91, 2.13, 3.5 log CFU reduction of intracellular bacteria respectively which may be due to higher uptake of the particles by the infected cells release of the peptide inside the cells (Figure 5.5).

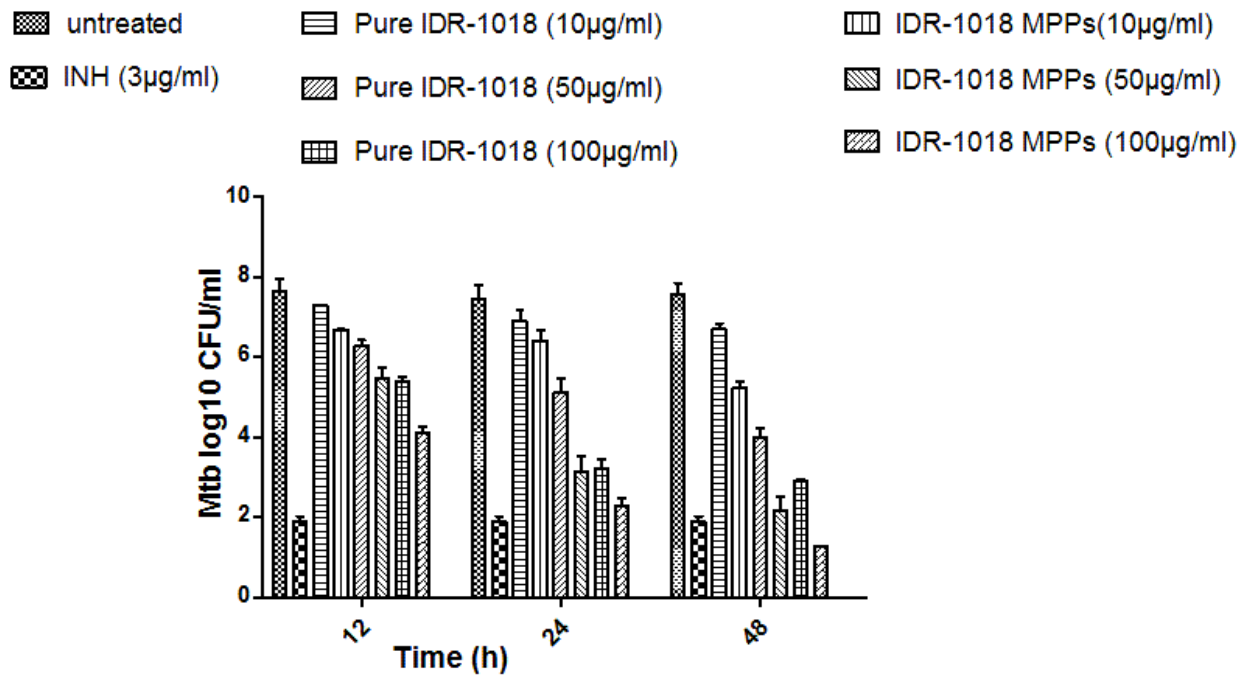

Figure 5.5. Colony Forming Unit (CFU) Assay: CFU of Mtb counted at 21-days after plating lysates recovered 12, 24 and 48 h after infection followed by treatment, with IDR-1018 MPPs). Results means (n=3, ± standard deviation).

- **Porous Nano Particles Aggregates (PNAP)**

In order to evaluate the effect of MIAP-PNAP on mycobacterial viability in different time period intervals, mono-layered cells were infected with virulent Mtb (H37Rv) (MOI 10:1 bacteria/macrophage) and treated with different concentrations of free and encapsulated MIAP for different time intervals (12, 24, 48h). The number of viable bacteria was enumerated by CFU assay of cell lysate. In the absence of treatment, there was growth of the mycobacterium tuberculosis (H37Rv) and the colony count was 6.14±1.15 Log_{10}CFU/ml. Free MIAP and MIAP-PNAP demonstrated significant dose and time dependent mycobactericidal effect (Figure 8A). Compared with either negative control (no treatment) or blank PNAPs, treatment of Mtb infected RAW264.7 cells with either pure MIAP or MIAP-PNAP reduced the number of intracellular bacteria over a 48h of treatment. CFU assay showed that 10 µM of pure and encapsulated MIAP had no significant killing effect, whereas higher concentration of peptide killed significant number of Mtb population after 48h of incubation. We also evaluated the anti-TB activity of MIAP in combination with sub lethal dose of isoniazid, which is first line standard anti-TB drug.

Treatment of the infected RAW264.7 cells with MIAP-PNAP for 48h at a concentration of 100µM reduced CFU of intracellular Mtb by 2.1 Log_{10}CFU compared with negative controls versus 1.3 Log_{10}CFU for pure MIAP. In parallel experiments, blank PNAPs did not demonstrated significant activity against mycobacterium. Mycobacterial action of the MIAP may be due to either direct lysis of membrane or indirectly due to alternative activation macrophages. Data are representative of three independent experiments carried out. The combination of MIAP-PNAP and INH (1µg/ml) exhibited ~1.7-fold reduction in bacterial CFU compared to bacteria treated with MIAP-PNAP alone and ~2.6 fold reduction after 48 h of incubation. These results indicate that both MIAP-PNAP exhibits a significant synergistic/additive effect with anti-TB drug against Mtb figure 5.7.

Indolicidin PNAPs also showed dose dependent mycobactericidal activity at a concentration of 10µg/ml, 50 µg/ml, 100 µg/ml concentration as shown in figure 5.6.

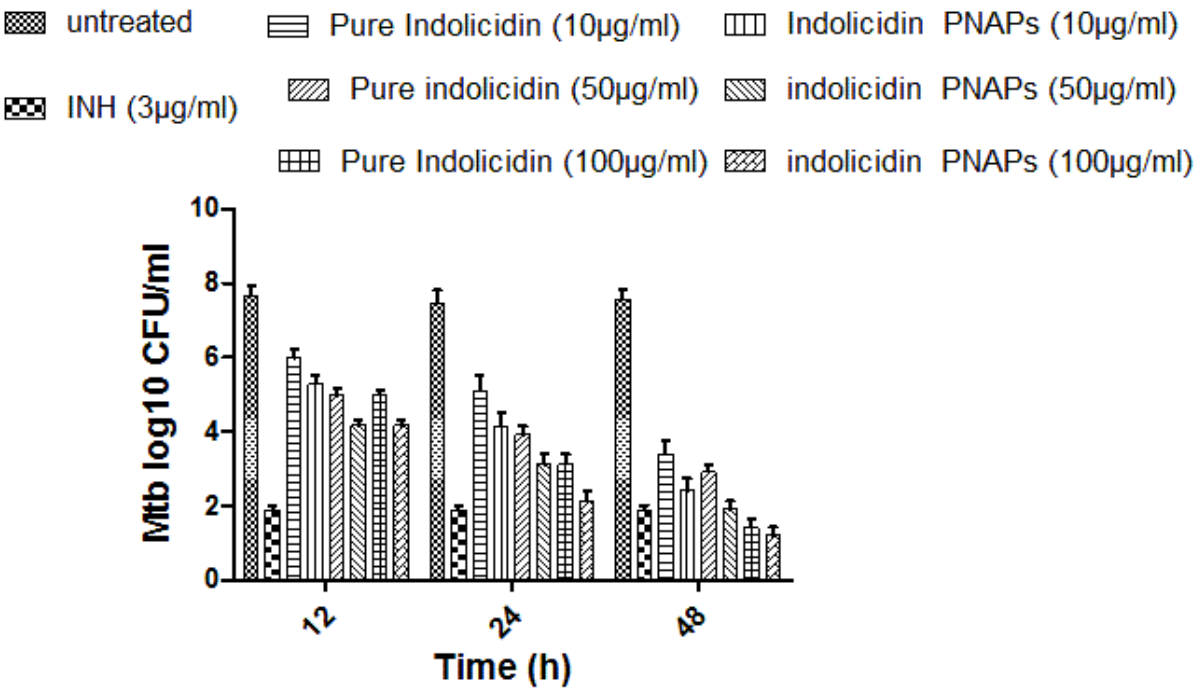

Figure 5.6. Colony Forming Unit (CFU) Assay: CFU of Mtb counted at 21-days after plating lysates recovered 12, 24 and 48 h after infection followed by treatment indolicidin PNAPs. Results means (n=3, ± standard deviation).

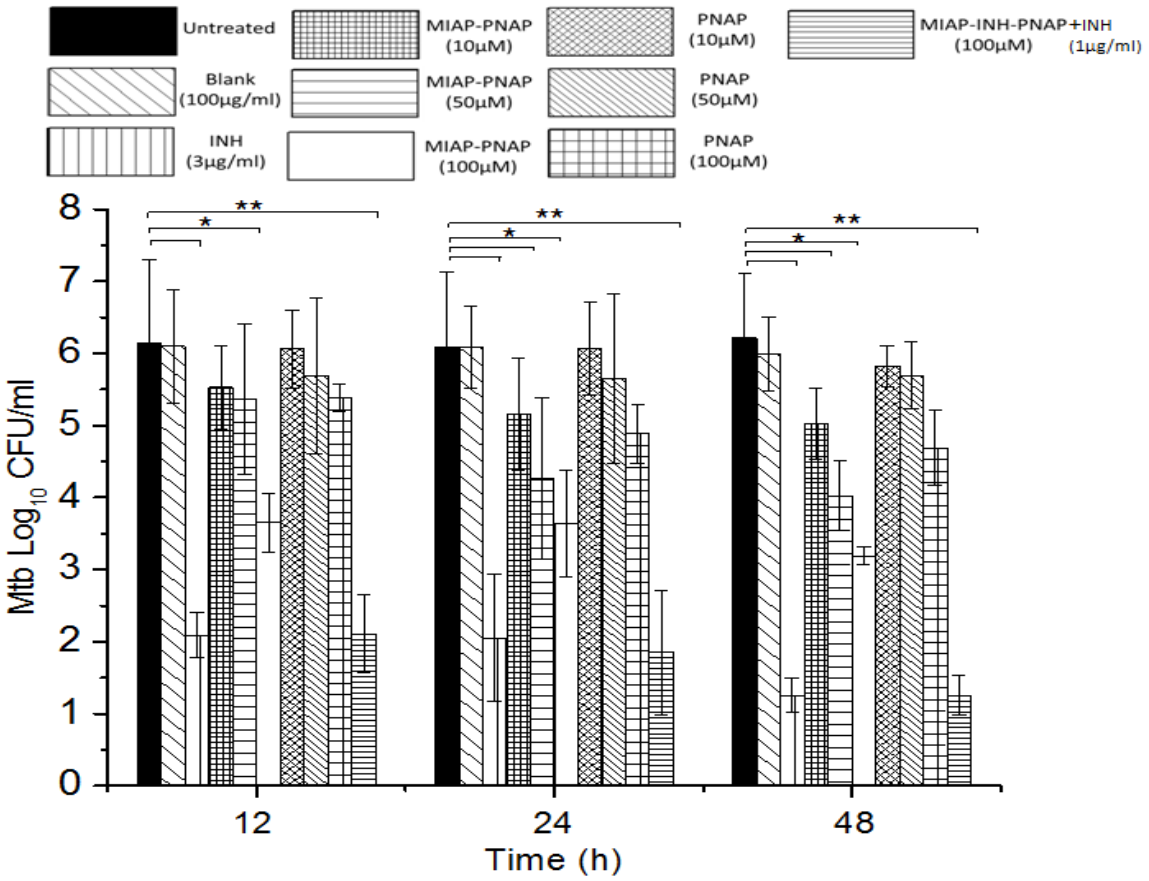

Figure 5.7: Colony Forming Unit (CFU) Assay: CFU of Mtb counted at 21-days after plating lysates recovered 12, 24 and 48 h after infection followed by no treatment, exposure to blank PNAP equivalent in weight to the highest PNAP dose (Blank). Results ar are means (n=3, ± standard deviation).

5.2.3.. Cytocompatibility

- **Porous Microspheres**

AMP cytotoxicity to mammalian cells is a significant concern for their development as clinical anti-TB agents. As a preliminary assessment of the biocompatibility of AMP and their suitability as anti-TB candidate, we measured their cytotoxicity against the Raw 264.7 mouse macrophage cell lines by an MTT colorimetric viability assay. The MTT assay was carried out on uninfected and infected/treated cells at different time-points over 96h following exposure to different doses of AMP. Extending the studies until 96h represents the clearance time of external particles from the lung. Pure and encapsulated peptide exhibited a dose-dependent cytotoxicity that increased with the incubation time. The observed effect on cell viability was also compared with the

unloaded formulation. Macrophages revealed a time-dependent effect ($p < 0.05$), which was particularly visible for AMP -MS for the highest concentration tested (100 µg/ml). As shown in Figure 5.10, all three peptides in soluble form were apparently more cytotoxic in comparison to MS containing equivalent amounts. Free peptides demonstrated pronounced dose dependent-toxicity such that viability of cells fell to 82.48±8.42; 78.66±6.71 and 81.02±4.64 %; by 96 h at highest concentration (100µg/ml) of AMP (Ub2, K4 and Aurein1.2 respectively). The general trend indicates that all three pure peptides used in studies responded with macrophages in a similar pattern and elicited considerable cytotoxicity. PLGA AMP -MS have been shown to be biocompatible when introduced in macrophage cultures with more than ~89% cell viability.

- **Mucus Penetrating Particles (MPP)**

MTT assay was carried out on the RAW 264.7 cells with different doses of pure and IDR-1018 loaded MPPs. Pure and encapsulated peptide exhibited a dose-dependent cytotoxicity that increased with the incubation time. As shown in figure 5.8 the pure peptide was more cytotoxic in comparison to peptide containing equivalent amount of formulation. Pure IDR-1018 showed 73.37 ± 2.8 at highest concentration (100µg/ml) and IDR-1018 formulation showed 89.56 ± 1.2%. cell viability The data generated from the MTT assay showed that the cytotoxicity of IDR-1018 was reduced when encapsulated MPPs shielded the cytotoxic effect of the free IDR-1018 on the viability of the cells. So the developed formulation managed to limit the toxicity of the same amount of IDR-1018 peptide against normal macrophage cells.

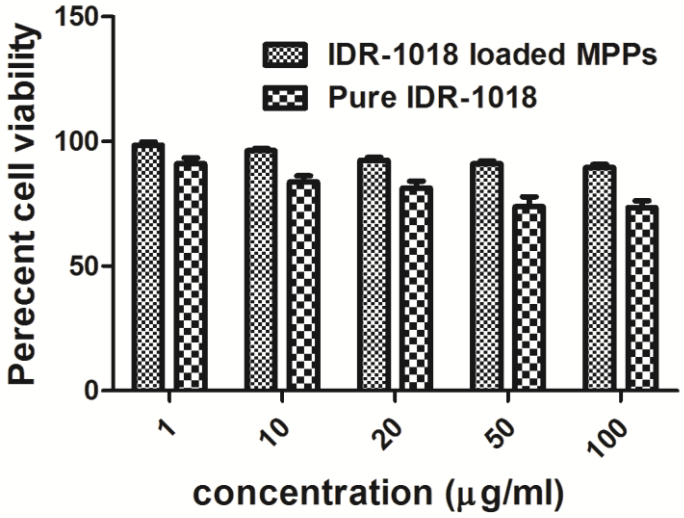

Figure 5.8. Cell viability of IDR-1018 MPPs formulation

- **Porous Nano Particles Aggregates (PNAP)**

The intrinsic cytotoxicity of AMP against mammalian cells is attributed to its reduced applicability as therapeutic agents. The MTT assay was carried out on uninfected and infected/treated cells at different time-points over 48 h following exposure to different doses of MIAP and PNAP. As shown in Figure 5.8, bare MIAP in soluble form was apparently more cytotoxic (73.58±7.14%) in comparison to MIAP-PNAP (85.24±6.29%) containing equivalent amounts. The differences however, were statistically significant (P<0.05) only when the 50 µM and 100 µM concentrations were compared in the case of bare MIAP and PNAP respectively.

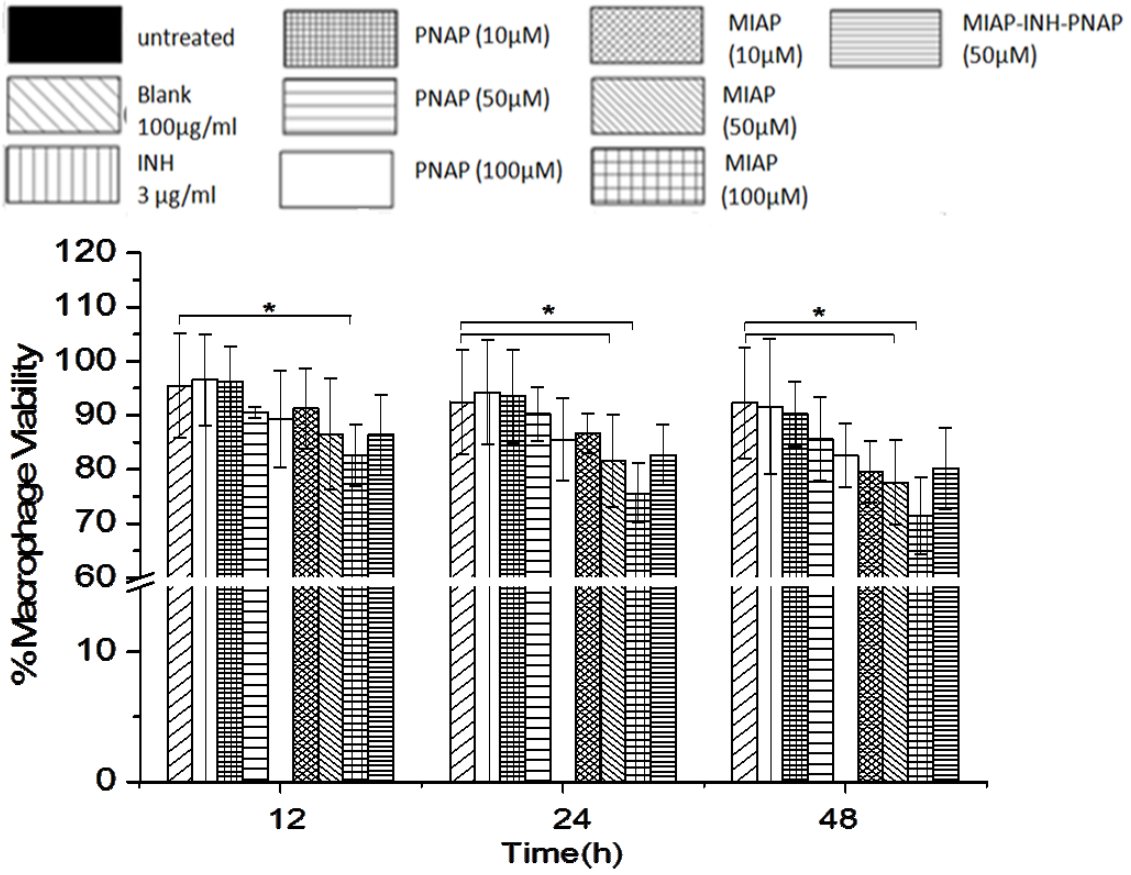

Figure 5.9. Cell viability assay of MIAP- porous nanoparticles aggregate particles formulation

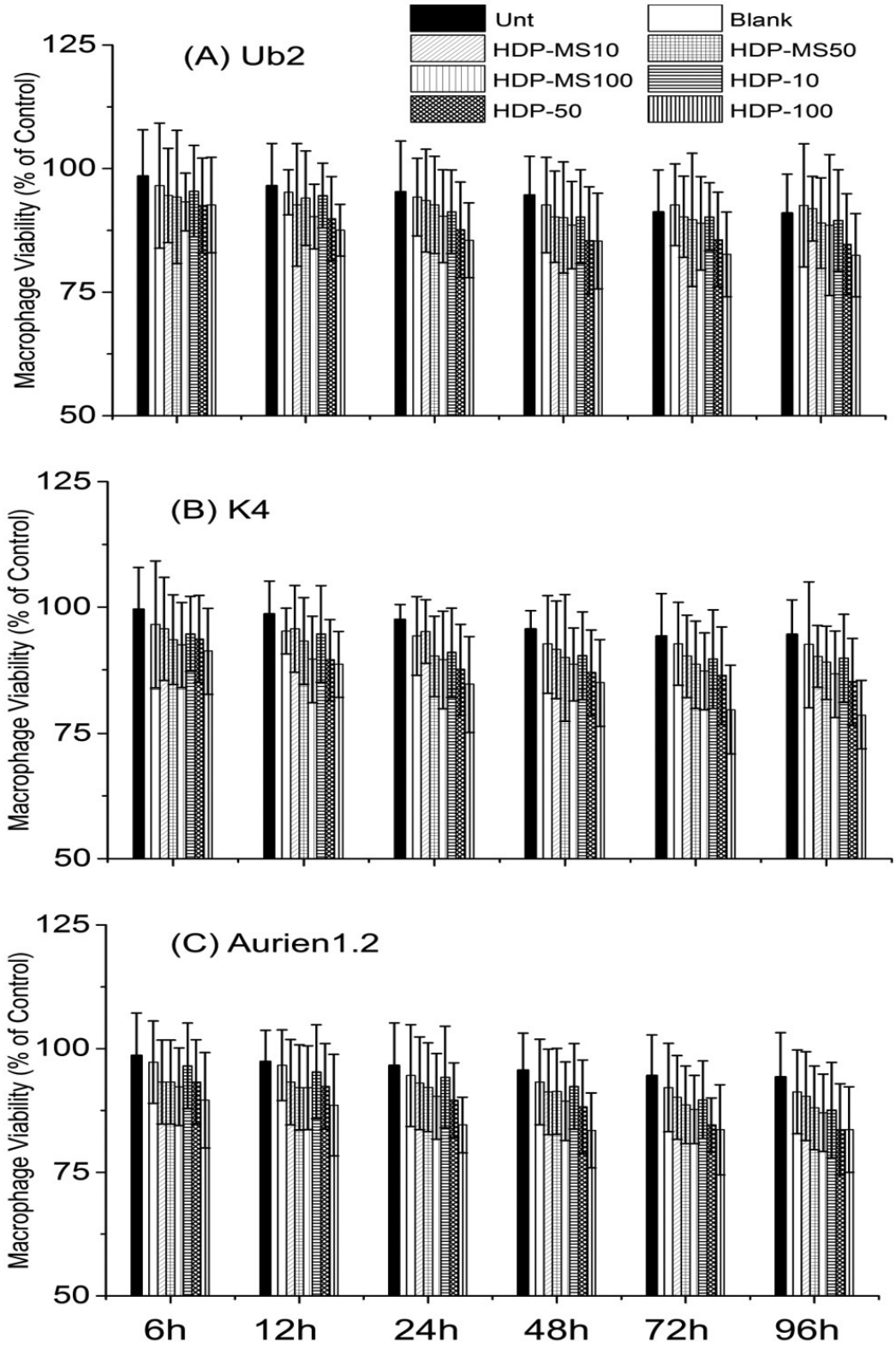

Figure 5.10. Cell viability assay of UB2, K4 and Aurein 1.2 peptide and their formulation

5.3. Conclusion

Formulations developed were actively phagocytosed by RAW264.7 macrophages cells in culture. Dose dependent killing of intracellular Mtb by different formulations were observed in comparison to equivalent amount of bare peptides in solution. Peptide Cytotoxicity was lower in formulation than that of dissolved peptides. So It was concluded that inhalable peptide loaded various formulations can aim AMPs to the infected macrophages and control the release of peptides in macrophage cytosol, and decrease M.tb burden. Thus, inhalable formulations containing AMPs are suitable for exploring as a way of combating pulmonary TB. Results observed here indicate that significant antimycobacterial activity may be achieved if macrophages infected with M.tb are exposed to AMPs.

In the previous study we found that AMP releasing formulations are capable of killing virulent M.tb directly as well as in cultured cells. However the mechanism of action of killing was not clear. Therefore in this chapter an attempt was made to elucidate mechanisms of action, by analyzing the effects of various AMP releasing formulations on a few molecular mechanisms of host response that M.tb evades to ensure its survival.

Resistance to anti-TB drugs is primarily due to unique intrinsic resistance mechanisms that mycobacterium possess. Most important determinant of resistance is a peculiar hydrophobic and multi-layered mycobacterial cell-wall structure with mycolic-acid and wax-D, which restricts permeability of both hydrophobic and hydrophilic drugs into bacteria. it was supposed that AMP which are known to permeabilize bacterial membranes may therefore help anti-TB antibiotics to target internal sites in bacteria.

The survival and pathogenesis of Mycobacterium tuberculosis (Mtb) inside macrophages and monocytes also depends on an ability to control the host cell machinery and evade host's defense mechanisms (103). TB bacteria (virulent H37Rv) successfully reside in macrophages due to its ability to "hijack" phago-lysosome biogenesis and inhibit host-cell apoptosis, as its survival strategy within the host macrophage (104, 105). Inside the macrophages, mycobacterium escapes the lethal effects of lysosomal enzymes and free radicals by halting phagosomal maturation(103). In this perspective, Desjardins and coworkers proposed an interesting "Kiss and Run" model for phagosome maturation in which microbe bearing phagosomes can momentarily/partially fuse (Kiss) with endosomes to permit exchange of some selective solutes, which is followed by quick fission (Run) but not result in complete and irreversible fusion of two membranes (106). Several reports suggested that the activated macrophages enhance the maturation of phagosomes containing mycobacterium and kills mycobacteria through innate antimicrobial effectors. As macrophages kills microbes by mechanisms, which involve participation of lysosomal contents, attention, has been focused on lysosomes in macrophages. Subsequent biochemical events in infected macrophages decide the fate of microbe and macrophage. Further, several reports illustrates virulent strain (H37Rv) inhibits apoptosis of host macrophages to facilitates its survival (103). Recognition of the innate immunity components (effector molecules) that contribute to phagosome-lysosome fusion (PLF) and apoptosis phenomenon will allow rational design of novel approaches to the treatment and prevention of tuberculosis.

6.1. Experimental

The effect of AMPs-releasing formulations on membrane lysis, phagosome-lysosome fusion and apoptosis or necrosis was investigated in RAW 264.7 macrophages infected with virulent ($H_{37}Rv$).

The experimental work is discussed under the following heads:

6.1.1. Materials

2, 7-Dichlorofluorescein Diacetate (DCFDA), Fluorescein Isothiocyanate (FITC), 4', 6-Diamidino-2-Phenylindole (DAPI), AnnexinV-Propidium iodide (PI) apoptosis detection kit, Paraformaldehyde and Triton-X-100 were purchased from Sigma chemical (St Louis, USA). Cell culture media and supplements were also obtained from Sigma chemical (St Louis, USA). Cytokine ELISA kits were procured from R&D Systems (Minneapolis, MN, USA). Other reagents and solvents used in the study were of analytical grade purchased from Merck chemicals (Bangalore, India).

6.1.2. Mycobacterial membrane integrity analysis

The interactions of selected AMP with intact M.tb were investigated using SEM and contact mode AFM. Direct observation of the effects induced by sustained released peptides from polymeric MS on bacterial cells was imaged (107). Mycobacteria (~2x107 cells/ml in Middle brook 7H-11 medium) were incubated with intermediate concentration (equivalent of 50µg/ml of peptide) of individual AMP-MS in separate experimental groups. After 12h of incubation, bacteria were centrifuged at 2000g for 15 minutes at 4°C and subsequently plated on coverslips (coated with poly-L-lysine) present in 6 well culture plate. Adhered bacterial cells were washed with 10µM PBS to remove microspheres. Bacterial samples were then fixed by treating them with 2% formaldehyde and 1% glutaraldehyde for 2 hours at 4°C. After critical point drying, samples were coated by gold sputter for SEM analysis (JEOL 6400; JEOL USA, Peabody, MA).

Similar studies were conducted over mica sheet for AFM analysis (Bruker MultiMode 8, NanoScope V controller, Bruker Co, USA).

6.1.3. Antibiotic accumulation assays

Exponentially growing *M.tb* was harvested at an optical density at 600 nm (OD_{600}) of 1.0, by centrifugation (3000 × *g*; 15 min). The pellets were then re-suspended in OADC free Middle brook broth which was adjusted to an OD_{600} of 4.0. Antibiotic uptake assay was conducted at an Isoniazid (INH) concentration of 10µg/ml for short period of 2h. The purpose of using higher antibiotic concentration (more than MIC value) in this procedure, to assure that the internalized antibiotic concentration fall under limit of detection (LOD) of the HPLC. Briefly, bacteria (~2×10^{12} Mtb/ 2ml) was pre-treated with intermediate concentration of individual AMP (50µg/ml; Ub2, K4 and Aurien1.2) in designated wells 6-well plate for interval of 6h. Further, bacteria in each well were incubated with 10µg/ml of Isoniazid for 2 h. In negative control group, cells were treated with similar concentration of INH without pre-treatment of HDP. After completion of incubation, bacteria were pelleted by centrifugation (10000 × *g*; 10 min) and washed twice with PBS (10mM). Bacilli were then re-suspended in 0.1 M glycine-HCl and finally disrupted by sonication. Bacterial lysates were centrifuged at 10000× *g* for 10 min at 4°C and the supernatants were separated. The resultant supernatant was filtered through 0.22µm PVDF membrane. INH was extracted with 1ml portions of Methanol-Acetonitrile (70:30, v/v) by vortexing for 1min followed by centrifugation at 4,000 *g* for 10 min. The supernatant was decanted, the process was repeated three times, and supernatants were pooled. The aqueous layer was separated by centrifugation of pooled supernatant at 4,000 *g* for 10 min. and 200 µl was aspirated from the top. RP-HPLC is performed using mixture of Triethylamine buffer (TEA) with ACN (3:97) as the mobile phase and measuring absorbance at 262 nm (108).

6.1.4. Phagosome-Lysosome Fusion (PLF) analysis

- **Labelling of bacteria**

Mycobacteria (4.5×107) to be used for Phagosome-lysosome fusion (PLF) studies were stained with Fluorescein Isothiocyanate (FITC). The bacteria were fluorescently labelled by incubation with 1 µg/ml FITC in 0.2M Na2CO3–NaHCO3 buffer containing 150 mM NaCl (carbonate

buffer, pH 9.2) for 2h at room temperature(109). The flourescent bacteria were washed five times in PBS buffer(110).

- **Bacterial infection and treatment**

Phagosome-Lysosome Fusion (PLF) (co-localization) experiment was performed in mouse macrophage cell line RAW264.7 adhered on 22× 22mm coverslips (Poly-L Lysine coated) (1.5×106 cells/well in a 6-well plate) (111). Cells were infected with fluorescein-labeled mycobacteria (MOI:10) for 2h, then washed with incomplete DMEM media to remove extracellular bacteria. Six different treatment groups were made, first was kept untreated; second was positive control, treated with 3µg/ml of Chloroquine (CQ) (Standard PLF inducer); third group cells were incubated with blank PNAP (equivalent to weighed amount of MIAP-PNAP taken in the experiment); fourth, 100µM of pure MIAP; fifth, MIAP-PNAP equivalent to 100µM of MIAP; and sixth group was treated with standard anti-TB drug, Isoniazid (INH) (3µg/ml). Formulations and free peptides/drug were incubated for 3h followed by washing of cells with incomplete DMEM media to remove extracellular drug /formulations. Cells were further incubated for 24h.

- **Labelling of lysosomal compartments**

LysoTracker Red was added to each well at the 1:10,000 dilution concentrations and incubated for 2h.

- **Cell permeation and fixation**

After completion of incubation, cells were washed three times with PBS and treated with para-formaldehyde (4%) for 20 min at 4°C to fix the cells. Cells were then washed two times and permeabilized with TritonX-100 solution (0.01% in PBS). Cells were washed three times with PBS and then stained with nucleus specific dye DAPI (4, 6-diamidino-2-phenylindole, Dihydrochloride) (0.5µg/ml) for 10 min.

- **Confocal scanning Laser Microscopy (CLSM)**

Cells were washed five times and, coverslips were mounted using buffered-glycerol (90% glycerol in PBS) and sealed with nail polish. Confocal microscopy was performed on Nikon C2plus CLSM using NIS element software. An argon/krypton laser (excitation-488 nm/

emission-530 nm) was used for evaluation of FITC fluorescence, and a helium/neon laser (excitation-543 nm/emission-585nm) for recognition of LysoTracker Red. The percentage of M.tb phagosomes colocalizing with the marker of interest was determined by counting 20 different fields per condition. Intracellular FITC labelled mycobacterium were green colored; Acidified lysosomes stained with lysotracker dye were red in color; and florescent intracellular bacteria fused with lysosomes emerge orange-yellow(112). PLF endpoints were evaluated by scoring for the percentage of orange-yellow cells in the field of view (110).

6.1.5. Reactive Oxygen Species (ROS)

Intracellular Reactive oxygen Species (ROS) levels were evaluated using flow cytometry in macrophages, cultured in serum-free medium and loaded with the redox-sensitive dye DCFH-DA(113). Briefly, RAW264.7 macrophages (1.5×10^6 cells/well in a 6-well tissue culture plate) were infected with mycobacteria at an MOI of 10 and washed after 3h. The cells were washed with serum-free DMEM to remove extracellular bacteria, complete medium was replaced, and culture plates maintained at 37°C in 5% CO_2. Four experimental groups were made. The first was kept untreated; the second was incubated with blank MP (equivalent to weighed amount of MIAP-PNAP taken in the experiment; third was incubated with MIAP (100µM), and forth with MIAP-PNAP (equivalent to 100µM of MIAP). At the time intervals of 12 and 48h following treatment to infected cells, 10µM DCFDA was added to each well and incubation was allowed to proceed for 20 min. Cells were washed, harvested from wells by scraping and analysed for intracellular fluorescence using a BD-Facscan instrument (BD, USA) and Cell Quest software.

6.1.6. Quantitation of free NO

Nitrite accumulation/release into culture supernatants was measured as an indicator of NO production by uninfected/TB infected macrophage exposed to MIAP alone (100µM) and encapsulated after 48h. The results were further, compared with nitric oxide generated by cells treated with equivalent amount of blank formulation. Fresh culture supernatants from different groups were mixed with identical quantity of Griess reagent (1% Sulfanilamide, 0.1% Napthyl-ethylenediamine, 2.5% H_3PO_4), incubated at room temperature for 15 min and the absorbance was measured at 546 nm using a microplate reader (Biotek, USA).

6.1.7. Apoptosis

Apoptosis or necrosis examination of the RAW264.7 macrophages after uptake of bare and encapsulated MIAP was evaluated in uninfected and *M.tb*-infected cells by flow cytometry. Early apoptotic changes were evaluated by staining macrophages with FITC-conjugated Annexin-V-PI apoptosis kit according to the manufacturer protocol (Sigma, St Louis, USA). Briefly, RAW264.7 macrophages (1.5×10^6 cells/well in a 6-well tissue culture plate) were infected with mycobacteria at an MOI of 10 and washed after 3h. Infected macrophages in designated wells were incubated with (i) Cyclohexamide (CHX, 100µg/ml, standard pro-apoptosis drug) (ii) Blank-PNAP (equivalent to weight of MIAP-PNAP) (iii) Free MIAP (100µM) and (iv) MIAP-PNAP (equivalent to 100 µM MIAP) for 48h. Cells were washed with incomplete DMEM medium to remove extracellular particles and peptide/drug. Macrophages were harvested by trypsinization, centrifuged at 300×g for 10min. Further, cell were suspended in 500µl PBS containing 5µl annexinV-FITC and 10µl of a propidium iodide solution (PI) (50µg/ml) (Sigma, Saint Louis, USA) incubated in dark for 30 min at 4°C and then washed with Annexin-binding buffer and the cells were analyzed by FACS (FACS calibur, Becton Dickinson Mansfield, MA, USA**).**

6.2. Results and discussion

6.2.1. Interaction between AMP compromise Mycobacterium wall

Mycobacterial morphology and membrane integrity were directly visualized by SEM and AFM upon incubation with sustained released peptides for 12h. Treatment with AMP at the 50µg/ml for 12h induced recognisable membrane damage as compared to the control group of bacterial cells, which exhibited an intact and smooth surface (Figure-6 Panel:1 & 2). *M.tb* cell wall is relatively less permeable towards AMP as compared to membranes of other Gram-negative or Gram-positive bacteria. These short peptides are ought to intercalate in lipid membrane and permeabilize it by the micellar aggregate channel model (114). Exposure of released AMP induced alteration in the cell-wall of mycobacterium by permeabilization of bacterial membranes, which ultimately lead to bacterial death. AFM (Figure-6 Panel: 1) and SEM (Figure-6 Panel: 2) results showed that all three active peptides interacted with the rigid mycobacterial cell envelope and killed bacilli by destroying the integrity of their membranes. Some of the AMP treated *Mtb* cells appeared corrugated and rough with certain depressions and

blisters on the membrane surface. Eventually, some bacterial cells lost their original structure with blebbing of cell membranes. The cell wall surface of mycobacterium treated with Ub2 showed more blebbing, corrugation, and intracellular content leakage compared to K4 and Aurien1.2. The results correspond to bacterial killing assay and revealed discontinuities in the cell membrane with occasional blebs suggests that the membrane is the target of AMP action.

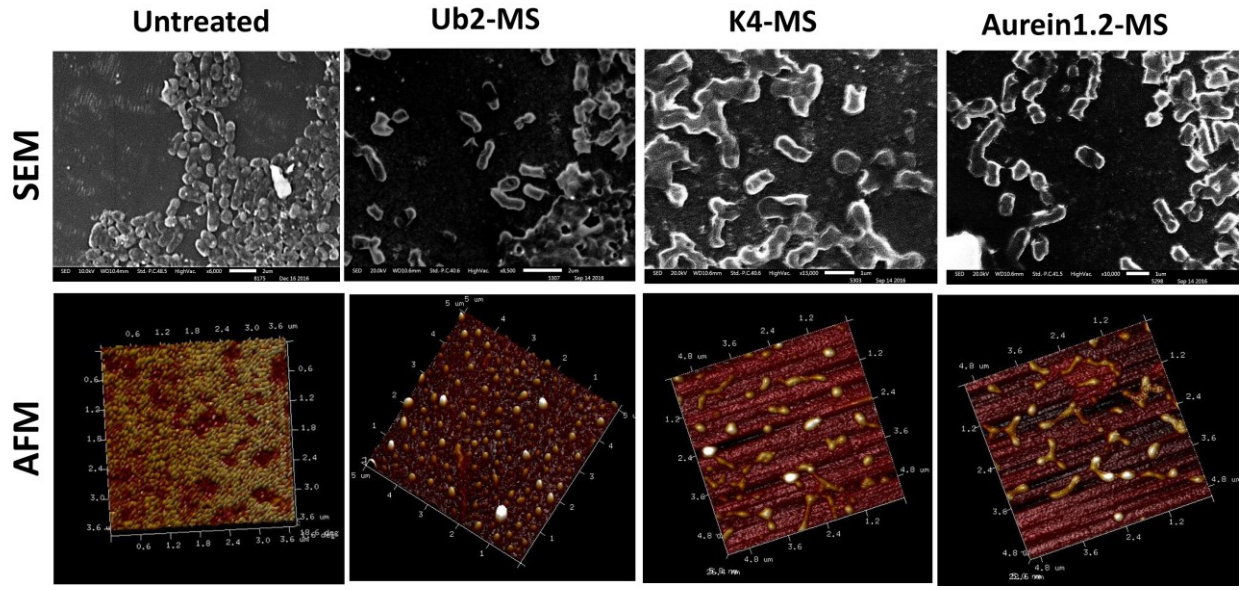

Figure 6.1: Interaction study of sustained released AMP with mycobacterium Morphology analysis of mycobacterium by SEM (Panel.1) and AFM (Panel.2) revealing the interaction of sustained released AMP with mycobacterium cell wall leading to damage of cell

6.2.2. Enhanced penetration of antibiotic into Mycobacterium

Drug penetration-assay in exponentially growing *M.tb* was performed in the presence of standard anti-TB antibiotic (INH, 10µg/ml) after pre-treatment with sub-optimal concentration of individual AMP (10 µg/ml) in separate experimental groups. Internalized INH was extracted from bacterial lysate (in glycine buffer) using solvent (Methanol-Acetonitrile 70:30v/v) extraction method. Subsequently, drug concentration was determined using the reverse phase HPLC method. After incubation of mycobacterium (~2×10^{12}) with INH (10µg/ml) for 2h, intracellular accumulation of approximately ~220.68±59.54 ng was observed in negative control group (without AMP pre-treatment). Pre-treatment of bacterial cells with suboptimal concentration (10µg/ml) of individual AMP for 6h, drastically increased (up to 4times) intracellular amount of antibiotics compared to negative control cells. As a result, the total

intracellular uptake of INH is shown in Figure-7. INH accumulated to intracellular concentrations was evaluated as approximately ~ 956.28±129.87ng (Ub2), 553.15±151.24ng (K4) and 768.65±109.28ng (Aurien1.2) in ~2×10^{12} of mycobacterium. The statistical significance was shown between the negative control and AMP pre-treated mycobacterium ($p < 0.05$), suggesting that INH uptake by AMP treated cells were significantly greater than the control mycobacterial cells. Ub2, K4 and Aurien1.2 enhanced penetration of antibiotic into bacteria by ~4.34, 2.51 and 3.5 folds as compared to untreated bacteria (Negative control group). Antibiotic permeation into mycobacteria is an important factor that influences anti-bacterial activity. Collectively, our results reveal that the extent of drug penetration in *M.tb* was significantly augmented by all three AMP used in the study.

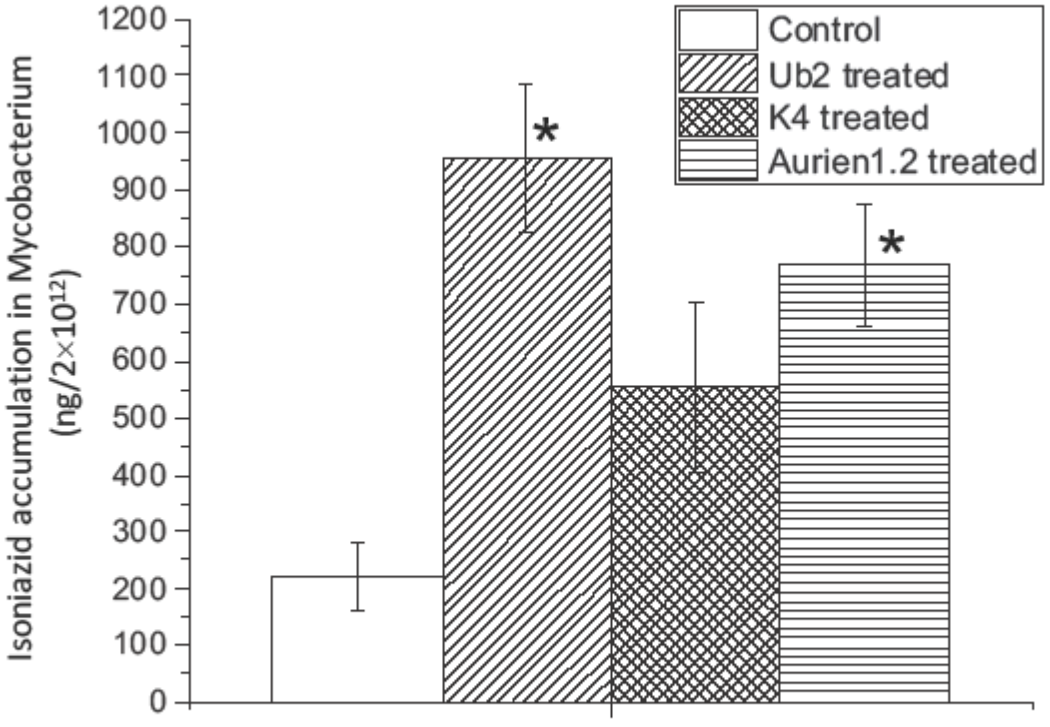

Figure 6.2. Antibiotic uptake in Mycobacterium tuberculosis H37Rv: Intracellular INH contents of replicating Mtb measured by RP-HPLC

6.2.3. Mycobacterium hijack phagosome

Colocalization of the lysosome specific-acidotropic dye LysoTracker Red DND-99 with phagosomes containing live virulent *M.tb* in mouse macrophages was examined by confocal microscopy. For each field, three images were recorded: First for the cell nuclei (blue), second for the FITC-labeled mycobacterium-positive compartment (Green) and third for LysoTracker-DND-99 positive compartment (red). Nucleus was stain with DAPI for precise positioning and cell number quantification of macrophages. This procedure improves the visualization of PLF phenomenon by the development of an orange-yellow color on fusion of the green-fluorescent phagosome compartment with the red-fluorescent lysosomal compartment. Twenty fields of each treatment groups were observed and evaluated. In untreated control group, the majority of phagosomes containing H37Rv *M.tb* did not co-localized with the acidic lysosomes (LysoTracker dye) in 24h (Figure.5A, Panel-1) demonstrating the ability of H37Rv *M.tb* to prevent phagosomal maturation. The fraction of bacteria co-localizing with LysoTracker-positive staining was less than ~6% in cells infected with *M.tb*. Similar observation was noted in the group where infected cells were treated with blank PNAP for same interval (Figure.5A Panel-3). The results indicate *M.tb* successfully resides in macrophages due to its ability to arrest phagosome maturation and creating a less acidic intracellular compartment, as its survival strategy within the host macrophage. *M.tb* manipulates the host cell machinery so as to limit the fusion between endosomes with phagosomes and thus avoid its microbicidal properties.

6.2.4. AMP-PNAP enhance PLF

The ability of *M.tb* to prevent phagosomal maturation was significantly compromised, as high magnitude of phagosome-lysosome fusion (PLF) was observed in the cells treated with MIAP-PNAP (equivalent to soluble peptide 100μM). Within 24h of treatment with MIAP-PNAP, there was 78.57±12.58% of PLF (Figure.5A Panel-5). The intensity of co-localization of the LysoTracker containing lysosomes with *M.tb* containing phagosomes was relatively lesser in the cells treated with bare peptide (24.88±9.17%) (Figure.). These results suggest that exposure of *M.tb* infected macrophages to exogenous MIAP; render mycobacterial phagosomes susceptible to acidification. Infected cells treated with standard anti-TB drug Isoniazid (3μg/ml), did not show to promote phagosome maturation in phase of 24h (Figure.5A, Panel-6) but within 72h it shoots up to 27.5±10.20 % (Data not shown). It appears that, in early 24h majority of

mycobacteria is live which prevents PLF, but in later hours, bacteria was killed by drugs these dead *M.tb were* not able to prevent phagosomal maturation.

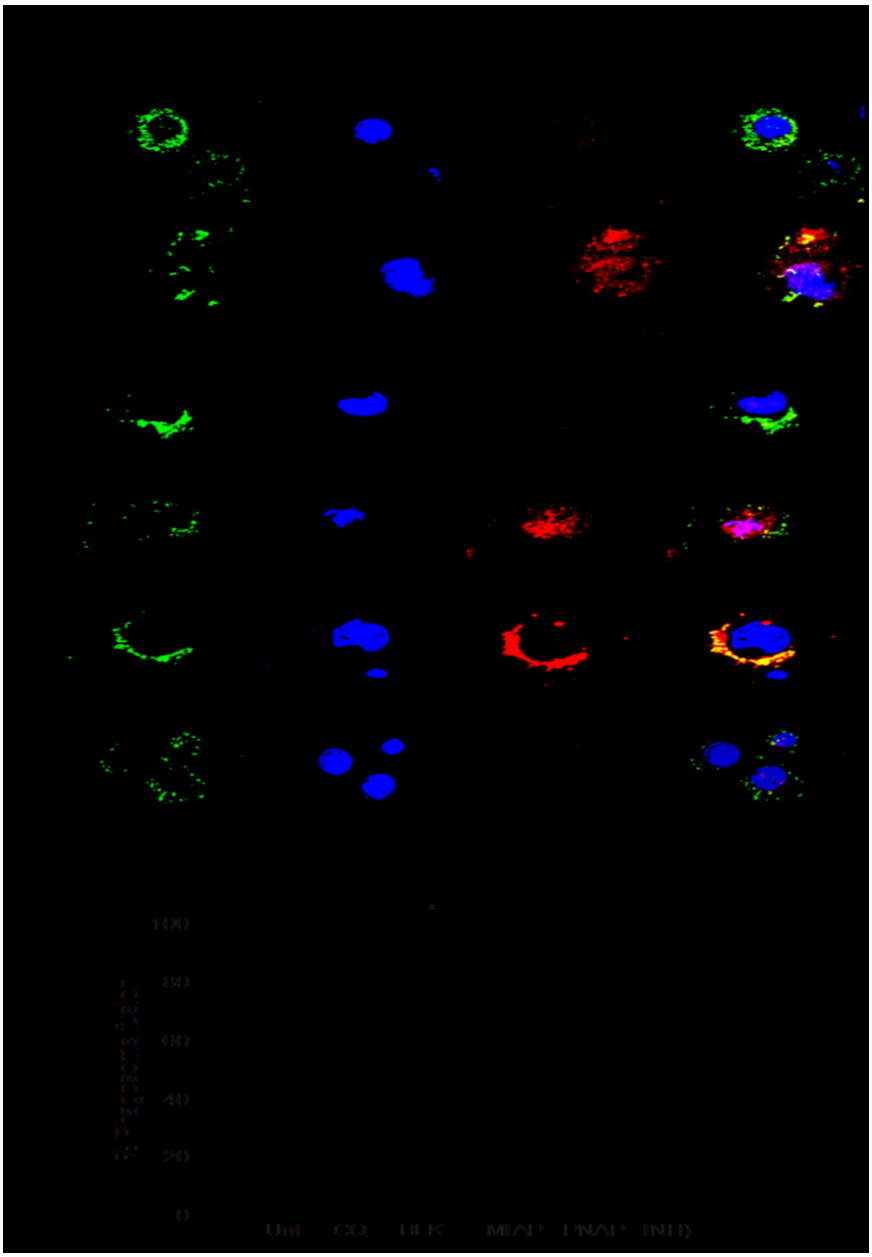

Figure.6.3. Phagosome–lysosome fusion: (A) Quantification of Mtb intracellular trafficking into acidified lysosomal compartments by confocal microscopy. Macrophages were infected with FITC (Green)-labeled Mtb H37Rv and stained with LysoTracker red DND (Red) for acidic lysosome and with DAPI (blue) for cell nuclei. Panel-1 Untreated cells; Panel-2 Positive control Chloroquine; Panel-3 Blank PNAP; Panel-4 pure MIAP ; Panel-5 MIAP-PNAP; Panel-6 Standard anti-TB drug Isoniazid treated cells. (B) Comparative quantitative analysis of percentage of Mtb phagosomes colocalizing with LysoTracker-stained lysosomes.

6.2.5. ROS production

The interplay between *M.tb* and host macrophage during the oxidative burst is complex, relying on both; the ability of the macrophage to produce ROS and the ability of *M.tb* to counteract this response. Untreated *M.tb* infected cells (Yellow colour) showed enhanced ROS generation in 6h after mycobacterial infection which was slightly reduced in next 24h (Figure.6A).

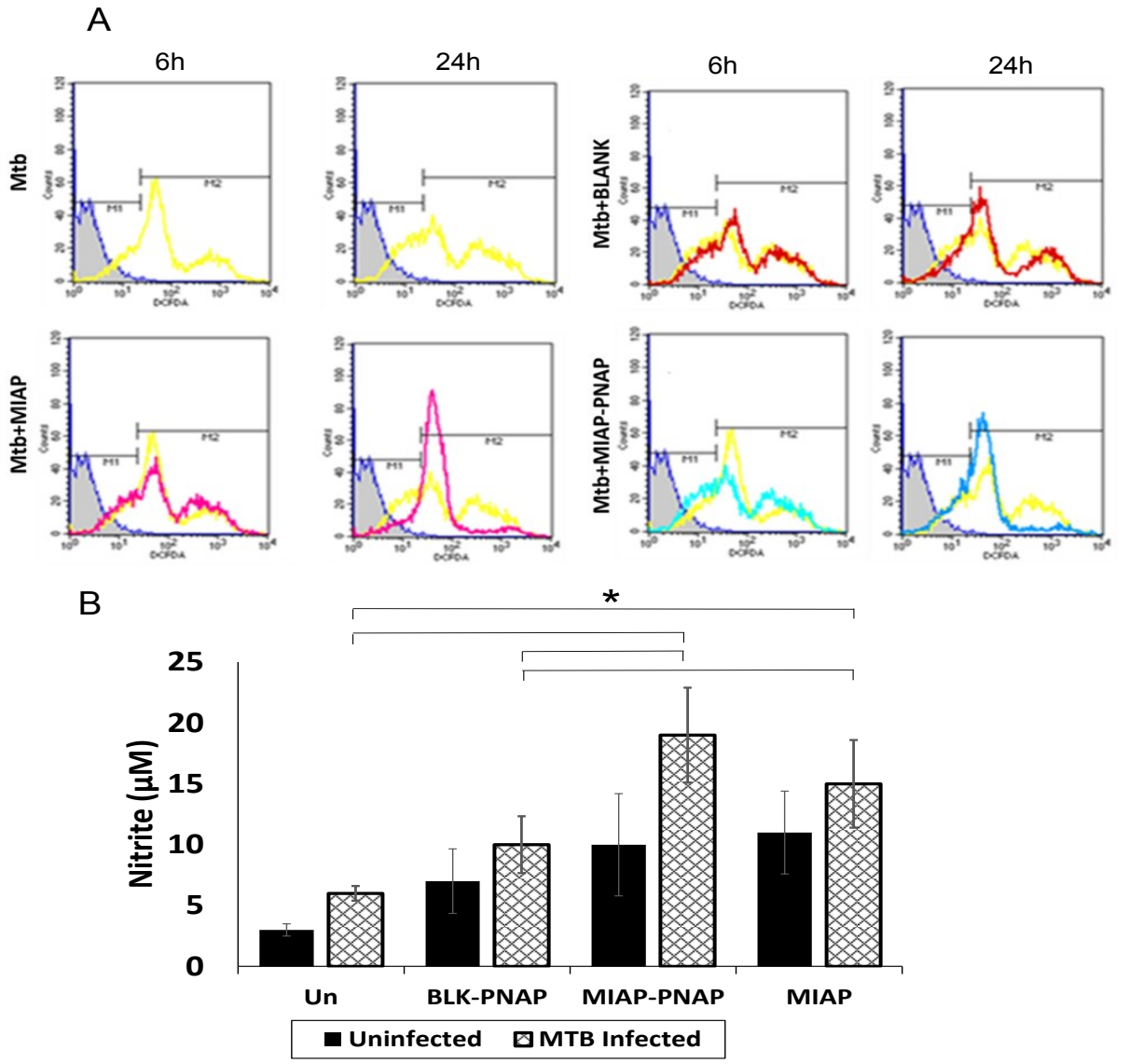

Figure 6.4. Free radical generation: (A) Reactive Oxygen Species (ROS) generation in response to different modes of treatment at 6 h and 24 h (B) Nitric oxide released in cell culture supernatant

Enhancement of ROS generation in the initial phase of infection may be attributed to initial innate response by infected macrophage in attempt to eradicate *M.tb*. After 24h of infection, reduction in ROS may be interpreted as successful implementation of the survival strategies of *M.tb* to inhibit ROS production. Blank PNAP enhanced ROS production (Red Colour) to some extent at both of the time points in infected cells. Both, MIAP alone and encapsulated peptide demonstrated significant augmentation of ROS generation in respect to uninfected controls. ROS generation was relatively high in the infected cells treated with bare peptide compared to formulation treated macrophages. This phenomenon of ROS generation may be attributed to two specialized mechanisms; (i) ROS generation after interaction of plasma membrane with peptide via NAPDH-oxidase mechanism; and (ii) through mitocondrial ROS generation mechanism after ingestion of peptide inside the cells. Microencapsulated peptides produces ROS by through mitocondrial ROS generation mechanism only. These results also indicate that exogenous MIAP stimulate macrophages to generate ROS which may enhance superoxide and contribute to bactericidal activity of macrophage by formation of free radicals.

6.2.6. Quantitation of free NO

Inhibition of intracellular nitric oxide (NO) production and scavenging of nitrosative free radicals is one of the evade mechanisms by M.tb. A small amount of NO was secreted by uninfected macrophages (3.15±0.41μM) which increased up to 6.18±0.52μM after mycobacterium infection. The amount nitric oxide released from uninfected macrophages was significantly lower as compared with infected cells in all treatment groups. MIAP caused a substantial increase in nitric oxide production (15.21±3.64μM) as compared to untreated and blank-formulation (9.11±2.39μM) treated cells. Higher NO concentration (19.45±4.01μM) was detected in respect of cells treated with PNAP-MIAP rather than with MIAP alone in solution. The differences between NO released by the cells treated with encapsulated PNAP and bare MIAP were statistically significant ($P<0.05$, ANOVA) after 96h(115).

6.2.7. Apoptosis induction in infected macrophages

To establish the regulatory role of sustained delivery of MIAP peptide on macrophage apoptosis and whether exogenous MIAP alone is able to modulate macrophage apoptosis independently of M.tb infection, we treated uninfected and TB infected cells with MIAP alone and encapsulated peptide. The results are demonstrated in Figure 6.5 correspond to the representative scatter dot

plots of AnnexinV-PI staining in TB infected macrophages, and enumerated proportion of apoptotic cells.

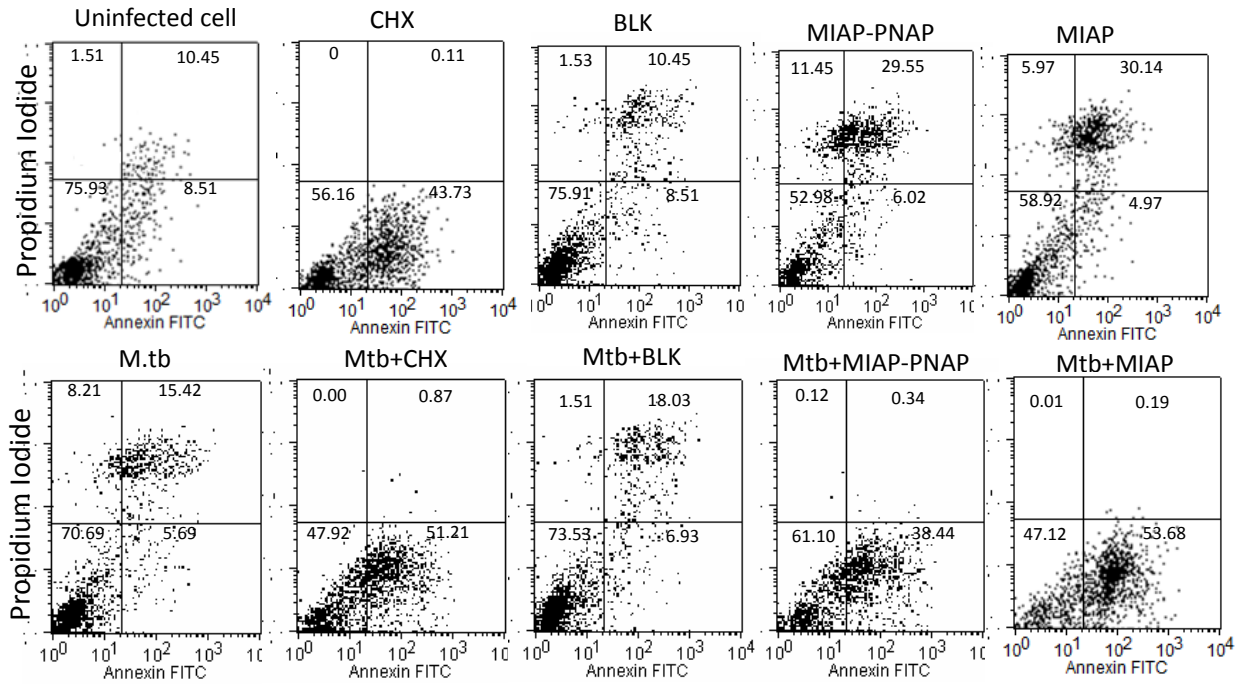

Figure 6.5. Flow cytometry profile represents Annexin-V-FITC staining on the X-axis and PI on the Y-axis. The numbers represent the percentage of cells in each quadrant.

Standard pro-apoptotic drug cyclohexamide at concentration of 50µg/ml show ~41% and ~52% of apoptosis in uninfected and infected macrophage cell population respectively. Blank-PNAP, MIAP-PNAP and free peptide (100µM) alone at equivalent concentrations were not able induce considerable apoptosis in uninfected cells. Similar concentrations of MIAP alone or MIAP-PNAP induced significant magnitude of apoptosis in M.tb infected (Virulent H37Rv) macrophages. The incidence of early apoptosis in infected cells was 52.25±9.54% and 37.41±6.58% in pure-MIAP and MIAP-PNAP treated group respectively. A very small number of macrophages showed apoptosis in the untreated and blank-PNAP treated cells. These observations infer that combination of microbial infection and treatment is required for optimal apoptosis induction in macrophages. Uninfected cells incubated with pure and encapsulated MIAP show some incidence of necrosis with unknown mechanism. The apoptosis of M.tb infected macrophages can be an important anti-TB defense mechanism, and there is a dysregulation of these mechanisms in infected macrophages. The results suggest that pure MIAP and MIAP-PNAP are able to revert the apoptosis mechanism in infected macrophages. These

findings implicate MIAP as an important factor in host-mediated macrophage apoptosis during TB infection. Further, it also suggests, that the presence of this AMP allows removal of activated macrophages by apoptotic process that is likely to minimize local inflammatory damage to tissue(116).

6.3. Conclusion

We investigated effects of sustained delivery of exogenous AMPs on some cellular and molecular mechanisms by which Mtb evades host responses. Our investigations suggest that AMPs releasing MIAP PNAPs reduce ROS in infected cells. This suggests that mycobacterial killing by exogenous AMPs at low concentration is not through generation of superoxide. Finally, it can be concluded that at low doses, AMPs-releasing formulation kill intracellular *M.tb* by activation of macrophage responses such as PLF and apoptosis. The permeabilization of the outer mycobacterial membrane by AMP enhanced the intrinsic efficacy effect of the INH by allowing access of internal target sites.

Most of the delivery systems relied on oral or parentral route to target lungs which is not suitable for local delivery to the lungs. Administration of oral or intravenous AMP may led to various side effects hence we preferred targeted lung delivery to overcome the adverse effects, which require small dose and minimize bioavailability in systemic circulation. Inhalable particles with optimum aerodynamic properties can release the drug directly to the lungs and may create new opportunities for the pulmonary diseases like tuberculosis. Based on our previous results in vitro activity the optimized MPPs and PNAPs formulation was selected for the *in vivo* activity. Inhalable AMP releasing formulations, offer benefits associated with targeting very small doses to lung macrophages to achieve high intracellular levels. Sustained release of AMP from formulations (MS coated to form MPPs and PNAP) straight to the lungs offers numerous returns including enhanced targeting to Mtb containing alveolar macrophages and decline in systemic side effects by diminishing dose and frequency. As the addition of prior study, in the present segment, we wanted to assess the *in-vivo* efficacy of inhalable AMP containing formulations as adjunct therapy and to come across a position in typical regimen of tuberculosis therapy. Here, we account *in vivo* anti-TB activity of inhalable indolicidin and IDR-1018 AMP releasing formulations after each day dosing with and devoid of standard anti-TB drugs i.e. Isoniazid in Mtb infected Swiss mice up to 6 weeks (5 days/ week). The AMP IDR-1018 and indolicidin were selected for in vivo efficacy because these two peptides were having good MIC values and have good results in *In Vitro* experiments. The results obtained were compared with oral chemotherapy with conventional anti TB drug. The efficacy of the formulation was determined by quantifying lung and spleen bacillary load by calculating colony-forming units (CFU), morphology of the lungs and spleen and histopathology of lungs and spleen.

7.1. MATERIALS

7.1.1. Chemicals

Isoniazid and Rifampicin was procured from sigma. Oral gavage cannula (20 gauges) was procured from Alzet Accessories, USA. Purified water from a Milli Q (Millipore corp. USA) water purification system was used in all experimental procedures. All additional materials were the same as described above.

7.1.2. Animals

Seventy six male Swiss mice weighing 25–30 g, were obtained from the Laboratory Animals facilty of Indian institute of Toxicology Research (IITR), Lucknow and maintained in the animal biosafety level-3 (ABSL-3) lab throughout the study of the National JALMA Institute for Leprosy & Other Mycobacterium Diseases; Agra, India. All the animal work was done according to the guidelines and approval of the Ethical Committee for Experimentation in Animals of the National JALMA Institute for Leprosy & Other Mycobacterium Diseases; Agra, India and all efforts were made to minimize suffering. Prior consent and procedure approval were taken from Institute's Animal Ethical Committee (IAEC) for animal experimentation**.**

7.2. Fabrication and optimization of in-house inhalation apparatus

7.2.1. Fabrication of in-house Inhalation apparatus

The inhouse inhalation apparatus for dry powder inhlation consist of 15 ml (Tarson) tube in which two holes are made (figure 7.1). One whole (on the tapering end) is connected with a tube and at the end of the tube one pipette bulb is connected and other hole is made at the cap of the tube. This hole should be enough to act as delivery port of the AMP loaded particles. Te size of the tubing connected was 1.5mm×0.8mm×3mm . The apparatus reported here was designed to fluidise a powder bed within the boundaries of the centrifuge tube by revenue of a disorderly air stream (1).

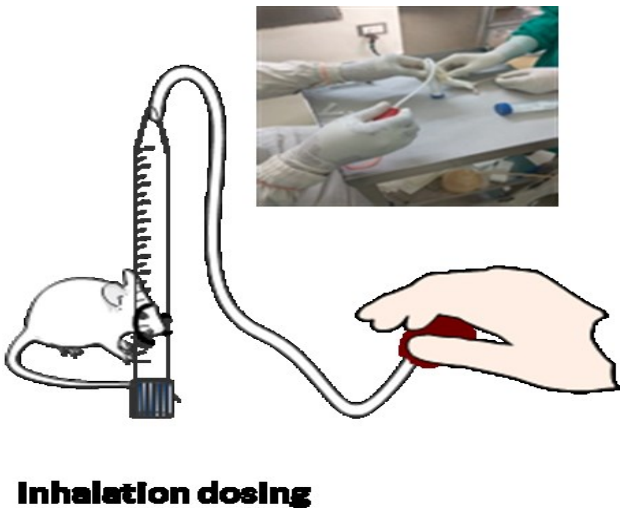

Figure 7.1: Fabrication of In-house inhalation apparatus for nose only pulmonary delivery of formulation

7.2.2. Operation of the apparatus

AMP loaded particles were weighed and positioned in the cap of the 15 ml tube. An experimental animal was then restrained with its nares inserted in the release port, without touching the particle bed. The pipette bulb was pressed and released once every second over the desired period of exposure, to fluidise the particles bed and generate a 'dusty' environment for the animal to breathe in (117).

7.2.3. *Determination of emitted dose (dose available for inhalation)*

AMPs (20 mg) were taken for fluidisation. Different amount of particles (10, 20, 30 mg) were fluidized for 30 sec. Pre-weighed wads of cotton wool (~300 mg) were used to completely occlude the delivery port during operation. For each dose 6 wads were used. The surface of the wad exposed to the fluidized powder remained flush with the inner wall of the tube and the area of the wad exposed to the aerosol was the same in each determination. The amount of MP collected on the plug was first determined by weighing on a 5-digit analytical balance (Mettler AE163).

7.2.4. Experimental model pulmonary tuberculosis in BALB/c mice

Seventy two Swiss mice were infected through aerosol route (Glascol- Inhalation Exposure System, USA) with 10 mL of suspension of Mtb H37Rv (~ 2×106/mL) figure 7.2. Briefly BALB/c mice of 8 weeks of age were exposed to bacterial aerosol generated by the nebulizer

coupled with the apparatus (Bacterial load 6.33X106). Approximately 100 bacilli were introduced into the respiratory tract of each animal. Infected mice were separated in groups of 6 cages en suited with micro isolators.

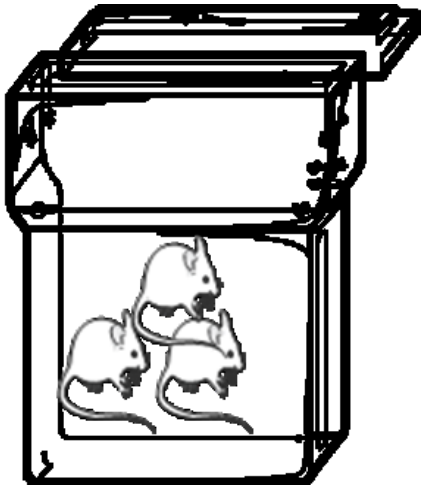

Figure 7.2. Schematic presentation of glasscol inhlation apparatus used for infection of mice presentation

7.3. Dosing & chemotherapy

4 weeks of infection, mice were randomly divided in to 11 groups. Dosing was underway 30 days after infection when the disease was established. Untreated animals (Group 1), inhalation 10mg IDR-1018 MPPs (group 2), inhalation 20mg IDR-1018 MPPs (group 3), inhalation 30mg IDR-1018 MPPs (group 4), inhalation 10 mg IDR-1018 MPPs along with oral INH 5mg/kg (group 5), indolicidin PNAPs formulation 10mg (group 6), indolicidin PNAPs formulation 20mg (group 7), indolicidin PNAPs formulation 30mg (group 8), indolicidin 20mg plus INH(group 9),, positive control oral 10mg/kg Rifampicin plus INH 5mg/kg (group10), inhalation 10mg blank MPPs (group 11) Daily inhalation dosing was done 5 days/week up to 6 weeks each group was having 6 mice. The efficacy of the formulation was determined by quantifying lung and spleen bacillary load by calculating colony forming units (CFU).

Inhalation of the dry powder formulation was done using an in-house inhalation assembly. Developed powdered formulation was exactly weighed and added to the cap of the inhalation apparatus and mice were restrained with their nostrils inserted inside chamber to inhale the aerosolized particles when the actuation was started. Powder was aerosolized by applying 30

actuations over 30 s (1) (Figure 7.3 B). Oral dosing of the standard drugs was delivered using ball tipped 20 gauge cannula (Figure 7.3 A)

in the present thesis we have focused on two approaches for treating tuberculosis first approach was exploration and utilization of various antimicrobial peptides for tuberculosis. So out of all the selected AMPs some peptides have good anti TB activity and further we evaluated their MIC values so out of all the selected peptides IDR-1018 and Indolicidin have good MIC values so we have done further *in vivo* activity with these two peptides. Second approach was to optimize delivery system which will be suitable for inhalation with these two selected peptides. so out of all the developed delivery systems we found Porous nanoparticle aggregates particles (PNAPs) and Mucus penetrating particles (MPPs) were found to be more suitable in lung delivery. So we have preceded further studies with these two delivery systems containing IDR-1018 and indolicidin peptides.

Table 7.1: Experimental groups of animals

Animal Groups	**Treatment**
Group-A	Untreated Control
Group-B	Blank MP (~10mg)
Group-C	Inhalation (IDR-1018) (~10mg)
Group-D	Inhalation (IDR-1018) (~20.0mg)
Group-E	Inhalation (IDR-1018) (~30.0mg)
Group-F	Inhalation(IDR-1018) (~20.0mg)+Oral(INH) (5mg/kg)
Group- G	Inhalation (indolicidin) (~10.0mg)
Group-H	Inhalation (indolicidin) (~20.0mg)
Group-I	Inhalation (indolicidin) (~30.0mg)
Group-J	Inhalation(indolicidin)(~20.0mg)+Oral(INH) (5mg/kg)
Group-K	Oral(INH+Rif) (10mg/kg)

Figure 7.3. Animal dosing in Biosafety level-3 laboratory. Panel A- Oral dosing using ball tipped 22 gauge cannula; Panel B- Inhalation of dry powder inhalable MPPs/PNAP via In-house nose only inhalation apparatus

7.4. Determination of viable bacilli in lungs and spleen

Lung and spleen from all of the four mice was used to determine CFU while one mice lung was used for histopathology. Each lung and spleen tissue was homogenized with polytron (Kinematica, Lucerne, Switzerland). The homogenates were plated in duplicate on Middlebrook 7H11 agar plates supplemented with oleic acid-albumin-dextrose-catalase (OADC) enrichment medium (BBL) and antibiotics (Cyclohexamide 25µg/mL, AmphotericinB 10µg/mL and Vancomycin 5µg/mL). The plates were incubated at 37°C in BOD incubator and CFU counts were scored after 4 weeks. CFU counts were expressed in Log10.

7.5. Histopathology

For histopathological analysis lung and spleen of each animal were removed and fixed in 10% neutral buffered formalin for 24 hours at room temperature. Tissue samples were dehydrated in a series of ethanol and embedded in paraffin wax. Sections of around 5µm were cut and mounted

on slides and stained with Haematoxylin–Eosin staining and subsequently processed for histopathological examination under light microscope.

7.6. Results and discussion

7.6.1. Determination of emitted dose

Determination of emitted dose was calculated by actuating the apparatus for 30 seconds for 30 times and weighing the amounts of particles collected. (Table 7.2). Consistent results were obtained. Results show that about 22 to 25% of total particles weighed into the 15 mL inhalation apparatus is available for inhalation by mice. This shows that the inhalation tool is competent for delivering reliable inhalation doses to laboratory animals.

Table- 7.2. : Emitted Dose estimation

Expt. No.	Powder weighed on cap (mg) ± SD	Emitted Dose (mg) ± SD	Actuation time(sec)	Percent delivery
1	12.14 ± 0.04	3.123 ± 0.024	30	25.72
2	22.17 ± 0.08	5.247 ± 0.038	30	23.66
3	27.12 ± 0.11	6.120 ± 1.214	30	22.56
4	32.22 ± 0.212	7.467 ± 2.443	30	23.17
5	44.24 ± 0.314	9.764 ± 1.412	30	22.07

7.6.2. In vivo anti tubercular therapeutic efficacy

The efficacy of the encapsulated IDR-1018 MPPs and indolicidin PNAPs formulation delivered by pulmonary delivery was compared alone as well as with standard therapy. For this experiment six-six mice were infected with H37Rv and after 4 weeks of infection animals were treated with different inhalation dose of IDR-1018 MPPs and oral INH plus Rifampicin 5 days per week for 6 weeks. The quantity of viable bacteria was enumerated in terms of Log10CFU/g of tissue of homogenate of lungs and spleens of animals.

As shown in Fig-7.4, 7.5, IDR-1018 MPPs and fig. 7.6,7.7indolicidin PNAPs showed significant activity in the Swiss mice at all concentrations used and was active in a dose-dependent mode.

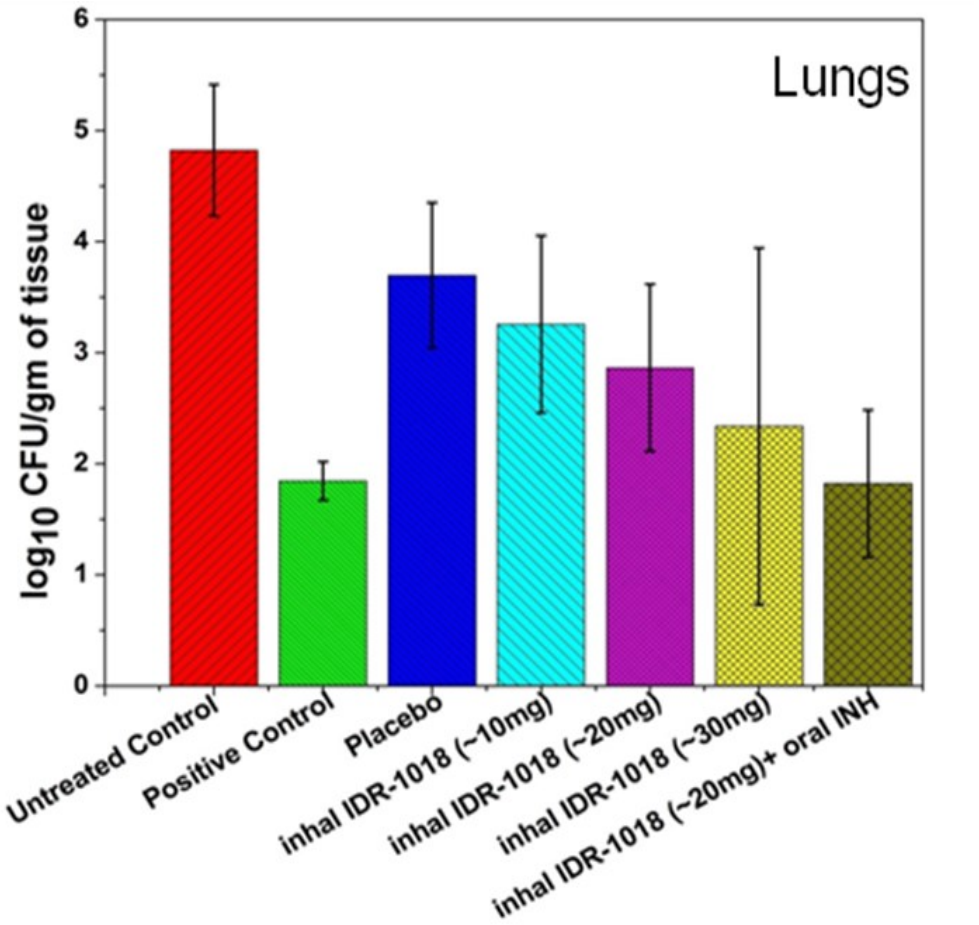

Figure 7.4. Number of viable bacteria (Log10 CFU/g of tissue) in Lungs of Swiss mice after receiving different treatment (IDR-1018 peptide loaded MPPs, free drugs and in combination of both) daily for 28 days in Mtb (H37Rv) infected animals. All values are mean±S.D for six animals

Following treatment with increasing doses of IDR-1018 MPPs and indolicidin PNAPs formulation, bacterial burden was reduced At 30.0mg; IDR-1018 MPPs in mice produced a more pronounced reduction of bacterial burden (Log10CFU) in the lungs in dose dependent manner as compared to the growth in the untreated control group (2.48 Log10CFU/g)), at 20.0 mg it produced about a (1.95 Log10CFU/g)), and at 10.0mg it produced about a (1.56 Log10CFU/g) log reduction (Table 1). In the same experiment, administration of IDR-1018 MPPs (~20 mg) plus oral therapy of half the standard dose of anti-tuberculosis drugs for 42 days significantly reduced bacterial load from both lung and spleen and resulted approximately (2.99 Log10CFU/g)respectively in magnitude reduction in bacterial Log10CFU in lungs and (1.7 Log10CFU/g) respectively in spleen (Table- and Figure-). No significant difference in the

reduction in the numbers of CFU in the spleen could be observed in the different treatment groups and there was not any noticeable decrease in bacterial survival. IDR-1018 MPPs (30mg) exhibited significantly enhanced reduction in CFU in both lung (2.48 Log10CFU/g) and spleen (1.65 Log10CFU/g) as compared with control group. It seems that, the bacterial clearance in spleen is mainly attributed to the standard anti-TB drugs. The results evidently showed the therapeutic potential of pulmonary delivery IDR-1018 with oral therapy of standard antituberculosis drugs.

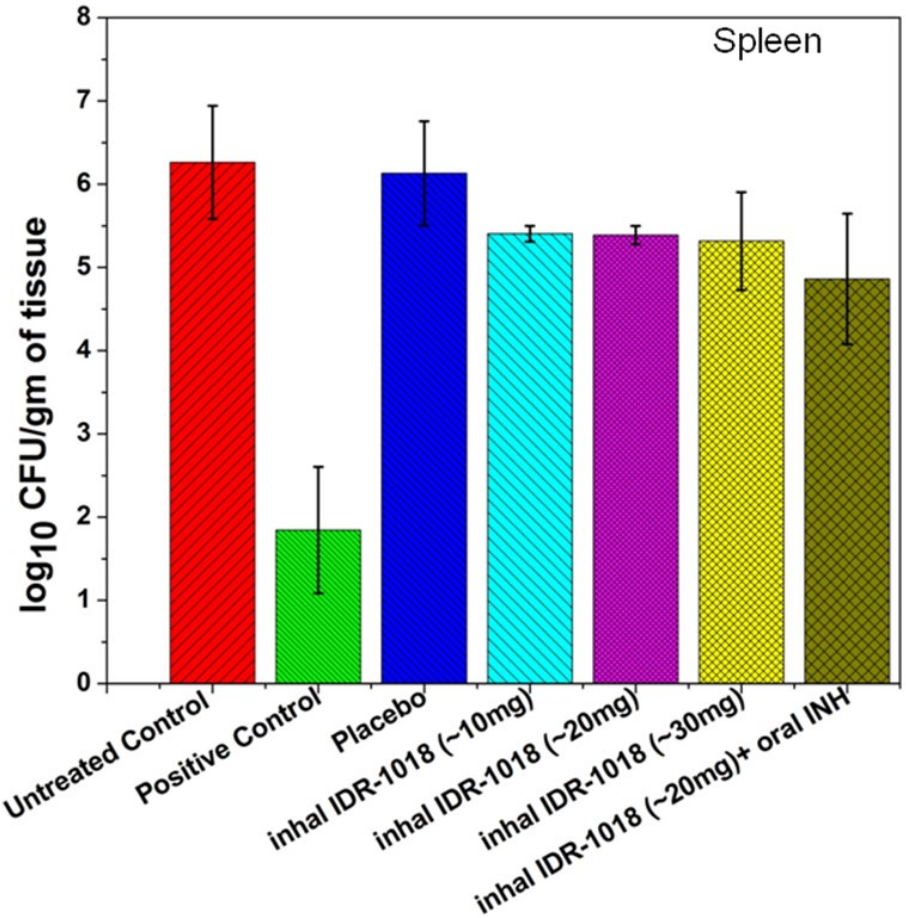

Figure 7.5. Number of viable bacteria (Log10 CFU/g of tissue) in Spleen of Swiss mice after receiving different treatment (IDR-1018 peptide loaded MPPs free drugs and in combination of both) daily for 28 days in Mtb (H37Rv) infected animals. All values are mean±S.D for six animals

Indolicidin formulation also reduces the bacterial burden in both lungs and spleen in dose dependent manner. Different doses of indolicidin formulation alone (~10, 20 and 30 mg) showed approximately 0.68, 1.42 and 1.37 fold reduction of bacterial load in lungs as compared to

control animals. The results evidently showed the therapeutic potential of pulmonary delivery IDR-1018 and indolicidin formulation with oral therapy of standard antituberculosis drugs. The results revealed that lung lobes of control group animals were enlarged and nodular, with caseous necrosis and lymphocyte infiltration. Lungs showed large areas with lymphocyte rich ill-formed granulomas. The severity of infection was observed to decrease with the administration of increasing doses of inhalable IDR-1018 and indolicidin formulation, as shown by the general trend seen in the grading.

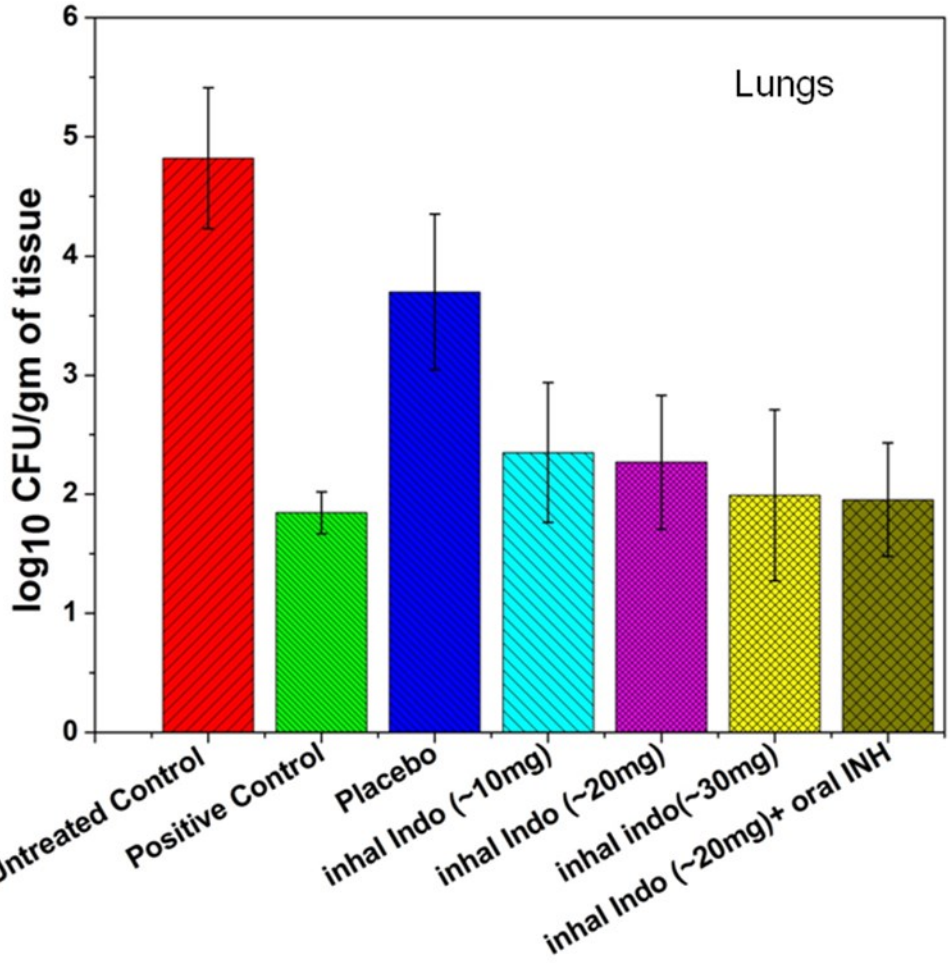

Figure 7.6: Number of viable bacteria (Log10 CFU/g of tissue) in Lungs of Swiss mice after receiving different treatment Indolicidin peptide loaded PNAPs, free drugs and in combination of both) daily for 28 days in Mtb (H37Rv) infected animals. All values are mean± S.D for six animals

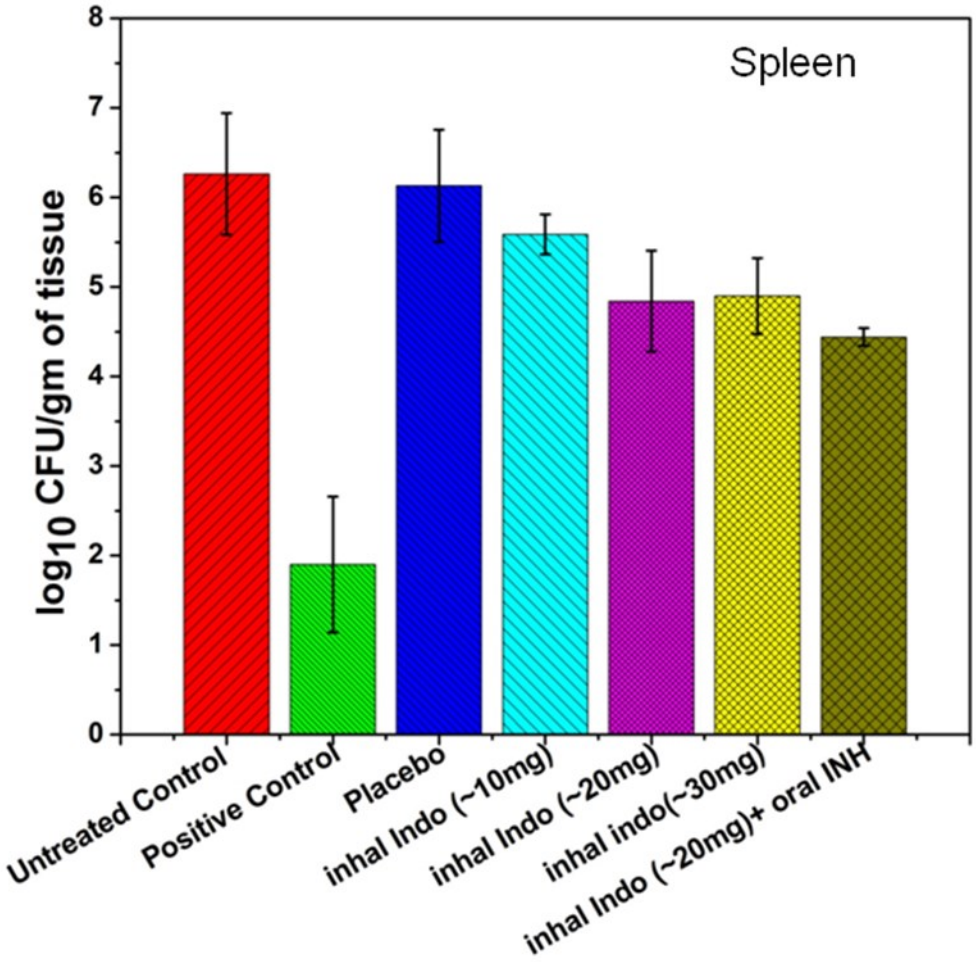

Figure 7.7. Number of viable bacteria (Log10 CFU/g of tissue) in spleen of Swiss mice after receiving different treatment Indolicidin peptide loaded PNAPs, free drugs and in combination of both) daily for 28 days in Mtb (H37Rv) infected animals. All values are mean± S.D for six animals

7.7. Morphological analysis of organs

At the time of sacrifice, the weights of the organs (lungs, and spleens) and the whole body weights of the treatment groups and the control mice were determined. After 28 days of treatment, body weights of treatment groups and control group were similar. The spleen weights and the lungs weights between the different treatment groups were slightly different from those of the untreated controls. In order to analyze the effect of the IDR-1018 MPPs and indolicidin PNAPs formulations the mice were administered inhalation of various doses of formulations. After 6 weeks of dosing animals were euthanized and diagnostic autopsy of lungs and spleen proved that no significant malformation were observed and morphology of the lungs were

improved as the dose was increased. At the time of sacrifice, the weights of the organs (lungs, and spleens) and the whole body weights of the treatment groups and the control mice were determined. After 6 weeks of treatment, body weights of treatment groups and control group were similar. The spleen weights and the lungs weights between the different treatment groups were slightly different from those of the untreated controls. In case of untreatment goups their were more nodule formation observed in lungs as compared to treatment groups (figure 7.8, figure 7.10). The weight of lung and spleen of untreated controls was slightly larger than treated groups. No clinical sign of significant toxicity was observed. There was hardly any significant difference in body weights of mice after treatment in pre and post experimentation whereas there was significant difference in organ weight and morphology between control and treatment groups (Figure7.9 & Figure 7.11) spleen of control animals.

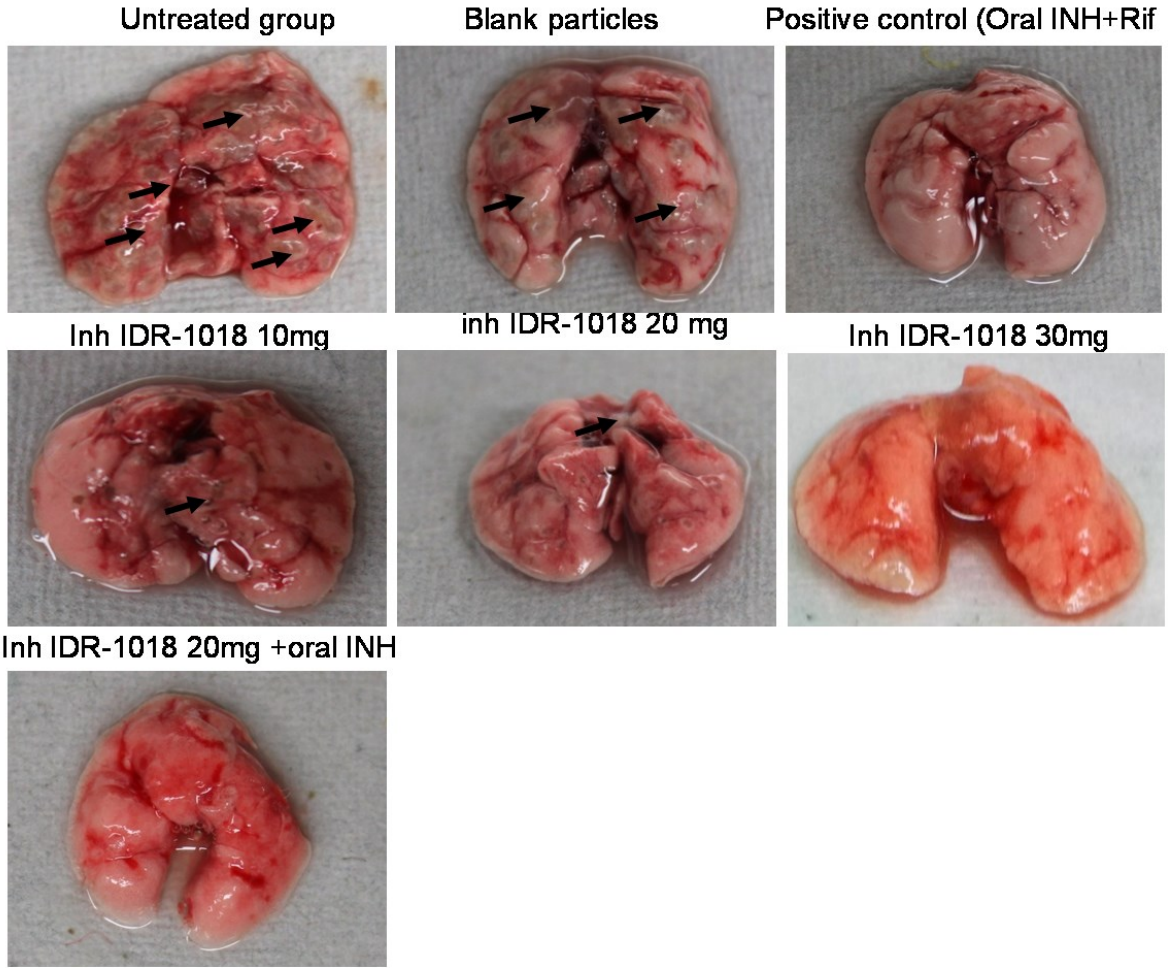

Figure 7.8. Morphology of lungs from mice after infection and different treatment of IDR-1018 formulation**.**

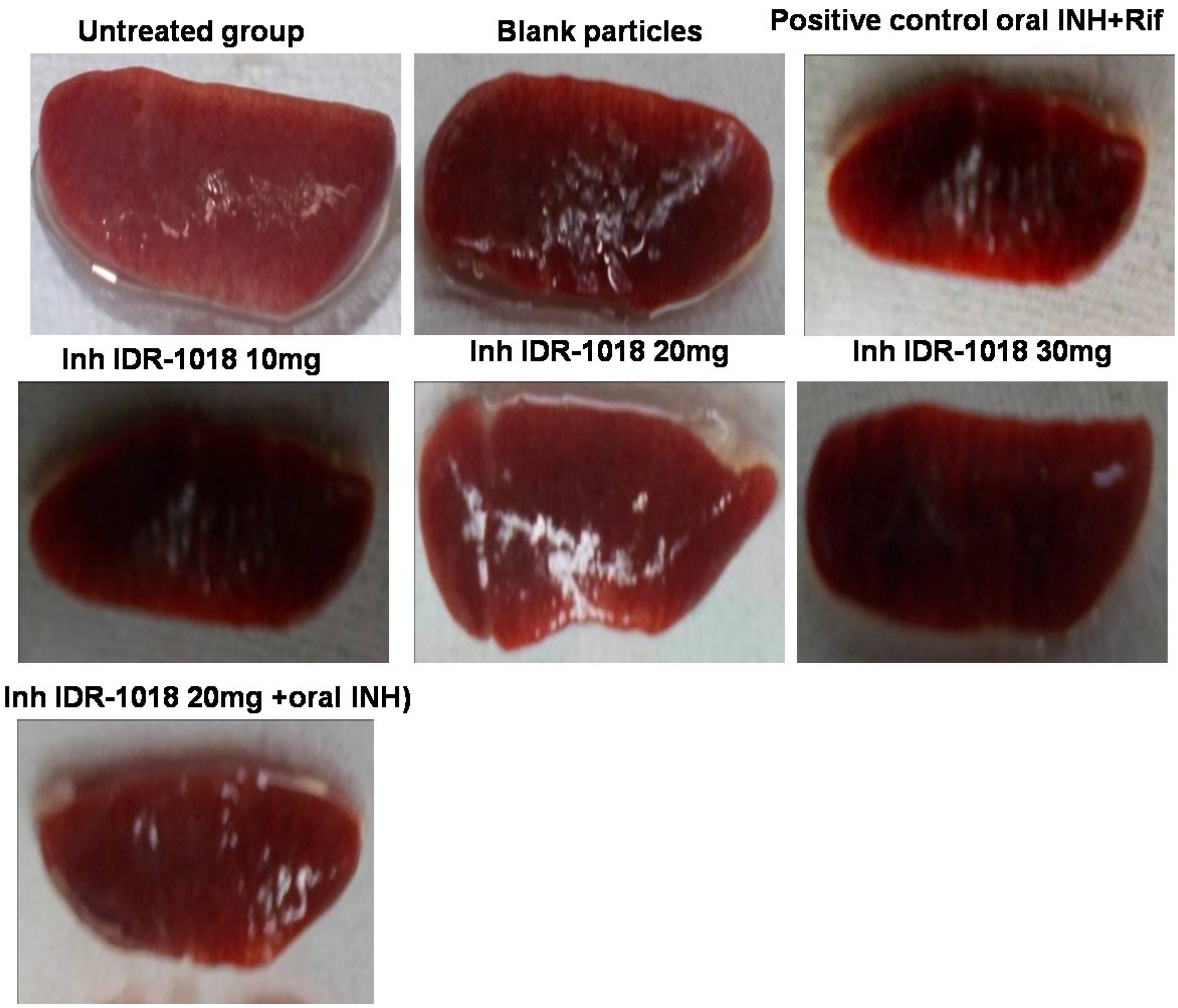

Figure 7.9. Morphology of spleen from mice after infection and different treatment of IDR-1018 formulation

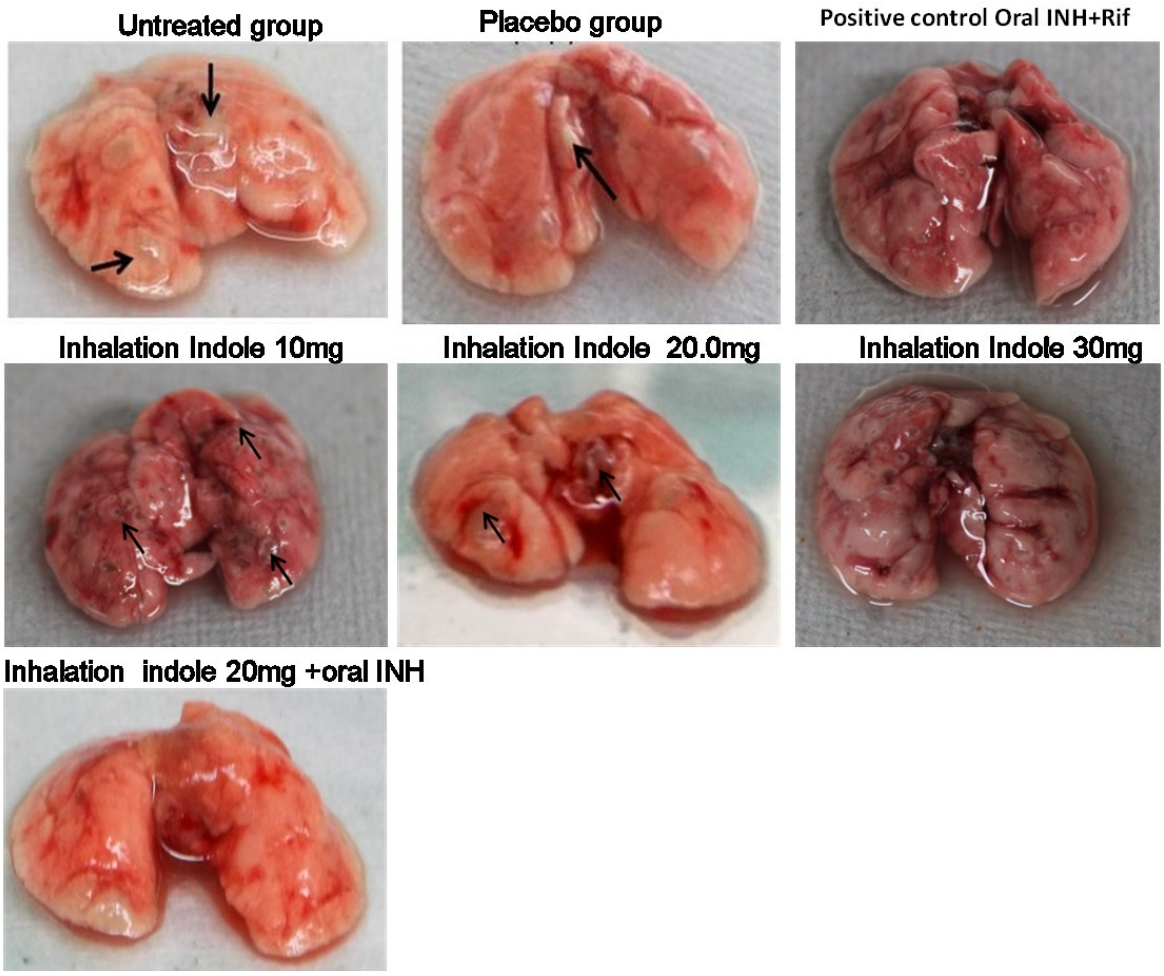

Figure 7.10. Morphology of lungs from mice injected after infection and different treatment indolicidin formulation**.**

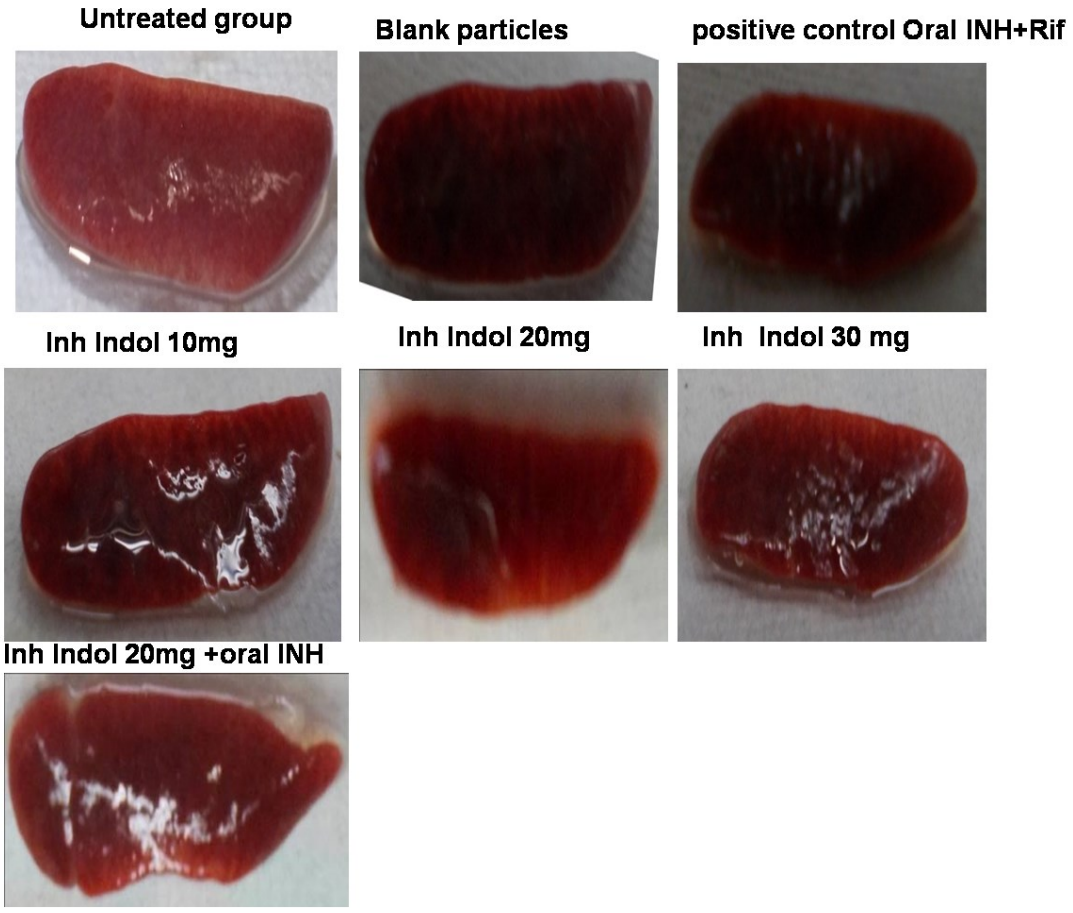

Figure 7.11. Morphology of spleen from mice after infection and different treatment indolicidin formulation**.**

7.8. Histopathological analysis

Histopathological results supported the CFU results of lungs and spleen (Fig-7.12). H &E staining of lungs and spleen tissue illustartes that lung lobes of control groups were enlarged and nodular with caseous necrosis, aggregation of foamy macrophages and reduced number of alveoli and its size. Lung shows a large area with lymphocyte rich ill-formed granulomas.

Lungs- The extent of infection, reflected by the pathology seen in the histological sections, which was reduced as the drug concentration increased. The results revealed that lung lobes of control group (group1) animals were enlarged and nodular, with caseous necrosis and lymphocyte infiltration. Lung shows a large area with lymphocyte rich ill-formed granulomas. Animals receiving blank microparticles alone showed no effect on histology improvement of organs. In some animals of IDR-1018 MPPs alone treatment, eosinophil rich regions was found,

this may be attributed due to immune reaction elicited by particles. These evaluations revealed that all treated animals typically had less severe infections than the untreated control animals. The severity of infection was observed to decrease with the administration of increasing doses of inhalable IDR-1018 MPPs (30mg), as shown by the general trend seen in the grading. Moreover, a dose of 10 mg seemed to significantly improve the histology in the lungs of these mice compared with the level of histology in mice treated with lower doses of IDR-1018 MPPs.

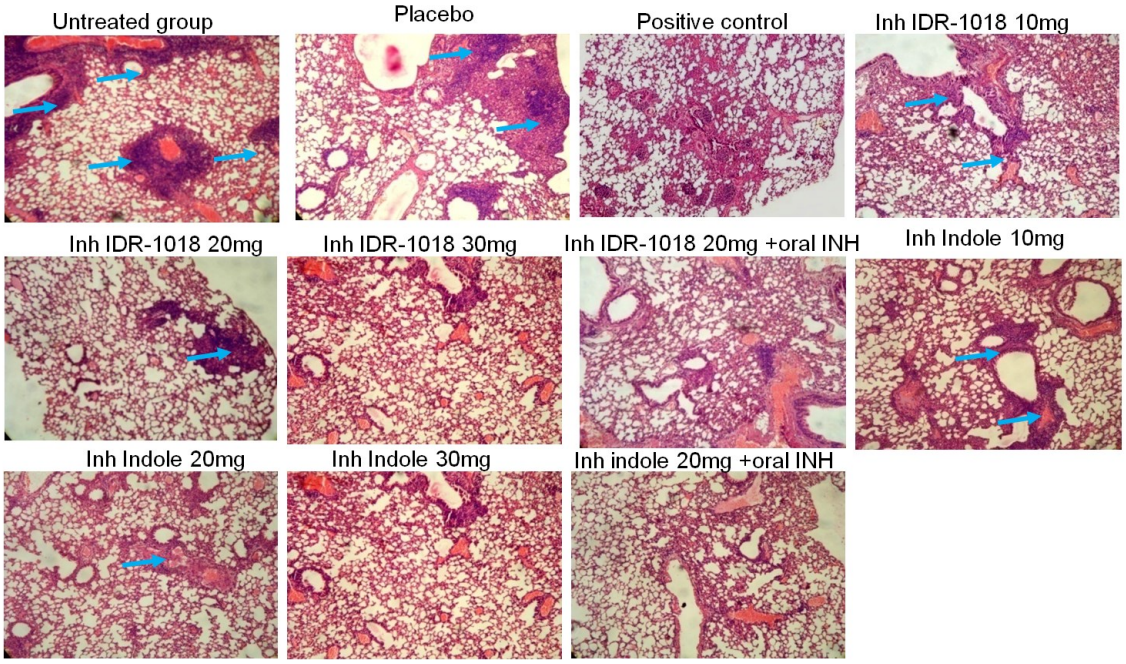

Figure 7.12. Histopathology of lungs tissue of TB infected mice after different treatments with IDR-1018 and indolicidin formulation

Histological assessment has shown that the TB infected granulomatous area inside lung was significantly reduced as compared to untreated mice. Fascinatingly, the amount as well as the cellular constitution was also somewhat different. In untreated mice the foamy macrophages was higher in the granuloma which are surrounded by lymphocytes. In case of group treated with indolicidin PNAPs formulation also showed improved histopathology of the lungs and the appearance of the granuloma rich region disappeared as the dose of the formulation was increased. In case of the treatment groups receiving oral INH (5mg/kg)+ inhalation IDR-1018 formulation (20mg) also have improved lung histopathology and no granuloma was observed which showed the additive effect of the IDR-1018 formulation with suboptimal concentration of

INH. In treatment group receiving indolicidin (20mg)+ INH(5mg/kg) also showed same effect so we proposed that these formulation can be effective adjunctive therapy for tuberculosis.

7.9. Conclusion

Pulmonary delivery of multiple doses of AMPs formulations exhibited appreciable anti-TB activity in mice infected with a low inhalation dose of virulent Mtb and improved the morphology and histology of the infected lungs in animals. The results reveal that formulation loaded with IDR-1018 and indolicidin put forth significant antimycobacterial activity against virulent M.tb *in vivo.*IDR-1018 MPPs had dose dependent anti tb activity by themselves, but also improved the efficacy of standard anti-TB drugs. MP containing combinations of AMPs with anti-TB drugs showed better efficacy than those containing anti-TB drugs alone. Histopathological studies revealed that the lungs had reduced inflammation, lymphocyte infiltration, number of quasi-granulomatous lesions and tissue damage in treatment groups.

Based on this investigational data, it is apparent that pulmonary drug delivery systems for sustained and intracellular delivery of AMPs show promise in anti-TB therapy. Moreover, AMPs are not likely to generate cross resistance with other anti TB drugs. The data suggest that these formulations work in synergy with conventional anti-TB drugs, if administered as adjunct therapy. The result of this study advocates that inhaled AMPs releasing MP represents a novel approach which can be used as effective adjunct/supplement therapy with current oral regimen against pulmonary TB.

Summary of the work

Tuberculosis infection can be in any organ and pulmonary tuberculosis is the most common form of tuberculosis. In pulmonary tuberculosis lungs are major site of infection (85). Current strategy of cure are distant and from optimal and improved ones are being required to conquer the rising extend of drug susceptible as well as drug resistant strains of TB. Conventional antimicrobials do not work and new pragmatic approach with novel drugs or combinations is essential to control this fatal ailment.

In order to decrease the dosing period of treatment and minimize toxicity there is need to develop new treatment strategy that kill mycobacterium more proficiently at the target site (86). Host-directed therapies have emerged as potential alternative to combat TB by reducing treatment time and preventing development of resistance (87-89). These antimicrobial peptides released in the body in small quantity, involved in body's own immune response against various infections. Endogenous host defense peptides (HDP) are well recognized components of the innate immunity and have been suggested to have an important role in TB infections(88). It has been reported that alterations in the production of these molecules increases susceptibility to infectious diseases, including TB(90). There are several reports of the immuno-modulatory effects of these peptides in TB and other models(91). Such peptides possibly inhibit microbial growth either directly through membrane/nucleic acid disruption or indirectly through immune-modulation to efficiently clear the infection.

Even though TB is an infectious disease that can invade on several organ of the body, but lung is the chief entrance for Mycobacterium tuberculosis and therefore the site of the early immune reaction as well as an essential site of reactivation. Inhalation drug delivery technology has been used to treat wide variety respiratory diseases in which drug loaded particles are directly delivered to the pulmonary region through dry powder inhalers. Within pulmonary drug delivery system development, we focus on particle development to add further value to the formulation. Micron sized nano-assemblies, Porous nano Particles Aggregates (PNAP), hybrid Nano in micro (NIM) systems, microparticles; porous micropshres accompanied with various properties were generated using different methods like spray freeze drying, double emusion method. Micron size (1-5 μm) supposed to imparts optimum aerodynamic properties for maximal deposition, whereas

nanoparticles (200-300nm) in case of PNAP and NIM provide relatively better entrapment of peptides and dispersion in lung lumen(92). Generally, the spray drying procedure which is a heating process is used for generation of micro-sized particles. It is challenging to maintain the potency and activity of the peptide in this procedure; hence we utilized spray freeze drying procedure for particle formation.

The key objective of this work was to develop antimicrobial peptides loaded inhalable delivery systems by spray freeze drying and double emulsion method using various biodegradable polymers for targeted and sustained delivery AMP to alveolar macrophages.

8.1 Peptide synthesis

The first chapter deals with the synthesis of antimicrobial peptides. Solid phase peptide synthesis (SPSS) is method of choice for chemical synthesis of antimicrobial peptides. In the current study, a series of AMP of less than 20 amino acid sequence were synthesized by Fmoc Solid Phase Peptide Synthesis (SPPS) method using Liberty-blue™ automated microwave peptide synthesizer (CEM Corporation, NC, USA) (Sharma et al., 2018a). Fmoc-Rink amide resin was utilized as the solid support. De-protection of Fmoc-amino acids and resins was performed by cleaving it from the support-resin using a cocktail solution of tri-fluoro-acetic acid (90%), thio-anisole (5%), ethane-diol (3%), and anisole (2%) for 3 hours. The precipitation of the peptide from the filterate after cleavage was done with cold diethyl ether. The crude peptide was purified by semi-preparative reversed-phase high-performance liquid chromatography (Waters Corporation, USA) on a C18 column with an acetonitrile-water gradient. The purity of lyophilized peptides was confirmed by analytical RP-HPLC [Waters Spherisorb, C18, (250×4.6mm, 5µm)] and MALDI-TOF mass spectrometry (Applied bio-systems 4700 proteomics analyzer, MA USA) (Sharma et al., 2018).

8.2 Preparation and characterization of inhalable formulations

Antimicrobial peptides are promising candidates in various chemotherapy, immunotherapy, and resistant cases of various diseases. This section described how various novel formulations can improve their therapeutic index, protecting their activity and controlling their release. In this chapter Preparation and characterization of various inhalable PLGA formulations loaded with

one of different peptides. Following types of particles were prepared by using spray freeze drying, double emulsions solvent evaporation method.

1) Microspheres
2) Porous microsphere
3) Mucus Penetrating Microparticles
4) Porous Nanoparticle aggregates (PNAP)

The particles produced were characterized in terms of particle size, size distribution, morphology, shape, *in vitro* drug release, stability and aerodynamic diameter using a cascade impactor.

- **Preparation of microspheres**

Microspheres (MS) are viewed as an effective tools especially for the inhalation of a range of drugs and biomolecules. In order to improve the dispersion properties of the powder, vander-waals forces between the particles need to be reduced significantly. Micropshres were prepared by double emulsion method. The release of the biotherapeutics from these nonporous particles was not in suatained manner so we proceed for The porous MS with good permeability of molecules, larger surface area/volume ratio, lower density, wider dispersion and improved aerodynamic characteristics as compared to non-porous MS of same size.

- **Preparation of porous microspheres**

We report a simple strategy to design hierarchically porous PLA-MS with variable pore architecture for controlled delivery of a variety of loaded biotherapeutic molecules of different sizes, using W1/O/W2 (Water/Oil/Water) double emulsion solvent evaporation method. The concentration of porogen/osmogen was specifically and precisely optimized, depending upon the prerequisite pore size in MS. The various parameters that influence the ultimate morphology of PLA-MS were individually evaluated for the formation of pores and morphology. It was established that, a delicate balance in ratio of porogen reagent and polymer in the reaction mixture is necessary to synthesize MS with desirable porosities. Four model drugs and biomolecules with significant size and solubility difference were used in the study to be encapsulated inside the MS of hierarchically porosity. The presence of mucus tarp the particles in the lungs so again we proceed for another delivery system that is mucus penetrating particles.

- **Mucus penetrating particles**

Polymeric mucus (PLGA, 50:50) penetrating microspheres loaded with individual AMP were prepared by w/o/w double emulsion–solvent evaporation method with minor modifications (1, 93). Briefly, 200 mg PLGA was dissolved in 5 mL dichloromethane (organic phase) and aqueous solution (0.5ml) containing different types of HDP (5mg) was prepared separately (inner aqueous phase). Primary emulsion (w/o) was prepared by adding aqueous peptide solution into organic polymer phase with intermittent episodes of sonication (5 second each), which was further added drop-wise to aqueous solution of 1% (w/v) poly vinyl Alcohol (PVA) with continuous mechanical stirring. The emulsion was stirred with a mechanical stirrer at 600rpm for 12h to ensure complete solvent evaporation of organic solvent. Microspheres (MS) formed were separated by centrifugation (10,000 ×g for 20 minutes at 4°C) and washed to remove excess of PVA. Finally the coating of N-acetyl cysteine which is a mucolytic agent was done and presence of NAC on surface of the particles can clear the thck mucus by breaking the disulphide bonds in mucus plug.

- **Porous Nanoparticle Aggregate Particles (PNAP) using spray freeze drying**

To obtain optimal aerodynamic properties and maximum deposition in lungs, PLGA nanoparticles (~300nm) prepared using double emulsion solvent evaporation method were processed into porous micron scale inhalable nano-assemblies i.e. “Porous Nanoparticle Aggregate Particles” (PNAP)(~1-6µm) using spray freeze dying(SFD) technique. Freshly prepared NP (20 mg/ml) were suspended in mannitol (10mg/ml) solution and sprayed into liquid nitrogen using 0.7mm spray dryer nozzle (Techno Search instruments, India). Liquid nitrogen was kept in 3L closed container which was continuously agitated using magnetic stirring(94).

- **N-acetyl cysteine coated mucus penetrating particles**

In normal lungs, inhaled matter is naturally trapped in airway mucus and then cleared from the lungs via whipping performance of cilia or hair-like strands, to the stomach to be ultimately ruined. unhappily, this necessary defensive machinery also prevents a lot of inhaled therapeutics from getting their objective(23). Researchers have discovered that coating of polymeric nanoparticles with various pharmaceutical excipients like polyethylene glycol(95), can minimize adhesion of the particles to the mucus surface(96). The coating of N-acetyl cysteine (NAC) can enhance mucus penetrating potential and allow the particles to reach the infected cells and

tissues(97). Researchers are developing the mucus penetrating particles (MPPs) loaded with various drugs to find the new strategy to treat against various diseases(98, 99). Less entanglement helps MPPs to disseminate swiftly in the mucus network fibers while uncoated microparticles are characteristically utterly trapped(95, 100, 101). To date only few studies have been reported on the use of MPPs for various purposes.

IDR-1018 microspheres were developed using double emulsion solvent evaporation method. Coating of PLGA MPs with NAC was optimized using different NAC concentrations, like 0.5, 1, 2, 4, 8, 12 and 20 mg/mL. PLGA MPs were incubated with a solution of 0.2M Sigma-Aldrich) and diferent NAC concentrations, in 0.1 M (N-morpholino)ethanesulfonic acid (MES; Sigma-Aldrich) buffer at pH 7.2, for 2 h, at 37 °C and 100 rpm. NAC coated PLGA MPs were centrifuged at 10000 rpm and then rinsed twice and lyophilized.

8.3. Characterization of Inhalable particles

- ***Particle Size Distribution***

Particle size was measured using Malvern Mastersizer 2000 (Malvern, UK). The particles displayed a log-normal distribution of cumulative volume-average sizes between 1 and 10μm, with median particle size of 3.1 ± 0.9μm. The addition of precisely optimized concentrations of various porogens leads to the formation of range of micron-sized porous PLA-MS (5.4 ± 1.6 to 10.7 ± 3.4 mm) which possess well defined pores and voids in nano-scale range (2.4 to 872.4 nm).

PNAP-nanoassemblies product was recovered from spray freeze drying (SFD) at mean percentage yields of 68.72± 13.08% of starting material. Hybrid Nano-in-Micro platforms "Porous nanoparticle-aggregate particles (PNAPs)" of 1-6 micron size were developed by atomization. PNAP supposed to disperse into primary AMP loaded nanoparticles from aggregates as soon as it delivered into lungs. The median hydrodynamic diameter of the prepared primary NP was found to be 312.6 ± 17.8 nm as determined by DLS. All the developed formulation were in inhalable range.

- ***Morphology of particles***

Scanning electron microscopy (SEM) was performed to study the particle geometry (morphology and size) of particles. Spherical shaped hierarchically porous PLA-MS particles with uniform

size distribution and regular pore morphology were obtained. Porogens induced well-distributed pores of diameter ranged from 2.4 nm to 872.4 nm on the surface, with well-ordered interconnected three dimensional channels inside the matrix. Owing the internal porous structure with numerous binding sites can solve the drawback of nonporous MS with low encapsulation efficiency and slow release of bio-therapeutics. The pore size was tuned in a range of spanning from diameter near to the size of small molecular drugs like INH, RIF to larger peptide and protein drugs.

Scanning electron microscopy (SEM) analysis of PNAPs and hybrid nano-in micro assemblies, NAC coated PLGA microspheres confirmed the size range, monodispersity, spherical shape with smooth surface topology. The mannitol matrix and lipid coating of PNAPs and hybrid nano-in micro sytems is supposed to be dissolved upon contact with lung fluid and surfactant, liberating AMP loaded nanoparticles for uptake by bacteria infected macrophages. In case of nano-in micro systems lipid matrix may soften upon contact with lung fluid

- ***Drug content, content uniformity and Entrapment efficiency***

The amount of drug that was entrapped in the particle powder after spray freeze drying was determined as the mass ratio of the entrapped drug to the theoretical amount of drug used in the preparation. The product was recovered from spray freeze drying (SFD) at mean percentage yields of 68.72± 13.08% of starting material. All particles showed high entrapment efficiency and drug loading. The encapsulation and loading efficiencies of MIAP in NP were 41.92±8.545% and 13.19± 4.85%, respectively.

- ***Aerodynamic Characterization***

All developed particles were evaluated for in-vitro lung deposition using Andersen Cascade impactor. The emitted fractions (EFs) of all developed MS (PL1-PL9), PNAPs from Rotahaler apparatus were in the range of 92.6 ± 15.9 to 96.1 ± 6.4%. Dry powder MS inhalation produced fine particle fractions (FPF) in range of 32.3 ± 5.8 to 56.6 ± 6.8% and mass median aerodynamic diameters (MMAD) as low as 3.1 ± 1.5 to 5.2 ± 1.3 μm. MS under investigation had a mean geometric deviation ranging from 1.3 ± 0.6 μm to 2.0 ± 0.7 μm and mass densities of approximately 0.08-0.76 g/cm3 (Table 1). Increase in porosities and reduction of density in MS of almost similar geometric size led to decrease in aerodynamic diameters. Large porous PLA-MS (>5 μm) hold smaller MMAD and FPF than non-porous MS of the almost similar size. In

this respect, porous PLA-MS under study with geometric size 5 μm appear to be more suitable for pulmonary delivery of bioactives with good aerodynamic properties with high lungs deposition.

Experimental studies by cascade impactor demonstrated the distribution of inhalable PNAPs in different respiratory strata according to particle size. The MMAD, GSD and FPF of emitted dose of optimized Blank-PNAP (3.17 ±0.89μm, 1.81±0.62μm and 67.95±5.58%) found to be in range that is appropriate for powder dispersibility and inhalation delivery. These aerodynamic values of the particles indicate that PNAP have adequate mass fraction of particles 1-5 μm, suitable for getting into interior regions of respiratory tree. Aerodynamic result suggests that the PNAPs were highly respirable and likelihood of carrying large fraction of formulations gets deposited to the mid region of the lung available for alveolar uptake.

- ***In Vitro* Drug Release Studies**

The developed DPI formulations were further characterized for in vitro drug release in simulated lung buffer at 37±2°C. Therapeutic outcomes are critically dependent on onset, release and duration of retention of drug in lungs. The *in-vitro* release profiles indicate the differences between PLA-MS caused by the variability in porosity. The pore geometry and internal structure of micro-matrix significantly influenced the release profile of the incorporated molecules. Indeed, the release of the bioactives from different MS was temporally diverse. The delivery rate of biotherapeutics in release medium from porous PLA-MS increases with increase in pore size from ~2.4 to 872 nm.

The release kinetics of peptides from the optimized formulations of NS and PNAP were studied for 10 days in simulated lung buffer (PBS, pH 7.4) at 37±2°C and observed continuous peptide release throughout this interval. AMP release from both NS and PNAP demonstrated dual biphasic pattern that was categorized by initial burst, followed by slower secondary linear sustained release pattern (apparent zero order phase) of peptide. The IDR-1018MPPs and Indolicidin PNAPs also controlled the release up to 2 days.

8.4. *In vitro* efficacy studies (intracellular efficacy on M.tb infected cells)

In the present chapter intracellular antitubercular efficacy and drug delivery of the developed AMP formulation were evaluated.

- *Inhibition of M.tb growth inside macrophages*

Differentiated cells were infected with Mtb at a multiplicity of infection (MOI) of 10 for 3 h. Wells were then washed with media to remove extracellular bacteria. MP sterilized by γ-radiation (irradiation dose 5 kGy using a ^{60}Co-radiation source) were suspended in sufficient amount of RPMI to obtain theoretical concentrations of 10, 50, and 100μM of AMP loaded particles, added to designated wells and incubated for 3 h. In the absence of treatment, the colony count was 6.21±1.09. Incubation with AMP led to reduction in CFU of Mtb, particularly if the drug was incorporated in MP. Placebo or blank particles equivalent to the highest dose did not demonstrate significant bactericidal activity(102). Comparing formulations containing different AMP, Indolicidin MPs and IDR-1018 MPs had the significantly higher activity than MP containing AMP. So animal studies were carried out with these two formulations(103).

- *Macrophage uptake studies*

The uptake and internalization of FITC labelled particles by macrophages was measured by flow cytometry and confocal microscopy. The flow cytometry instrument was set to collect 10000 events for each sample. Differentiated RAW264.7 macrophages demonstrated efficient uptake of all type of particles. Porous micropsheres and AMP loaded PNAPs, demonstrated almost similar phagocytic uptake. Confocal microscopy results illustrate the percentage of phagocytic cells containing microparticles following incubation of the cells with the particles for 3h. Macrophages showed internalization of blank, microparticles respectively.

Nonporous and low porosity spherical particles were efficiently phagocytized in higher numbers compared to particles with high porosity. Evidently, in addition to particle size and surface properties, the cellular association and uptake was also found to be porosity dependent. The internalization of PLA-MS into macrophages was in the order PL1 > PL2 > PL3 > PL4 > PL5> PL7 > PL8> PL6> PL9.

- *Cytotoxicity towards RAW 264.7 mouse macrophages*

AMP cytotoxicity to mammalian cells is a significant concern for their development as clinical anti-TB agents. As a preliminary assessment of the biocompatibility of AMP and their suitability as anti-TB candidate, we measured their cytotoxicity against the Raw 264.7 mouse macrophage cell lines by an MTT colorimetric viability assay. The MTT assay was carried out on uninfected and infected/treated cells at different time-points following exposure to different doses of HDP. The general trend indicates that all pure peptides used in studies responded with macrophages

in a similar pattern and elicited considerable cytotoxicity. PLGA-AMP formulations have been shown to be biocompatible when introduced in macrophage cultures with more than ~89% cell viability.

8.5. Therapeutic efficacy studies in tb infected animal model

In the present chapter *in vivo* efficiency of inhalable AMP IDR-1018 and indoclicidin-containing PNAPs as adjunct therapy was evaluated. Multiple dosing (5 days/ week) of mice infected with virulent Mtb was carried out, with and without concurrent administration of inhaled or orally-administered INH and RIF. The CFU count, morphometry and histopathology of excised lungs and spleen were documented to examine the therapeutic efficacy.

The efficacy of the encapsulated IDR-1018 formulation delivered by pulmonary delivery was compared alone as well as with standard therapy. For this experiment six-six mice were infected with Mtb H37Rv and after 4 weeks of infection animals were treated with different inhalation dose of IDR-1018 MPPs and oral INH plus Rifampicin 5 days per week for 6 weeks. The quantity of viable bacteria was enumerated in terms of Log10 CFU/g of tissue of homogenate of lungs and spleens of animals.

IDR-1018 MPPs showed significant activity in the Swiss mice at all concentrations used and was active in a dose-dependent mode. Following treatment with increasing doses of IDR-1018 MPPs, bacterial burden was reduced At 30 mg; IDR-1018 formulation in mice produced a more pronounced reduction of bacterial burden (Log10 CFU) in the lungs in dose dependent manner as compared to the growth in the untreated control group (2.48 Log10 CFU/g)), at 20 mg it produced about a (1.95 Log10 CFU/g)), and at 10 mg it produced about a (1.56 Log10 CFU/g) log reduction (Table 1). In the same experiment, administration of IDR-1018 formulation (~20 mg) plus oral therapy of half the standard dose of anti-tuberculosis drugs for 42 days significantly reduced bacterial load from both lung and spleen and resulted approximately (2.99 Log10 CFU/g) respectively in magnitude reduction in bacterial Log10 CFU in lungs and (1.7 Log10 CFU/g) respectively in spleen. No significant difference in the reduction in the numbers of CFU in the spleen could be observed in the different treatment groups and there was not any noticeable decrease in bacterial survival. IDR-1018 MPPs (30 mg) exhibited significantly enhanced reduction in CFU in both lung (2.48 Log10 CFU/g) and spleen (1.65 Log10 CFU/g) as compared with control group. It seems that, the bacterial clearance in spleen is mainly attributed to the standard anti-TB drugs. The results evidently showed the therapeutic potential of

pulmonary delivery IDR-1018 with oral therapy of standard antituberculosis drugs. The results revealed that lung lobes of control group animals were enlarged and nodular, with caseous necrosis and lymphocyte infiltration. Lungs showed large areas with lymphocyte rich ill-formed granulomas. The severity of infection was observed to decrease with the administration of increasing doses of inhalable IDR-1018 and indolicidin formulation, as shown by the general trend seen in the grading. In these treatment groups, white pulp was much condensed as compared to untreated ones. Animals receiving MP alone shown little effect on histology improvement of spleen while the group receiving oral treatment along with IDR-1018 MPs showed maximum improvement in both lung and spleen histology

8.6. Mechanistic study

We found that AMP releasing formulations are capable of killing virulent M.tb directly as well as in cultured cells and also in murine model of tuberculosis. However the mechanism of action of killing was not clear. Therefore in this chapter an attempt was made to elucidate mechanisms of action, by analysing the effects of various AMP releasing formulations on a few molecular mechanisms of host response that Mtb evades to ensure its survival.

- *Interaction between AMP with Mycobacterium wall.*

In this course of study, since high concentration of AMP might be noxious to mammalian cells our hypothesis was to use suboptimal concentrations of AMP to permeablize the bacteria which might help in accelerating influx of anti-TB antibiotic into bacteria.

Mycobacterial morphology and membrane integrity were directly visualized by SEM and AFM upon incubation with sustained released peptides formulations for 12h. Treatment with AMP at the 50µg/ml for 12h induced recognisable membrane damage as compared to the control group of bacterial cells, which exhibited an intact and smooth surface *M.tb* cell wall is relatively less permeable towards AMP as compared to membranes of other Gram-negative or Gram-positive bacteria. These short peptides are ought to intercalate in lipid membrane and permeabilize it by the micellar aggregate channel model. Exposure of released AMP induced alteration in the cell-wall of mycobacterium by permeabilization of bacterial membranes, which ultimately lead to bacterial death(104).

- *Phagosome-Lysosome Fusion (PLF) estimation by Confocal microscopy*

The ability of the microbe to arrest phagosome maturation is considered one major mechanism that allows its survival within host macrophages. We examine, whether exogenous AMP, an important component of host innate immunity, can alter the maturation of Mtb- phagosomes, we examined the co-localization of the lysosomes (stained with acidotropic dye LysoTracker Red DND-99) with phagosomes containing virulent FITC-H37Rv Mtb in macrophage cells after treatment with pure and encapsulated AMP, using Confocal Laser microscopy.

In untreated controls, the majority of phagosomes containing H37Rv did not co-localize with the LysoTracker dye at any time intervals of observation. Out of the all the synthesized peptides only MIAP peptide was showing phago-lysosomal fusion so we have shown the data of the MIAP formulation. The ability of Mtb to prevent phagosomal maturation found to be compromised and high intensity of phagosome-lysosome fusion (PLF) was observed in the cells treated with MIAP-PNAP (equivalent to soluble peptide 100µM). Within 6h of treatment, there was 78.57±12.58% of PLF. The intensity of colocalization of the LysoTracker dye with Mtb phagosomes was lesser in the cells treated with bare peptide (24.88±9.17%); but it also significantly enhanced the PLF in infected cells These results suggest that exposure of Mtb infected macrophages to exogenous MIAP; render mycobacterial phagosomes susceptible to acidification. When infected cells were treated with standard anti-TB drug Isoniazid (equivalent to 3µg/ml of drug), did not appear to promote phagosome maturation in initial phase of 6 h but within 12h it shoots upto 27.5±10.20 %. It appears that, in early 6 h majority of mycobacteria is live which prevents PLF, but in later hours, bacteria was killed by drugs these dead Mtb were not able to prevent phagosomal maturation(62).

- *Reactive Oxygen Species (ROS) estimation using flow cytometry*

The generation of ROS is one of the powerful mechanisms to inhibit microbial growth. Activated macrophages are known to produce and release of a variety of ROS such as the superoxide anion (O2-) and H_2O_2. The interplay between Mtb and the host macrophage during the oxidative burst is complex, relying on both the ability of the macrophage to produce ROS, and the ability of Mtb to counteract this response. The results also indicate that exogenous AMP formulation stimulates macrophages to generate ROS which enhance superoxide mediated bactericidal activity of macrophage by formation of free radicals.

- *Apoptosis studies by Flow cytometery*

To establish the regulatory role of sustained delivery of AMP on macrophage apoptosis and whether exogenous AMP alone is able to modulate macrophage apoptosis independently of Mtb infection, we treated uninfected cells with bare and encapsulated MIAP(48). Apoptosis is characterized by AnnexinV-PI dual staining followed by flow cytometry. AnnexinV-PI dual staining distinguish early apoptotic (annexinV +ve, PI -ve), necrotic (PI -ve) and viable cells (Annexin-V and PI -ve) depending on the staining. The percentage of apoptotic/necrotic cells was analyzed by flow cytometry at 48 h post-treatment. Blank-PNAP, MIAP-PNAP and free peptide alone at concentrations (100μM) did not able induce considerable apoptosis in uninfected cells while significant magnitude of apoptosis was observed in Mtb infected (Virulent H37Rv) macrophages at same concentration of MIAP. The incidences of early apoptosis in infected cells were 52.25±9.54% and 39.41±6.58% in MIAP-PNAP and pure-MIAP treated group respectively(62). Very small number of macrophages showed apoptosis in the uninfected and blank-PNAP treated cells. These results suggest that combination of microbial infection and MIAP is required for optimal apoptosis induction in macrophages. Uninfected cells incubated with pure and encapsulated MIAP show some incidence of necrosis with unknown mechanism. These results provide new insight into the effect of exogenous HDP on macrophage cell responses during Mtb infection.

Conclusively, the applicability of AMP releasing inhalable porous particles, PNAPs, MPPs was explored as an unconventional advancement to fight against TB. Inhalable particles suitable for deep lung deposition, i.e. within respirable size range (1-10μm) and aerodynamic diameter of ~2.5 μm were developed and characterised. PNAP demonstrated dual biphasic pattern that was categorized by initial burst, followed by slower secondary linear sustained release pattern (apparent zero order phase) of peptide. MIAP-PNAPs show sustained liberation of peptide for longer period of time (8 days) as compared with MIAP-NP (5 days) leading to total cumulative release to ~95%. The release profiles of Ub2, K4 and Aurien1.2 from respective microspheres**.** All the HDP were gradually released from porous MS matrix in a biphasic mode. The first phase is characterized by a fast release which probably results from the solubilisation of peptides that usually present near the surface. The second phase is characterized by a slow release which could be attributed to the degradation of polymer matrix leading to the diffusion of the entrapped peptide. All the formulations MIAP, IDR-1018, indolicidin, K4, aurin1.2, UB2 at concentration

10, 50 and 100µg/ml showed significant *in vitro* anti TB activity. The results reveal that formulation loaded with IDR-1018 and indolicidin put forth significant antimycobaterial activity against virulent Mtb *in vivo.* The *in vivo* antitubercular efficacy of the formulation was compared with standard oral INH and rifampicin (10 mg/kg). After histopathological examination of the lungs and spleen revealed that treatment with inhaled formulation considerably reduce inflammation and minimal granulomatous involvement compared to untreated control. Almost similar response was observed in case of oral INH and rifampicin therapy. We made an attempt to elucidate some cellular and molecular mechanism by which AMP kills Mtb at very low concentrations. Results suggest that different types of AMP showed different or multiple mechanisms to kill bacteria residing in alveolar macrophages. These data provide evidence for the potential of AMP therapy for the treatment of TB and combination of microencapsulated AMP with standard anti-TB hold great potential as new regimen for treatment of tuberculosis.

FUTURE SCOPE

Based on the present investigation, the following studies may be pursued:

- It is apparent that pulmonary drug delivery systems (microparticles) for sustained delivery of AMP undoubtedly have the potential for anti-tubercular therapy. MDR-TB and XRD-TB which are not responding to usual TB treatment is another circumstance where inhaled therapy of AMP releasing formulations can be applied. Due to multiple mechanism of action of exogenous AMP which is different from conventional antituberculosis drugs, it may offer additional advantage against MDR/XDR TB and hence, selected AMP releasing formulations can be tested against MDR/XDR TB strains of *Mycobacterium tuberculosis*.

- Preliminary results propose that these formulations may work in synergy with conventional therapy, if used as adjunct therapy. The formulations were found to be effectual in laboratory small animals, now, there is need of efficacy and toxicity studies in non-human primates and they capacity to extrapolate the therapeutic results from laboratory animals to human clinical trials.

Conclusively, the applicability of AMP releasing inhalable porous particles, PNAPs, MPPs was explored as an unconventional advancement to fight against TB. Inhalable particles suitable for deep lung deposition, i.e. within respirable size range (1-10 μm) and aerodynamic diameter of ~2.5 μm were developed and characterised. PNAPs demonstrated dual biphasic pattern that was categorized by initial burst, followed by slower secondary linear sustained release pattern (apparent zero order phase) of peptide. MIAP-PNAPs show sustained liberation of peptide for longer period of time (8 days) as compared with MIAP-NP (5 days) leading to total cumulative release to ~95%. The release profiles of Ub2, K4 and Aurien1.2 from respective microspheres. All the HDP were gradually released from porous MS matrix in a biphasic mode. The first phase is characterized by a fast release which probably results from the solubilisation of peptides that usually present near the surface. The second phase is characterized by a slow release which could be attributed to the degradation of polymer matrix leading to the diffusion of the entrapped peptide. All the formulations MIAP, IDR-1018, indolicidin, K4, aurin 1.2, UB2 at concentration 10, 50 and 100 μg/ml showed significant in vitro anti TB activity. The results reveal that formulation loaded with IDR-1018 and indolicidin put forth significant antimycobacterial activity against virulent M.tb in vivo. The in vivo antitubercular efficacy of the formulation was compared with standard oral INH and rifampicin (10 mg/kg). After histopathological examination of the lungs and spleen revealed that treatment with inhaled formulation considerably reduce inflammation and minimal granulomatous involvement compared to untreated control. Almost similar response was observed in case of oral INH and rifampicin therapy. We made an attempt to elucidate some cellular and molecular mechanism by which AMP kills M.tb at very low concentrations. Results suggest that different types of AMP showed different or multiple mechanisms to kill bacteria residing in alveolar macrophages. AMP kill the bacterium by direct membrane lysis as well as can activate cells via phagosomal-lysosomal fusion and apoptosis. These data provide evidence for the potential of AMP therapy for the treatment of TB and combination of microencapsulated AMP with standard anti-TB hold great potential as new regimen for treatment of tuberculosis.

1. Giovagnoli S, Blasi P, Schoubben A, Rossi C, Ricci M. Preparation of large porous biodegradable microspheres by using a simple double-emulsion method for capreomycin sulfate pulmonary delivery. International journal of pharmaceutics. 2007;333(1-2):103-11.

2. Harries A, Dye C. Tuberculosis. Annals of tropical medicine and parasitology. 2006;100(5-6):415-31.

3. Pradhan S, Mathur A, Patil A. ADVANCES IN ANTI-TUBERCULOSIS DRUGS. Journal of Drug Delivery and Therapeutics. 2014;4(5):69-73.

4. Goble M, Iseman MD, Madsen LA, Waite D, Ackerson L, Horsburgh Jr CR. Treatment of 171 patients with pulmonary tuberculosis resistant to isoniazid and rifampin. New England journal of medicine. 1993;328(8):527-32.

5. Fox W, Ellard GA, Mitchison DA. Studies on the treatment of tuberculosis undertaken by the British Medical Research Council tuberculosis units, 1946–1986, with relevant subsequent publications. The International Journal of Tuberculosis and Lung Disease. 1999;3(10):S231-S79.

6. Pena R, Sbarbaro D, editors. Integral variable structure controllers for small wind energy systems. IECON'99 Conference Proceedings 25th Annual Conference of the IEEE Industrial Electronics Society (Cat No 99CH37029); 1999: IEEE.

7. Francalanci L, Tommasini S, Conticelli S, Davies GR. Sr isotope evidence for short magma residence time for the 20th century activity at Stromboli volcano, Italy. Earth and Planetary Science Letters. 1999;167(1-2):61-9.

8. Alwarthan AA. Chemiluminescence detection of sodium nitroprusside using flow injection analysis. Talanta. 1994;41(10):1683-8.

9. Sharma A, Sharma S, Khuller G. Lectin-functionalized poly (lactide-co-glycolide) nanoparticles as oral/aerosolized antitubercular drug carriers for treatment of tuberculosis. Journal of Antimicrobial Chemotherapy. 2004;54(4):761-6.

10. Anisimova Y, Gelperina S, Peloquin C, Heifets L. Nanoparticles as antituberculosis drugs carriers: effect on activity against Mycobacterium tuberculosis in human monocyte-derived macrophages. Journal of Nanoparticle Research. 2000;2(2):165-71.

11. Kaur M, Malik B, Garg T, Rath G, Goyal AK. Development and characterization of guar gum nanoparticles for oral immunization against tuberculosis. Drug delivery. 2015;22(3):328-34.

12. Reljic R, Hart P, Copland A, Kim M, Tran AC, Poerio N, et al. Immunization with Mycobacterium tuberculosis antigens encapsulated in phosphatidylserine liposomes improves protection afforded by BCG. Frontiers in Immunology. 2019;10:1349.

13. Khademi F, Taheri RA, Momtazi-Borojeni AA, Farnoosh G, Johnston TP, Sahebkar A. Potential of cationic liposomes as adjuvants/delivery systems for tuberculosis subunit vaccines. Reviews of Physiology, Biochemistry and Pharmacology, Vol 175: Springer; 2018. p. 47-69.

14. Momin MA, Sinha S, Tucker IG, Das SC. Carrier-free combination dry powder inhaler formulation of ethionamide and moxifloxacin for treating drug-resistant tuberculosis. Drug development and industrial pharmacy. 2019:1-11.

15. Patil TS, Deshpande A, Shende PK, Deshpande S, Gaud R. Evaluation of Nanocarrier-Based Dry Powder Formulations for Inhalation with Special Reference to Anti-Tuberculosis Drugs. Critical Reviews™ in Therapeutic Drug Carrier Systems. 2019;36(3).

16. Singh J, Garg T, Rath G, Goyal AK. Advances in nanotechnology-based carrier systems for targeted delivery of bioactive drug molecules with special emphasis on immunotherapy in drug resistant tuberculosis–a critical review. Drug delivery. 2016;23(5):1676-98.

17. Pham D-D, Fattal E, Tsapis N. Pulmonary drug delivery systems for tuberculosis treatment. International journal of pharmaceutics. 2015;478(2):517-29.

18. Nguyen L, Pieters J. The Trojan horse: survival tactics of pathogenic mycobacteria in macrophages. Trends Cell Biol. 2005;15(5):269-76.

19. Flannagan RS, Cosio G, Grinstein S. Antimicrobial mechanisms of phagocytes and bacterial evasion strategies. Nat Rev Microbiol. 2009;7(5):355-66.

20. Clemens DL, Horwitz MA. Characterization of the Mycobacterium tuberculosis phagosome and evidence that phagosomal maturation is inhibited. J Exp Med. 1995;181(1):257-70.

21. Keane J, Remold HG, Kornfeld H. Virulent Mycobacterium tuberculosis strains evade apoptosis of infected alveolar macrophages. J Immunol. 2000;164(4):2016-20.

22. Desjardins M. Biogenesis of phagolysosomes: the 'kiss and run' hypothesis. Trends Cell Biol. 1995;5(5):183-6.

23. Desjardins M, Nzala NN, Corsini R, Rondeau C. Maturation of phagosomes is accompanied by changes in their fusion properties and size-selective acquisition of solute materials from endosomes. Journal of cell science. 1997;110(18):2303-14.

24. Park H-S, Yu J-W, Cho J-H, Kim M-S, Huh S-H, Ryoo K, et al. Inhibition of apoptosis signal-regulating kinase 1 by nitric oxide through a thiol redox mechanism. Journal of Biological Chemistry. 2004;279(9):7584-90.

25. Dahl KE, Shiratsuchi H, Hamilton BD, Ellner JJ, Toossi Z. Selective induction of transforming growth factor beta in human monocytes by lipoarabinomannan of Mycobacterium tuberculosis. Infect Immun. 1996;64(2):399-405.

26. MacMicking J, Xie Q-w, Nathan C. Nitric oxide and macrophage function. Annual review of immunology. 1997;15(1):323-50.

27. Nguyen L, Pieters J. Mycobacterial subversion of chemotherapeutic reagents and host defense tactics: challenges in tuberculosis drug development. Annual review of pharmacology and toxicology. 2009;49:427-53.

28. Nigou J, Dover LG, Besra GS. Purification and biochemical characterization of Mycobacterium tuberculosis SuhB, an inositol monophosphatase involved in inositol biosynthesis. Biochemistry. 2002;41(13):4392-8.

29. Keane J, Remold HG, Kornfeld H. Virulent Mycobacterium tuberculosis strains evade apoptosis of infected alveolar macrophages. The Journal of Immunology. 2000;164(4):2016-20.

30. Dünnhaupt S, Kammona O, Waldner C, Kiparissides C, Bernkop-Schnürch A. Nano-carrier systems: strategies to overcome the mucus gel barrier. European Journal of Pharmaceutics and Biopharmaceutics. 2015;96:447-53.

31. Kolloli A, Subbian S. Host-directed therapeutic strategies for tuberculosis. Frontiers in medicine. 2017;4:171.

32. Khara JS, Wang Y, Ke X-Y, Liu S, Newton SM, Langford PR, et al. Anti-mycobacterial activities of synthetic cationic α-helical peptides and their synergism with rifampicin. Biomaterials. 2014;35(6):2032-8.

33. Giuliani A, Pirri G, Nicoletto S. Antimicrobial peptides: an overview of a promising class of therapeutics. Open Life Sciences. 2007;2(1):1-33.

34. Seyfi R, Kahaki FA, Ebrahimi T, Montazersaheb S, Eyvazi S, Babaeipour V, et al. Antimicrobial Peptides (AMPs): Roles, Functions and Mechanism of Action. International Journal of Peptide Research and Therapeutics. 2019:1-13.

35. Fjell CD, Hiss JA, Hancock RE, Schneider G. Designing antimicrobial peptides: form follows function. Nature reviews Drug discovery. 2012;11(1):37.

36. Batai I, Kerenyi M, Tekeres M. The impact of drugs used in anaesthesia on bacteria. European journal of anaesthesiology. 1999;16(7):425-40.

37. Yeaman MR, Yount NY. Mechanisms of antimicrobial peptide action and resistance. Pharmacological reviews. 2003;55(1):27-55.

38. Hamoen LW, Wenzel M. Antimicrobial peptides-interaction with membrane lipids and proteins. Frontiers in cell and developmental biology. 2017;5:4.

39. Arranz-Trullén J, Lu L, Pulido D, Bhakta S, Boix E. Host antimicrobial peptides: The promise of new treatment strategies against tuberculosis. Frontiers in Immunology. 2017;8:1499.

40. Brogden KA. Antimicrobial peptides: pore formers or metabolic inhibitors in bacteria? Nature Reviews Microbiology. 2005;3(3):238.

41. Ramón-García S, Mikut R, Ng C, Ruden S, Volkmer R, Reischl M, et al. Targeting Mycobacterium tuberculosis and other microbial pathogens using improved synthetic antibacterial peptides. Antimicrobial agents and chemotherapy. 2013;57(5):2295-303.

42. Clausen ML, Slotved HC, Krogfelt KA, Andersen PS, Agner T. In vivo expression of antimicrobial peptides in atopic dermatitis. Experimental dermatology. 2016;25(1):3-9.

43. Clowry J, Irvine AD, McLoughlin RM. Next-generation anti–Staphylococcus aureus vaccines: A potential new therapeutic option for atopic dermatitis? Journal of Allergy and Clinical Immunology. 2019;143(1):78-81.

44. Raftery T, Martineau AR, Greiller CL, Ghosh S, McNamara D, Bennett K, et al. Effects of vitamin D supplementation on intestinal permeability, cathelicidin and disease markers in Crohn's disease: results from a randomised double-blind placebo-controlled study. United European gastroenterology journal. 2015;3(3):294-302.

45. Law IK, Cheng MW, Shih DQ, McGovern DP, Koon HW. The Roles of Antimicrobial Peptides in the Regulation of Gastrointestinal Microbiota and Innate Immunity. Antimicrobial Peptides in Gastrointestinal Diseases: Elsevier; 2018. p. 35-60.

46. Hancock RE, Haney EF, Gill EE. The immunology of host defence peptides: beyond antimicrobial activity. Nature Reviews Immunology. 2016;16(5):321.

47. van Eijk M, van der Ent C, Aerts H, Kristensen M, de Cock H, van Dijk A, et al. Novel antimicrobial peptides to fight infections in patients with cystic fibrosis. 2017.

48. Payne JE, Dubois AV, Ingram RJ, Weldon S, Taggart CC, Elborn JS, et al. Activity of innate antimicrobial peptides and ivacaftor against clinical cystic fibrosis respiratory pathogens. International journal of antimicrobial agents. 2017;50(3):427-35.

49. Forde É, Schütte A, Reeves E, Greene C, Humphreys H, Mall M, et al. Differential in vitro and in vivo toxicities of antimicrobial peptide prodrugs for potential use in cystic fibrosis. Antimicrobial agents and chemotherapy. 2016;60(5):2813-21.

50. Chen C, Deslouches B, Montelaro RC, Di YP. Enhanced efficacy of the engineered antimicrobial peptide WLBU2 via direct airway delivery in a murine model of Pseudomonas aeruginosa pneumonia. Clinical Microbiology and Infection. 2018;24(5):547. e1-. e8.

51. Banaschewski BJ, Veldhuizen EJ, Keating E, Haagsman HP, Zuo YY, Yamashita CM, et al. Antimicrobial and biophysical properties of surfactant supplemented with an antimicrobial peptide for treatment of bacterial pneumonia. Antimicrobial agents and chemotherapy. 2015;59(6):3075-83.

52. Mangoni ML, McDermott AM, Zasloff M. Antimicrobial peptides and wound healing: biological and therapeutic considerations. Experimental dermatology. 2016;25(3):167-73.

53. Otvos Jr L, Ostorhazi E. Therapeutic utility of antibacterial peptides in wound healing. Expert review of anti-infective therapy. 2015;13(7):871-81.

54. Kwok PCL, Grabarek A, Chow MY, Lan Y, Li JC, Casettari L, et al. Inhalable spray-dried formulation of D-LAK antimicrobial peptides targeting tuberculosis. International journal of pharmaceutics. 2015;491(1-2):367-74.

55. Felício MR, Silva ON, Gonçalves S, Santos NC, Franco OL. Peptides with dual antimicrobial and anticancer activities. Frontiers in chemistry. 2017;5:5.

56. Alvar J, Mowdray C, Alves F, Yardley V, Martin J, Fernandez C, et al. Drug Discovery for Leishmaniasis: Royal Society of Chemistry; 2017.

57. do Nascimento VV, Mello ÉdO, Carvalho LP, de Melo EJ, Carvalho AdO, Fernandes KV, et al. PvD1 defensin, a plant antimicrobial peptide with inhibitory activity against Leishmania amazonensis. Bioscience reports. 2015;35(5).

58. Rodríguez-Carlos A, Martinez-Gutierrez F, Torres-Juarez F, Rivas-Santiago B. Antimicrobial Peptides-based Nanostructured Delivery Systems: An Approach for Leishmaniasis Treatment. Current pharmaceutical design. 2019;25(14):1593-603.

59. Mansour SC, de la Fuente-Núñez C, Hancock RE. Peptide IDR-1018: modulating the immune system and targeting bacterial biofilms to treat antibiotic-resistant bacterial infections. Journal of Peptide Science. 2015;21(5):323-9.

60. Portell-Buj E, Vergara A, Alejo I, López-Gavín A, Monté MR, San Nicolás L, et al. In vitro activity of 12 antimicrobial peptides against Mycobacterium tuberculosis and Mycobacterium avium clinical isolates. Journal of medical microbiology. 2018;68(2):211-5.

61. Linde CM, Hoffner SE, Refai E, Andersson M. In vitro activity of PR-39, a proline-arginine-rich peptide, against susceptible and multi-drug-resistant Mycobacterium tuberculosis. Journal of Antimicrobial Chemotherapy. 2001;47(5):575-80.

62. Rivas-Santiago B, Santiago CER, Castañeda-Delgado JE, León–Contreras JC, Hancock RE, Hernandez-Pando R. Activity of LL-37, CRAMP and antimicrobial peptide-derived compounds E2, E6 and CP26 against Mycobacterium tuberculosis. International journal of antimicrobial agents. 2013;41(2):143-8.

63. Martineau AR, Wilkinson KA, Newton SM, Floto RA, Norman AW, Skolimowska K, et al. IFN-γ-and TNF-independent vitamin D-inducible human suppression of mycobacteria: the role of cathelicidin LL-37. The Journal of Immunology. 2007;178(11):7190-8.

64. Pandya S, Gupta A, Ranjan R, Sachan M, Kumar A. Inhaled Drug Combinations. Delivery Systems for Tuberculosis Prevention and Treatment. 2016:212.

65. Patil J, Sarasija S. Pulmonary drug delivery strategies: A concise, systematic review. Lung India: Official Organ of Indian Chest Society. 2012;29(1):44.

66. Marple VA, Liu BY, Rubow KL. A dust generator for laboratory use. Am Ind Hyg Assoc J. 1978;39(1):26-32. Epub 1978/01/01.

67. Yadav AB, Sharma R, Muttil P, Singh AK, Verma RK, Mohan M, et al. Inhalable microparticles containing isoniazid and rifabutin target macrophages and 'stimulate the phagocyte' to achieve high efficacy. Indian J Exp Biol. 2009;47(6):469-74.

68. Verma RK, Singh AK, Mohan M, Agrawal AK, Verma PR, Gupta A, et al. Inhalable microparticles containing nitric oxide donors: saying NO to intracellular Mycobacterium tuberculosis. Mol Pharm. 2012;9(11):3183-9.

69. Parumasivam T, Leung SS, Quan DH, Triccas JA, Britton WJ, Chan H-K. Rifapentine-loaded PLGA microparticles for tuberculosis inhaled therapy: preparation and in vitro aerosol characterization. european journal of pharmaceutical sciences. 2016;88:1-11.

70. Gaspar MC, Grégoire N, Sousa JJ, Pais AA, Lamarche I, Gobin P, et al. Pulmonary pharmacokinetics of levofloxacin in rats after aerosolization of immediate-release chitosan or sustained-release PLGA microspheres. european journal of pharmaceutical sciences. 2016;93:184-91.

71. Sharma A, Vaghasiya K, Verma RK. Inhalable microspheres with hierarchical pore size for tuning the release of biotherapeutics in lungs. Microporous and Mesoporous Materials. 2016;235:195-203.

72. Cunha L, Rosa da Costa AM, Lourenço JP, Buttini F, Grenha A. Spray-dried fucoidan microparticles for pulmonary delivery of antitubercular drugs. Journal of microencapsulation. 2018;35(4):392-405.

73. Kaur R, Garg T, Malik B, Gupta UD, Gupta P, Rath G, et al. Development and characterization of spray-dried porous nanoaggregates for pulmonary delivery of anti-tubercular drugs. Drug delivery. 2016;23(3):872-7.

74. Pandey R, Sharma S, Khuller G. Nebulization of liposome encapsulated antitubercular drugs in guinea pigs. International journal of antimicrobial agents. 2004;24(1):93-4.

75. Chimote G, Banerjee R. In vitro evaluation of inhalable isoniazid-loaded surfactant liposomes as an adjunct therapy in pulmonary tuberculosis. Journal of Biomedical Materials Research Part B: Applied Biomaterials. 2010;94(1):1-10.

76. Khatak S, Semwal UP, Pandey MK, Dureja H. Investigation of Antimycobacterial potential of solid lipid nanoparticles against M. smegmatis. 2018.

77. Kumar K, Das M, Rajasekharan Pillai V. Syntheses of four peptides from the immunodominant region of hepatitis C viral pathogens using PS-TTEGDA support for the investigation of HCV infection in human blood. The Journal of Peptide Research. 2000;56(2):88-96.

78. Merrifield RB. Solid phase peptide synthesis. I. The synthesis of a tetrapeptide. Journal of the American Chemical Society. 1963;85(14):2149-54.

79. Lloyd-Williams P, Albericio F, Giralt E. Convergent solid-phase peptide synthesis. Tetrahedron. 1993;49(48):11065-133.

80. Sharma A, Vaghasiya K, Gupta P, Gupta UD, Verma RK. Reclaiming hijacked phagosomes: Hybrid nano-in-micro encapsulated MIAP peptide ensures host directed therapy by specifically augmenting phagosome-maturation and apoptosis in TB infected macrophage cells. Int J Pharm. 2018;536(1):50-62.

81. Sharma A, Vaghasiya K, Ray E, Verma RK. Nano-encapsulated HHC10 host defense peptide (HDP) reduces the growth of Escherichia coli via multimodal mechanisms. Artificial cells, nanomedicine, and biotechnology. 2018:1-10.

82. Leite CQ, Beretta AL, Anno IS, Telles MA. Standardization of broth microdilution method for Mycobacterium tuberculosis. Memorias do Instituto Oswaldo Cruz. 2000;95(1):127-9.

83. Muttil P, Kaur J, Kumar K, Yadav AB, Sharma R, Misra A. Inhalable microparticles containing large payload of anti-tuberculosis drugs. Eur J Pharm Sci. 2007;32(2):140-50. Epub 2007/08/08.

84. Alwarthan AA. Chemiluminescence detection of sodium nitroprusside using flow injection analysis. Talanta. 1994;41(10):1683-8.

85. Garcia-Contreras L, Fiegel J, Telko M, Elbert K, Hawi A, Thomas M, et al. Inhaled large porous particles of capreomycin for treatment of tuberculosis in a guinea pig model. Antimicrobial agents and chemotherapy. 2007;51(8):2830-6.

86. Sharma A, Vaghasiya K, Verma RK. Inhalable microspheres with hierarchical pore size for tuning the release of biotherapeutics in lungs. Microporous and Mesoporous Materials. 2016;235:195-203.

87. Giovagnoli S, Blasi P, Schoubben A, Rossi C, Ricci M. Preparation of large porous biodegradable microspheres by using a simple double-emulsion method for capreomycin sulfate pulmonary delivery. International journal of pharmaceutics. 2007;333(1-2):103-11.

88. Cheow WS, Ng MLL, Kho K, Hadinoto K. Spray-freeze-drying production of thermally sensitive polymeric nanoparticle aggregates for inhaled drug delivery: effect of freeze-drying adjuvants. International journal of pharmaceutics. 2011;404(1-2):289-300.

89. Saluja V, Amorij J, Kapteyn J, de Boer A, Frijlink H, Hinrichs W. A comparison between spray drying and spray freeze drying to produce an influenza subunit vaccine powder for inhalation. Journal of Controlled Release. 2010;144(2):127-33.

90. Sharma A, Vaghasiya K, Gupta P, Gupta UD, Verma RK. Reclaiming hijacked phagosomes: hybrid nano-in-micro encapsulated MIAP peptide ensures host directed therapy by specifically augmenting phagosome-maturation and apoptosis in TB infected macrophage cells. International journal of pharmaceutics. 2018;536(1):50-62.

91. Ravivarapu HB, Lee H, DeLuca PP. Enhancing initial release of peptide from poly(d,l-lactide-co-glycolide) (PLGA) microspheres by addition of a porosigen and increasing drug load. Pharm Dev Technol. 2000;5(2):287-96.

92. Muttil P, Kaur J, Kumar K, Yadav AB, Sharma R, Misra A. Inhalable microparticles containing large payload of anti-tuberculosis drugs. european journal of pharmaceutical sciences. 2007;32(2):140-50

93. Yadav AB, Misra A. Enhancement of apoptosis of THP-1 cells infected with Mycobacterium tuberculosis by inhalable microparticles and relevance to bactericidal activity. Antimicrobial agents and chemotherapy. 2007;51(10):3740-2.

94. Verma RK, Singh AK, Mohan M, Agrawal AK, Verma PR, Gupta A, et al. Inhalable microparticles containing nitric oxide donors: saying NO to intracellular Mycobacterium tuberculosis. Molecular pharmaceutics. 2012;9(11):3183-9.

95. Sharma R, Muttil P, Yadav AB, Rath SK, Bajpai VK, Mani U, et al. Uptake of inhalable microparticles affects defence responses of macrophages infected with Mycobacterium tuberculosis H37Ra. Journal of Antimicrobial Chemotherapy. 2007;59(3):499-506.

96. Verma RK, Singh AK, Mohan M, Agrawal AK, Verma PR, Gupta A, et al. Inhalable microparticles containing nitric oxide donors: saying NO to intracellular Mycobacterium tuberculosis. Molecular pharmaceutics. 2012;9(11):3183-9.

97. Reix N, Parat A, Seyfritz E, Van Der Werf R, Epure V, Ebel N, et al. In vitro uptake evaluation in Caco-2 cells and in vivo results in diabetic rats of insulin-loaded PLGA nanoparticles. International journal of pharmaceutics. 2012;437(1-2):213-20.

98. Paramonov SE, Bachelder EM, Beaudette TT, Standley SM, Lee CC, Dashe J, et al. Fully acid-degradable biocompatible polyacetal microparticles for drug delivery. Bioconjugate Chemistry. 2008;19(4):911-9.

99. Paramonov SE, Bachelder EM, Beaudette TT, Standley SM, Lee CC, Dashe J, et al. Fully acid-degradable biocompatible polyacetal microparticles for drug delivery. Bioconjug Chem. 2008;19(4):911-9. Epub 2008/04/01.

100. Verma RK, Agrawal AK, Singh AK, Mohan M, Gupta A, Gupta P, et al. Inhalable microparticles of nitric oxide donors induce phagosome maturation and kill Mycobacterium tuberculosis. Tuberculosis (Edinb). 2013;93(4):412-7.

101. Mohanty S, Jena P, Mehta R, Pati R, Banerjee B, Patil S, et al. Cationic antimicrobial peptides and biogenic silver nanoparticles kill mycobacteria without eliciting DNA damage and cytotoxicity in mouse macrophages. Antimicrob Agents Chemother. 2013;57(8):3688-98.

102. Lawlor C, O'Connor G, O'Leary S, Gallagher PJ, Cryan SA, Keane J, et al. Treatment of Mycobacterium tuberculosis-Infected Macrophages with Poly(Lactic-Co-Glycolic Acid) Microparticles Drives NFkappaB and Autophagy Dependent Bacillary Killing. PloS one. 2016;11(2):e0149167.

103. Flannagan RS, Cosio G, Grinstein S. Antimicrobial mechanisms of phagocytes and bacterial evasion strategies. Nature reviews Microbiology. 2009;7(5):355-66.

104. Clemens DL, Horwitz MA. Characterization of the Mycobacterium tuberculosis phagosome and evidence that phagosomal maturation is inhibited. The Journal of experimental medicine. 1995;181(1):257-70.

105. Keane J, Remold HG, Kornfeld H. Virulent Mycobacterium tuberculosis strains evade apoptosis of infected alveolar macrophages. Journal of immunology. 2000;164(4):2016-20.

106 Desjardins M. Biogenesis of phagolysosomes: the 'kiss and run' hypothesis. Trends Cell Biol. 1995;5(5):183-6.

107. Tamime R, Wyart Y, Siozade L, Baudin I, Deumie C, Glucina K, et al. Membrane characterization by microscopic and scattering methods: multiscale structure. Membranes. 2011;1(2):91-7.

108. Verma RK, Kaur J, Kumar K, Yadav AB, Misra A. Intracellular time course, pharmacokinetics, and biodistribution of isoniazid and rifabutin following pulmonary delivery of inhalable microparticles to mice. Antimicrob Agents Chemother. 2008;52(9):3195-201.

109. Teitelbaum R, Cammer M, Maitland ML, Freitag NE, Condeelis J, Bloom BR. Mycobacterial infection of macrophages results in membrane-permeable phagosomes. Proc Natl Acad Sci U S A. 1999;96(26):15190-5. Epub 1999/12/28.

110. Verma RK, Singh AK, Mohan M, Agrawal AK, Verma PR, Gupta A, et al. Inhalable microparticles containing nitric oxide donors: saying NO to intracellular Mycobacterium tuberculosis. Molecular pharmaceutics. 2012;9(11):3183-9.

111. Ramachandra L, Smialek JL, Shank SS, Convery M, Boom WH, Harding CV. Phagosomal processing of Mycobacterium tuberculosis antigen 85B is modulated independently of mycobacterial viability and phagosome maturation. Infect Immun. 2005;73(2):1097-105. Epub 2005/01/25.

112. Desai MP, Labhasetwar V, Walter E, Levy RJ, Amidon GL. The mechanism of uptake of biodegradable microparticles in Caco-2 cells is size dependent. Pharmaceutical research. 1997;14(11):1568-73.

113. Eruslanov E, Kusmartsev S. Identification of ROS using oxidized DCFDA and flow-cytometry. Methods Mol Biol. 2010;594:57-72. Epub 2010/01/15.

114. Hancock RE, Chapple DS. Peptide antibiotics. Antimicrob Agents Chemother. 1999;43(6):1317-23.

115. Shekunov BY, Chattopadhyay P, Tong HH, Chow AH. Particle size analysis in pharmaceutics: principles, methods and applications. Pharmaceutical research. 2007;24(2):203-27.

116. Muschel RJ, Bernhard EJ, Garza L, McKenna WG, Koch CJ. Induction of apoptosis at different oxygen tensions: evidence that oxygen radicals do not mediate apoptotic signaling. Cancer Research. 1995;55(5):995-8.

117. Kaur J, Muttil P, Verma RK, Kumar K, Yadav AB, Sharma R, et al. A hand-held apparatus for "nose-only" exposure of mice to inhalable microparticles as a dry powder inhalation targeting lung and airway macrophages. Eur J Pharm Sci. 2008;34(1):56-65. Epub 2008/04/05.

PUBLISHED

1. Sharma, A., Vaghasiya, K., Gupta, P., Singh, A. K., Gupta, U. D., & Verma, R. K. **(2020).** Dynamic mucus penetrating microspheres for efficient pulmonary delivery and enhanced efficacy of host defence peptide (HDP) in experimental tuberculosis. **Journal of Controlled Release**. **(IF 7.87)**

2. Sharma A, Vaghasiya K, Ray E, Gupta P, Gupta UD, Singh AK, Verma RK Jun 11. **(2020)**. Targeted pulmonary delivery of Epigallocatechin gallate (EGCG), a green tea polyphenol controls the growth of Mycobacterium tuberculosis by enhancing the autophagy and supressing bacterial burden. ACS Biomaterials Science & Engineering. 2020 **(IF 4.43)**

3. Vaghasiya K, Ray E, Sharma A, Katare OP, Verma RK. **(2020)**. Matrix metalloproteinase responsive mesoporous silica nanoparticles cloaked with cleavable-protein for "Self-actuating" on-demand controlled drug delivery for cancer therapy. ACS Applied Bio Materials. 2020 Jun 26.

4. Sharma A, Vaghasiya K, Gupta P, Gupta UD**,** Verma RK* **(2019)** Mycobactericidal activity of some micro-encapsulated synthetic Host Defense peptides (HDP) by expediting the permeation of antibiotic: A new paradigm of drug delivery for tuberculosis Mar 10;558:231-241 **International Journal of Pharmaceutics**. **(IF4.2)**

5. Vaghasiya K, **Sharma A,** Kumar K, Ray E, Adlakha S, Katare OP, Hota SK, Verma RK **(2019 Nov**). Heparin-Encapsulated Metered-Dose Topical "Nano-Spray Gel" Liposomal Formulation Ensures Rapid On-Site Management of Frostbite Injury by Inflammatory Cytokines Scavenging. ACS **Biomaterials Science & Engineering**. 6;5(12):6617-31. **(IF 4.43)**

6. Vaghasiya, K., Eram, A., **Sharma, A**., Ray, E., Adlakha, S. and Verma, R.K., **2019**. Alginate microspheres elicit innate M1-inflammatory response in macrophages leading to bacillary killing. ***AAPS PharmSciTech***, *20*(6), p.241. **(IF 2.45)**

7. Handa, M., **Sharma, A**., Verma, R.K. and Shukla, R., **(2019)**. Polycaprolactone based nano-carrier for co-administration of moxifloxacin and rutin and its In-vitro evaluation for sepsis. *Journal of Drug Delivery Science and Technology*, *54*, p.101286. **(IF 2.6)**

8. Adlakha, S., **Sharma, A**., Vaghasiya, K., Ray, E. and Verma, R.K., (**2019)**. Inhalation delivery of host defence peptides (HDP) using nano-formulation strategies: A pragmatic approach for therapy of pulmonary ailments. Current protein & peptide science. **(IF 2.1)**

9. Sharma A, Vaghasiya K, Gupta P, Gupta UD**,** Verma RK* **(2018)** Reclaiming *hijacked phagosomes*: Hybrid nano-in-micro encapsulated MIAP peptide ensures host directed therapy by specifically augmenting phagosome-maturation and apoptosis in TB infected macrophage cells **International Journal of Pharmaceutics**. Nov 24;536(1):50-62 **(IF 4.2)**

10. Sharma A, Vaghasiya K, Ray E**,** Verma RK* **(2018)** Nano-encapsulated HHC10 host defense peptide (HDP) reduces the growth of Escherichia coli via multimodal mechanisms. **Artificial Cells, Nanomedicine, and Biotechnology** 2018 Jul 23:1-10 **(IF 3.93)**

11. . **Sharma A**, Vaghasiya K, Ray E, Verma RK*** (2018)** Lysosomal targeting strategies for design and delivery of bioactive for therapeutic interventions **Journal of Drug Targeting** Vol 26, NO. 3, 208–221 **(IF 3.4)**

12. Sharma A, Verma RK* **(2017)** Hybrid Nano-in-Micro systems for lung delivery of Host Defence Peptides (HDP) as adjunct therapeutics for Pulmonary TB. **Drug Delivery to Lungs** (Proceedings) Vol 26, 3, 113–115. **(IF)**

13. Sharma A, Vaghasiya K, Verma RK* **(2016)** Inhalable microspheres with hierarchical pore size for tuning the release of biotherapeutics in lungs **Microporous and Mesoporous Materials** 235, 195-203 **(IF 4.18)**

Book sections

1. Ray E, **Sharma A**, Vaghasiya K, Verma RK* (2018) Molecular Medicines for Cancer: Concepts and Applications of Nanotechnology CRC Press/Taylor & Francis Publishers

2. **Sharma A**, Vaghasiya K, Yadav AB, Verma RK* (2018) "DNA nanostructures. chemistry, self-assembly and application, Emerging Applications of Nanoparticles and Architecture Nanostructures, Springer

3. Vaghasiya, K., **Sharma, A**., Ray, E., Adlakha, S. and Verma, R.K., (2020). Methods to Characterize Nanoparticles for Mucosal Drug Delivery. In Mucosal Delivery of Drugs and Biologics in Nanoparticles (pp. 27-57). Springer, Cham.)

4. Adlakha, S, Vaghasiya, K., **Sharma, A.,** Ray, E., and Verma, R.K., (2020). Inhalable polymeric dry powders for antituberculosis drug delivery. In Nanotechnology Based Approaches for Tuberculosis Treatment, Academic press